*Physiol Rev* 97: 939–993, 2017
Published May 3, 2017; doi:10.1152/physrev.00030.2016

# DENTAL ENAMEL FORMATION AND IMPLICATIONS FOR ORAL HEALTH AND DISEASE

**Rodrigo S. Lacruz, Stefan Habelitz, J. Timothy Wright, Michael L. Paine**

Department of Basic Science and Craniofacial Biology, College of Dentistry, New York University, New York, New York; Department of Preventive and Restorative Dental Sciences, University of California, San Francisco, San Francisco, California; Department of Pediatric Dentistry, School of Dentistry, University of North Carolina, Chapel Hill, North Carolina; Herman Ostrow School of Dentistry, Center for Craniofacial Molecular Biology, University of Southern California, Los Angeles, California

**Lacruz RS, Habelitz S, Wright JT, Paine ML.** Dental Enamel Formation and Implications for Oral Health and Disease. *Physiol Rev* 97: 939–993, 2017. Published May 3, 2017; doi:10.1152/physrev.00030.2016.—Dental enamel is the hardest and most mineralized tissue in extinct and extant vertebrate species and provides maximum durability that allows teeth to function as weapons and/or tools as well as for food processing. Enamel development and mineralization is an intricate process tightly regulated by cells of the enamel organ called ameloblasts. These heavily polarized cells form a monolayer around the developing enamel tissue and move as a single forming front in specified directions as they lay down a proteinaceous matrix that serves as a template for crystal growth. Ameloblasts maintain intercellular connections creating a semi-permeable barrier that at one end (basal/proximal) receives nutrients and ions from blood vessels, and at the opposite end (secretory/apical/distal) forms extracellular crystals within specified pH conditions. In this unique environment, ameloblasts orchestrate crystal growth via multiple cellular activities including modulating the transport of minerals and ions, pH regulation, proteolysis, and endocytosis. In many vertebrates, the bulk of the enamel tissue volume is first formed and subsequently mineralized by these same cells as they retransform their morphology and function. Cell death by apoptosis and regression are the fates of many ameloblasts following enamel maturation, and what cells remain of the enamel organ are shed during tooth eruption, or are incorporated into the tooth's epithelial attachment to the oral gingiva. In this review, we examine key aspects of dental enamel formation, from its developmental genesis to the ever-increasing wealth of data on the mechanisms mediating ionic transport, as well as the clinical outcomes resulting from abnormal ameloblast function.



## I. INTRODUCTION

Dental enamel is the hardest substance in the human body and serves as the wear-resistant outer layer of the dental crown. It forms an insulating barrier that protects the tooth from physical, thermal, and chemical forces that would otherwise be injurious to the vital tissue in the underlying dental pulp. Because the optical properties of enamel are also derived from its structure and composition (205), developmental defects or environmental influences affecting enamel structure are typically visualized as changes in its opacity and/or color. The impact of developmental insults on enamel is critical because, unlike bone, once mineralized, enamel tissue is acellular and hence does not remodel.

In mammals, dental enamel is the only epithelial-derived tissue that mineralizes in nonpathological situations (bone and dentin, the other principal mineralized tissues, are derived from mesenchymal cells). Enamel forms within an organic matrix composed of a unique grouping of extracellular matrix proteins (EMPs) that show little homology to proteins found in other tissues. The enamel organ is formed by a mixed population of cells. Among these are ameloblasts, which are primarily responsible for enamel formation and mineralization, and form a monolayer that is in direct contact with the forming enamel surface.

The process of enamel formation is referred to as amelogenesis. Enamel matrix proteins are secreted by ameloblasts into the enamel space, and are later degraded and proteolytically removed, also by ameloblasts. It is with a high level of precision that ameloblasts regulate the formation of a de novo hydroxyapatite-based (Hap-based) inorganic material within the enamel space. The formed enamel has a characteristic prismatic appearance composed of rods, each formed by a single ameloblast and extending from the dentino-enamel junction (DEJ) to the enamel surface, and the interrod enamel located around the enamel rods. Traces of EMP peptides are included in the fully formed enamel and are believed to contribute to the final structure, such that the fully formed (mature) enamel has unique morphological and biomechanical properties. By weight, mature enamel is ~95% mineral, ~1–2% organic material, and ~2–4% water (100, 331, 479, 509, 523, 548).

In this review, we discuss enamel from its developmental beginnings to its final structure. We will pay particular attention to the proteins comprising the enamel matrix, the role of ameloblast-mediated ion transport and mineralization, and the importance of extracellular pH regulation during enamel formation. There is also mounting information on the clinical outcomes that result from abnormal ameloblast function related to specific gene mutations, and we will summarize what is currently understood about enamel genotype-phenotype relationships.

## II. DENTAL TISSUES: HUMAN, RAT, AND MOUSE TEETH

All mammalian teeth share a similar structure: *1*) the enamel crown, formed by epithelial cells; *2*) the dentin found underlying the enamel, formed by mesenchymal cells and containing a large collagen component; *3*) the pulp, the organ generating/supplying the dentin-forming cells (odontoblasts), and also containing vasculature and nerve supply; *4*) the root, comprised primarily by the dentin, but also containing the root canal and surrounded by a thin layer of mineralized cementum; and *5*) the periodontal ligament, which is part of the dental socket that unites the cementum to the alveolar bone **(FIGURE 1)** (263, 333, 355, 403, 507, 655). Enamel is far more mineralized than the other tooth structures and serves to protect the dentin and pulp. Enamel contains no collagen, and once formed is devoid of any cells, so it cannot remodel.

Humans are diphyodonts (having 2 sets of teeth) with an initial/primary dentition of 20 teeth and a secondary/permanent dentition of 32 teeth. Rats and mice are monophydonts (having one set of teeth) with a single dentition of 16 teeth. Rats and mice have become widely used animal models to study tooth formation because rodents have continuously growing maxillary and mandibular incisors. This characteristic in rodents means that throughout the animal's lifespan, all stages of amelogenesis (see below) can be studied on a single incisor at any one time.

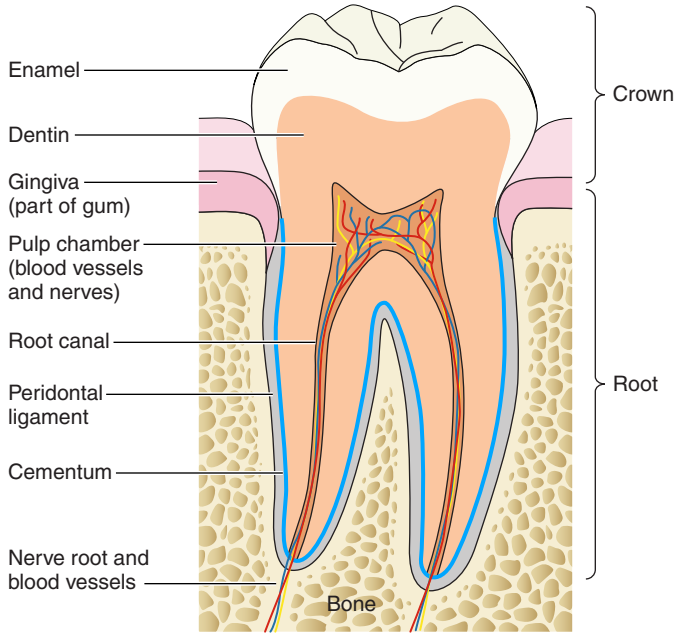


**FIGURE 1.** The anatomy of a human mandibular molar tooth. The major features of the mammalian tooth include the enamel, dentin, pulp contained within the pulp chamber, the root canal that carries the nerve and vasculature to the pulp, cementum, periodontal ligament, and the alveolar bone.

## III. AMELOGENESIS

### A. Embryological Development of Teeth

The staging of tooth formation has been studied histologically and morphologically for centuries. The principal stages include the initial development of a dental lamina comprising an inward growing band of thickened oral epithelium at specific sites determined by the localized expression of key transcription factors **(FIGURE 2)**. The dental lamina rapidly folds and penetrates the underlying mesenchyme to form the dental placode, followed by the bud, cap, and bell stages. These stages shape the crown, which is then followed by the development of the roots. The mesenchyme immediately underlying the dental epithelium is derived from cranial neural crest cells (74). Very early in tooth formation there is epithelial-mesenchymal molecular crosstalk initially orchestrated by the mesenchyme, such that epithelial cells destined to create enamel start to differentiate to form ameloblasts, and the underlying neural crest-derived mesenchyme differentiates into cells that will form the remainder of the tooth. It is beyond the scope of this review to discuss the morphogenesis and histology of mammalian tooth formation, or the cellular origins and molecular signals used locally to direct odontogenesis; however, the reader is directed to some outstanding publications that cover all these topics (74, 262, 271, 377, 378, 403, 594).

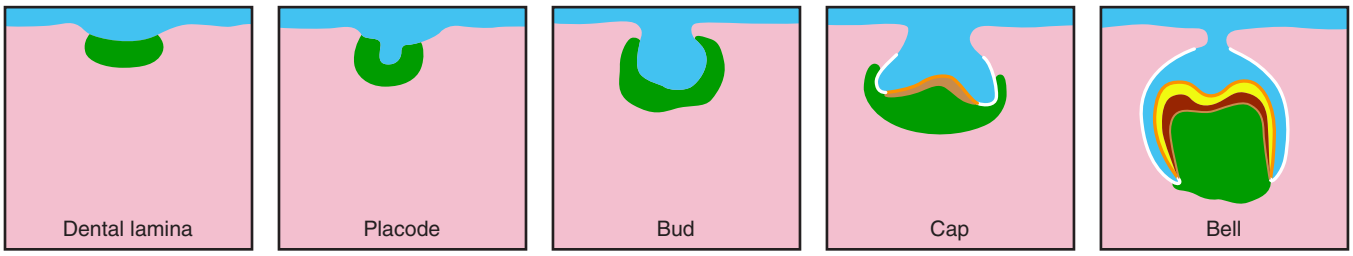


**FIGURE 2.** The principal stages of tooth formation. Thickening of the oral epithelium (blue) to form the dental lamina, the placode, bud, cap, and bell stages. The dental epithelium is shown in blue, the neural crest-derived mesenchyme in green, and all other (non-neural crest-derived) underlying mesenchyme in pink. At the cap and bell stage, the outer enamel epithelium is shown in white, the inner enamel epithelium (ameloblasts) is shown in orange, and the dentin-forming cells (odontoblasts) are shown as light brown. At the bell stage the forming enamel is yellow and the dentin dark brown. Green represents the (cranial) neural crest-derived mesenchymal cell population that migrates to the dental lamina and will eventually form the pulpal tissues seen in the bell stage.

## B. Amelogenesis

### *1. Overview of enamel formation*

Enamel development involves two major functional stages, secretory and maturation, with a brief transition between the two stages (403), although additional subdivisions may include: presecretory, early secretory, late secretory, transition, preabsorptive, early maturation, and late maturation stages (17, 273, 299, 464, 524). Throughout this review we focus primarily on the secretory and maturation stages as the bulk of data available to date, on the secretion of structural matrix proteins and proteinases, and on ionic transport, relates to these two stages.

### *2. The enamel organ*

Amelogenesis involves the formation of a number of epithelium-derived cell types. The innermost layer, the inner enamel epithelium, is a single layer of cells that differentiate into ameloblasts. The outermost layer is also a single layer of cells, referred to as the outer enamel epithelium. The inner and outer enamel epithelium converge at a region called the cervical loop, which is a niche for dental epithelial stem cells (47, 204, 272, 336, 379, 380, 420) and thus provides a constant source of enamel-forming cells until the enamel crown is fully formed with one exception. In rodent incisors, the long teeth in the upper and lower jaws, the stem cell niche in the cervical loop is retained for life, enabling the continuous growth of these teeth.

The cells comprising the enamel organ in the secretory stage and maturation stage are morphologically very different (228, 541). Hu et al. (228) illustrated the changing ameloblast morphologies throughout amelogenesis as viewed histologically. During the secretory stage, four cell populations are easily recognized: a single layer of secretory ameloblasts; the stratum intermedium, typically one or two cell layers thick; the stellate reticulum comprised of a larger grouping of star-shaped cells; and the single-layer outer enamel epithelium **(FIGURE 3)**. The vascular network that supplies nutrients to the developing enamel organ is associated with the outer enamel epithelium (275, 403). The anatomy of the enamel organ changes quickly and dramatically from secretory to maturation stage. Secretory ameloblasts transform, after a short transition period, and become shorter; they have frequently been referred to as squatter maturation cells (320, 403, 541). The other three epithelial cell populations identified in the secretory stage (stratum intermedium, stellate reticulum, and outer enamel epithelium) reorganize to become the papillary layer (PL) cells that are rich with blood vasculature weaving through its folds **(FIGURE 3)**.

The functional roles of these cell populations of the enamel organ, other than the ameloblasts, are poorly understood (343). The stratum intermedium has high alkaline phosphate (ALPL) activity (225, 640), suggesting that its function may be to facilitate transport of phosphate from the circulation to the developing enamel organ (640). Cells of the stellate reticulum maintain contact with each other through numerous desomosomes and gap junctions, giving them a star-like appearance (366, 367). The stellate reticulum cells express glycoaminoglycans such as perlecan, which accumulate in the intercellular spaces (245). The outer enamel epithelium is a single layer of cuboidal cells covering the entire enamel organ, thought to form a protective buffer isolating the other cells of the enamel organ (403). During the transition to maturation stage, the stratum intermedium, stellate reticulum, and possibly also the outer enamel epithelium reorganize to form the PL cells (61, 269). The PL cells are vascularized and participate in ion transport during the maturation stage, aiding the movement of ions from the blood circulation to the ameloblasts (61, 269).

### *3. Secretory-stage amelogenesis*

During the secretory stage, ameloblasts are highly polarized cells. The height (basal-apical distance) of a secretory

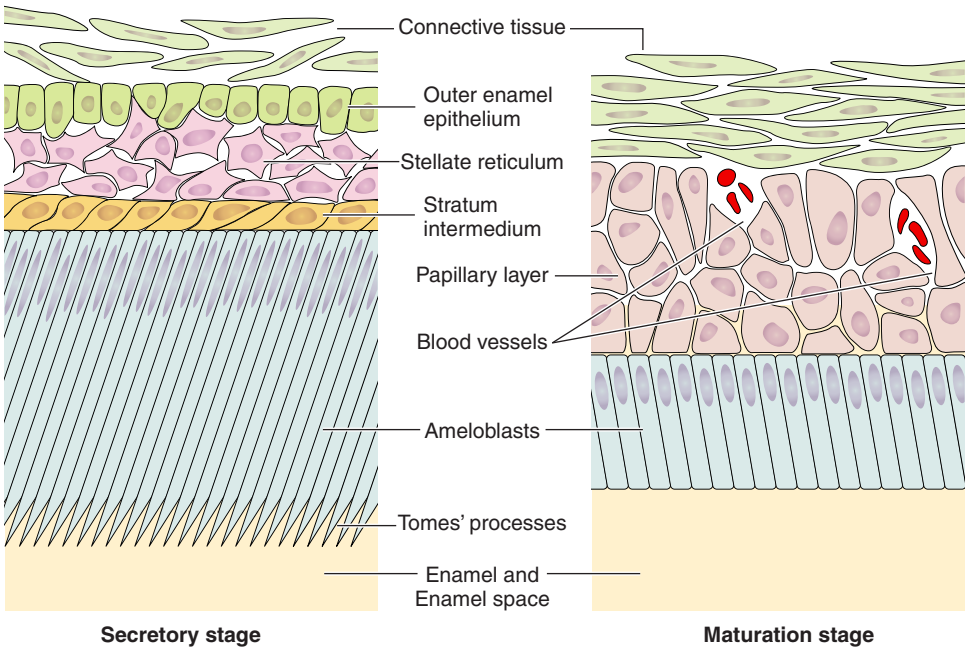


**FIGURE 3.** Secretory- and maturation-stage ameloblasts. *A*: highly polarized secretory ameloblasts (Am) with the Tomes' process (TP) projecting into the forming enamel front. *B*: shorter maturation ameloblasts. Connective tissue (CT), outer enamel epithelium (OEE), stellate reticulum (Sr), stratum intermedium (Si), and papillary layer cells are also identified, as is the enamel (En) or enamel space (ES) region which is in contact with the distal/apical pole of ameloblasts. Blood vessels (BV) can also be seen in the folds of the papillary layer cells.

ameloblast can be as great as 90 $\mu$m but is generally ~70 $\mu$m, while a narrow average diameter is ~5 $\mu$m, as detailed by Smith (541). These cells synthesize and secrete a limited number of structural enamel matrix proteins (EMPs), most notably amelogenin (AMELX), ameloblastin (AMBN), and enamelin (ENAM) (316, 541, 544). A unique characteristic observed in the morphology of secretory ameloblasts is the presence of the Tomes' processes (276, 450, 592, 621), triangular-shaped extensions of the cell found at the distal end and penetrating into the enamel matrix, giving an ameloblast monolayer a "picket-fence" appearance if viewed on a histological section (276, 403). The Tomes' process is important for exocytosing secretory vesicles and also plays a role in determining boundaries between rod and interrod regions (160, 403).

The precursors of the enamel crystals start to form during the early secretory stage in a protein-rich extracellular environment that is maintained at near-neutral pH conditions (316, 544). Thin hydroxyapatite-like (Hap-like) crystals [sometimes referred to as either enamel ribbonlike structures (97) or enamel ribbons (236, 543)] grow almost exclusively along their c-axis and elongate perpendicular to the DEJ under the influence of EMPs, in a direction that is finely coordinated with the movement of the ameloblasts traveling away from the dentin (148, 403). Historically, it was considered that initial formation of enamel crystallites (i.e., nucleation) occurred within the enamel matrix (115). However, some recent data have challenged this notion and suggest that enamel crystal growth is initiated on mineralized collagen fibers from the dentine (236, 543). These crystals then extend through the DEJ to the ameloblast membrane, and throughout the enamel (236, 543). Almost the entire thickness and volume of enamel is laid down during the secretory stage. It is a very soft tissue (gel-like) at this point, comprised of similar amounts of EMPs, mineral, and water by weight. Adjacent secretory-stage ameloblasts are tightly opposed and are connected to each other by intercellular junctional complexes on the lateral membrane at both the proximal/basal and distal/apical poles (240, 403, 503, 504, 506). These junctional complexes can be either tight, forming a beltlike and complete seal around the cell, as is frequently observed at the apical membrane, or they can be incomplete/leaky, as may be seen at the basal pole (240, 403, 504). These junctional complexes of secretory ameloblasts form a semipermeable barrier for intercellular movement/diffusion of mineral ions from the circulation to the enamel matrix (240, 579).

### *4. Transition stage*

The transition from secretory to maturation is brief (228, 603) and, in the rat lower incisor, spans ~170 $\mu$m (541) or ~30–40 cell widths. During this brief transition, significant morphological changes can be seen as ameloblasts become shorter and lose their secretory Tomes' process, and the PL is formed (274). These changes are accompanied by dramatic changes in gene expression profiles (318, 527, 664). The expression of EMP coding genes *AMELX*, *AMBN*, and *ENAM* are downregulated during this transition, whereas many other genes including those involved in ion transport, proteolysis, and pH homeostasis are upregulated (234, 318, 615, 664). During the transition stage, ~25% of ameloblasts die (550), presumably from apoptosis, which may result from the cells being in a metastable state due to calcium overload (240).

### *5. Enamel maturation*

Maturation-stage ameloblasts are shorter than secretory-stage ameloblasts, being ~40 $\mu$m in height. The major func-

tions of the ameloblasts during enamel maturation encompass many activities, including ion transport (541), acid-base balance (316), EMP debris removal/endocytosis (313, 524), and apoptosis (318). To date, many of the molecular mechanisms involved in ameloblast-directed enamel maturation remain unclear (320). However, in the past decade there have been significant contributions to the literature highlighting the importance of ion transport and pH regulation during enamel maturation (reviewed in Refs. 125, 320, 410).

Although crystal growth takes place during both the secretory and maturation stages, it is during the maturation stage that the crystals greatly expand in width and thickness, giving enamel its characteristic durability and hardness (541). To add complexity during the maturation stage, ameloblasts change morphology in a unique series of modulations (cyclical changes) between a ruffle-ended (RA) appearance and a smooth-ended (SA) appearance in coordinated groups, appearing as bands of similar morphology across the circumference of the crown in an oblique fashion (466, 622). SA waves appear at ~8.5-h intervals in rat incisors, and these ameloblasts change after 2 h into RA cells, reforming their characteristic cell specializations at the distal border (545). On average, the surface of a rat incisor in any histological section shows ~70% of maturation ameloblasts in the RA phase and ~20% of maturation ameloblasts in the SA phase (466). Transitional cells can also be identified (268). RA cells are characterized by a distinct distal striated or ruffled border (468). RA cells are cytoplasmically polarized with a large concentration of mitochondria proximal to the ruffle-border and supranuclear Golgi complex (268). Intercellular spaces are noticeable along the lateral region of RA cells, but these cells are tightly bound by junctional complexes at their apical (distal) ends (167, 240, 403, 466), limiting the movement of small molecules into the enamel space. RA cells are also associated with increased endocytotic functions (313, 403, 498). In contrast, SA cells show a complete absence of the distal ruffled border (501). SA cells contain many lateral cytoplasmic projections, and they are bound at their basal ends by tight junctions whereas the apical ends of the cells may have incomplete/leaky or absent junctional complexes (240, 313, 318, 403, 504, 536, 541). It is believed that this dynamic permeability pattern allows bidirectional diffusion of small molecules into and out of the enamel via intercellular spaces (269, 541).

To briefly summarize the distinct roles of RA and SA maturation-stage ameloblasts, RA cells with their ruffled apical membrane likely have greater capacity to transport ions into and away from the enamel organ, and also to endocytose the EMP debris. SA cells with incomplete junctional complexes may allow for intercellular movements of fluids that may in turn contribute to the neutralization of pH in the enamel matrix (403). Although SA cells show little endocytotic activity (403), clathrin-coated vesicles and endocytotic activity have been identified in both RA and SA cells (499, 500, 505).

The RA to SA modulations play a role in pH regulation and bicarbonate transport, which differ at each stage (316, 541, 581). Ameloblasts associated with the $Ca^{2+}$ chelator glyoxal bis-2-hydroxyanil (GBHA) showed SA morphology under a light microscope, indicating that neutral-alkaline conditions dominate at this stage. Alternatively, it has been proposed that extracellular pH conditions modulate the RA to SA transitions (64). Others have shown that $Ca^{2+}$ entry to the enamel increased during the RA stage (467).

Recent immunohistochemical analyses have reported a number of differences in certain protein localizations between RA and SA ameloblasts. These include the anion exchanger AE2 (a member of the *SLC4* gene family) that is differentially localized at the lateral or the basal part of the lateral membrane of primarily RA cells, and in the same location but to a lesser extent in SA cells (269). The expression of carbonic anhydrase-2 (CA2), an enzyme that is involved in the local production of bicarbonate, is upregulated in RA cells (269, 342). Protein subunits of the V-type ATPase proton pump are fairly evenly distributed in the cytoplasm of SA cells, but most highly concentrated at the apical membrane of RA cells (269, 342, 495). These data emphasize the greater capacity of RA cells to transport ions, and to influence and control changes in the extracellular pH during enamel maturation, although this is likely a simplified portrayal of the functions performed by each cell type.

## C. Crystal Structure of Apatite

Calcium ($Ca^{2+}$) and phosphate ($PO_4^{3-}$) ions are only sparsely soluble in water and thus precipitate at rather low concentrations as a crystalline or amorphous solid (671). Under physiological conditions, apatite has the lowest solubility among the calcium phosphate minerals and is therefore the most chemically stable mineral phase. Consequently, apatite constitutes the inorganic component in all sound mineralized tissues in vertebrate animals (120).

In saturated aqueous calcium phosphate solutions with physiological range of pH (6.0 to 7.4), precipitation of stoichiometric hydroxyapatite (Hap) can occur according to the following reaction (*Equation 1*)

$$10Ca^{2+} + 6HPO_4^{2-} + 2H_2O \rightarrow Ca_{10}(PO_4)_6(OH)_2 + 8H^+ \quad (1)$$

Precipitation of one mole of Hap will result in the release of eight protons, thus acidifying the solution and requiring active pH regulation by ameloblasts as will be described below.

The unit cell (the simplest repeating unit) of Hap corresponds to the chemical formula $Ca_{10}(PO_4)_6(OH)_2$ (289). Its crystal lattice has hexagonal symmetry and comprises $PO_4^{3-}$ tetrahedrae coordinated with $Ca^{2+}$ ions **(FIGURE 4)**. There are two types of $Ca^{2+}$ positions in the Hap-lattice, of which Ca (2) is unique as it forms channels that allow anions to move along the c-axis of the apatite crystal **(FIGURE 4)**. Hydroxyl ions are able to diffuse and be replaced by other ions such as fluoride ($F^-$), carbonate ($CO_3^{2-}$), or chloride ($Cl^-$) from aqueous solutions. This makes apatite composition highly adaptable to its solution environment, which is critical to its properties in biological apatites. Apatite crystals in bones and teeth are far from being stoichiometric. Instead, they are rich in defects and usually calcium-deficient (120, 667). To maintain electron neutrality upon calcium depletion, phosphate groups are protonated ($HPO_4^{2-}$) and/or phosphate groups are replaced with $CO_3^{2-}$. Carbonate ions can also replace two hydroxyl groups along Ca (2) channels. The chemical reactions below describe the formation of a calcium-deficient carbonated apatite (*Equation 2*) and a calcium-deficient carbonated hydroxyapatite (*Equation 3*)

$$9Ca^{2+} + 6HPO_4^{2-} + CO_3^{2-} \rightarrow Ca_9(PO_4)_4(HPO_4)_2(CO_3) + 4H^+ \quad (2)$$

$$18Ca^{2+} + 10HPO_4^{2-} + 2CO_3^{2-} + 4H_2O \rightarrow Ca_{18}(PO_4)_8(HPO_4)_2(CO_3)_2(OH)_4 + 12H^+ \quad (3)$$

Carbonate substitutions for phosphate ($PO_4^{3-}$) or hydroxyl ions ($OH^-$) affect the ideal crystal structure of apatite and lower its symmetry, resulting in lower binding energies and ultimately increase the chemical solubility of the mineral phase (332). Carbonated apatite is therefore much more susceptible to acidic dissolution and dissolves at pH around 5, which is readily produced by cariogenic (caries-producing) bacteria. In contrast, $F^-$ fit perfectly between Ca (2) triangles and stabilize the hexagonal symmetry and crystal lattice. Exchange of $CO_4^{3-}$ for $F^-$ therefore lowers the solubility by at least three orders of magnitude, and fluoroapatite can withstand a pH as low as 4 without dissolution. This partly explains the high benefit of fluoride supplements in toothpastes and drinking water for caries prevention and erosion reduction in teeth (393, 451, 671).

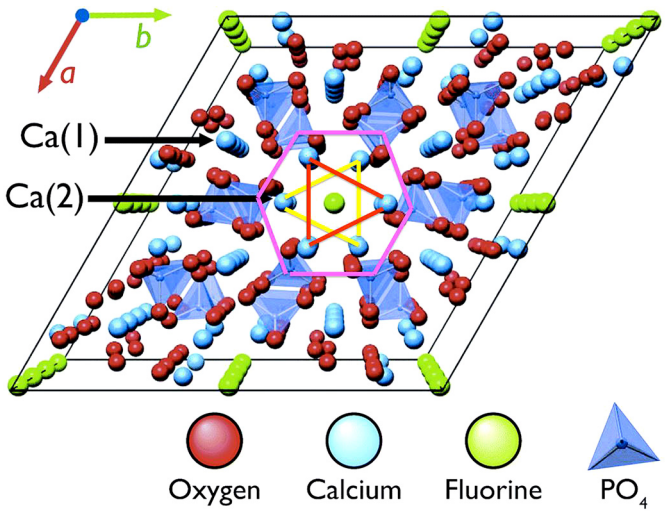


**FIGURE 4.** Crystal structure of calcium phosphate apatite shows hexagonal symmetry. Two types of calcium sites are indicated, with Ca (2) sites in triangular configuration (yellow and red lines) creating channels along which ions can move (green). Anions (green) such as $OH^-$, $Cl^-$, $CO_3^{2-}$, or $F^-$ can fill sites in the channels. $F^-$, the smallest of these species, can fit within the triangle created by the Ca sites forming the channel; larger anion species deform the lattice significantly when occupying these sites, leading to a reduced lattice stability and therefore higher solubility.

## IV. EVOLUTIONARY ORIGINS OF ENAMEL AND ENAMEL MATRIX PROTEINS

The evolution of enamel is tied to the appearance of teeth and in general with the development of skeletonized structures. Early vertebrates during the Cambrian period show mineralized structures in the oropharynx that were used for feeding, and which are likely related to the origins of teeth, although they were composed of a carbonated material dissimilar to enamel (286). These structures are comparable to pharyngeal teeth found in modern fish (teleosts). Some modern fish (e.g., hagfish and lampreys) show structures resembling teeth, but these are cartilaginous and, unlike true teeth, derive from ectomesenchyme rather than ectoderm (244). Modern vertebrate teeth may have evolved from oropharyngeal denticles or from dermal denticles such as those found in sharks. However, shark teeth (and their dermal denticles) are formed from enameloid, which contains a large component of collagen, unlike true enamel. Reptiles also have teeth, but unlike mammals, reptilian enamel lacks a rod/interrod (prismatic) structure. Mammalian enamel has a highly organized prismatic structure that forms as described in section III*B* **(FIGURE 5)**. The prismatic or rod/interrod architecture seen in mature mammalian enamel can be appreciated in **FIGURE 6**. Mammalian enamel is rather heterogeneous in its microstructure, even within the same species. For example, rodent incisor and molar microanatomy differ, which has been ascribed to different functional requirements by each tooth type during mastication (185, 297, 354, 472, 473). Also of note is that with the introduction of interdigitating rods, which are angled to apatite fibers in the interrod enamel, crack resistance is increased (198), while fracture toughness of prismatic mammalian enamel is about double that of prismless reptile enamel (663).

The origin of the main structural proteins secreted by ameloblasts, AMELX, AMBN, ENAM, and the relatively newer amelotin (AMTN) and odontogenic, ameloblast-associated protein (ODAM), dates back to over ~600 million years ago (532). They are all members of the secretory calcium-binding phosphoprotein (SCPP) gene family derived from the ancestral *SPARC/Osteonectin* gene (482). ENAM appears to be the original protein from which the others, in-

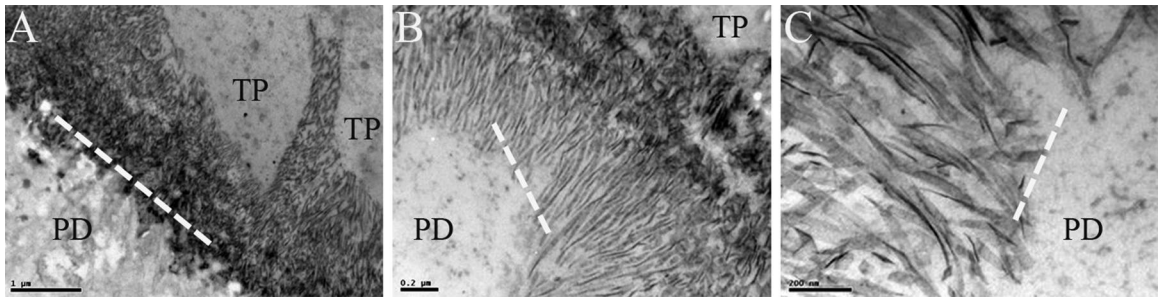


**FIGURE 5.** Transmission electron micrographs (TEM) of early enamel development. TEM images of the mouse showing early enamel formation. *A*: ameloblast Tomes' process (TP; right) surrounded by enamel crystallites seen adjacent to the dentino-enamel junction (DEJ; broken line) that is located diagonal to frame, and with pre-dentin (PD; unmineralized dentin) to the left. Scale = 1 $\mu$m. *B*: initial enamel crystallite formation for the first 1–1.5 $\mu$m (shown in panel). TP, PD, and DEJ (broken line) are also identified. Scale = 0.2 $\mu$m. *C*: this panel shows a higher magnification of the DEJ area very early in enamel crystallite formation. Scale = 200 nm.

cluding AMBN, are derived. AMELX, the most abundant matrix protein, arose via gene duplication from AMBN (532). Additional information on the evolution of SCPP genes, and their role in tooth formation, can be found in a number of recent papers (104, 169, 170, 280–288, 532–534).

The human genome contains two amelogenin genes, one located on the X chromosome (*AMELX:* locus Xp22.3-p22.1) and the second on the Y chromosome (*AMELY:* locus Yp11) (325, 492, 496). Both the X and Y amelogenins are expressed in males; however, the X-chromosome-derived amelogenin is expressed at significantly higher levels (492). It is estimated that >90% of the amelogenin gene transcripts in male primates are derived from the X chromosome (103, 428, 492). The close proximity of *SPARCL1, AMBN, ENAM, AMTN*, and *ODAM* on the human chromosome 4q13-q21.1 has resulted in detailed investigation of this chromosome region by enamel researchers as it hosts genes responsible for inherited dental diseases (94, 165, 228, 561, 641). This region contains many of the genes responsible for the mineralization of hard tissues (285, 287, 288, 532, 534).

For significance, since amelogenin is expressed on both the X and Y chromosome in some mammals such as primates, cow, pig, horse, and sheep (175, 209, 256, 325, 400, 448, 462, 492), the nucleotide differences between the X- and Y-derived amelogenins allow for quick, PCR-based, sex determination in utero, or in forensic medicine (129, 159, 428, 611).

## V. ENAMEL MATRIX PROTEINS AND WHAT WE HAVE LEARNED FROM ANIMAL MODELS

### A. Overview

The most abundant of the secreted structural proteins of the enamel matrix are amelogenin (AMELX), ameloblastin (AMBN), and enamelin (ENAM) (228, 428, 430). While some studies have suggested that AMELX (112, 196, 211) and AMBN (152, 557) are expressed in nondental tissues in nonpathological states, there is wide consensus that all three proteins are most highly expressed in the enamel organ. Moreover, Amelx (178), Ambn (164), and Enam (230, 231) mutant mice show pathologies that appear to be limited only to the dental enamel, suggesting that the levels and biological roles of these two proteins in nondental tissues are negligible. Our current understanding is that AMELX, AMBN, and ENAM are the major secreted products of secretory-stage ameloblasts, while AMTN and ODAM are secreted by maturation-stage ameloblasts.

It has been estimated that amelogenin proteins contribute ~90% of the enamel organic matrix, based on both protein analyses and unbiased RNA and protein profiling (67, 305, 364, 475, 530, 591). AMBN composes ~8–10% of the enamel organic matrix (369), while ENAM appears to be present in trace amounts only (66, 369). These figures for relative protein levels also appear reasonable when looking at mRNA levels; for example, mRNA profiling from a rat enamel organ demonstrated that 20.0% of all gene transcripts were to Amelx and 2.9% of gene transcripts were to Ambn (305, 364). At the time of this study the "ameloblastin" mRNAs identified were to an unknown gene, and designated as only as clones Y224, Y243, and Y275 (364), but further characterization resulted in the cloning of a full-length Ambn transcript, and the subsequent naming of this gene (305).

Knockout or mutant mouse models for all these enamel-specific genes have been generated and all appear healthy and are fertile. The enamel of *Amelx* (180), *Ambn* (164), and *Enam* (230) mutant mice are severely impacted, showing disorganized enamel; these mice require a soft diet because the occlusal surfaces of their teeth wear easily. The *Amtn* and *Odam* mutant mice show either only a mild

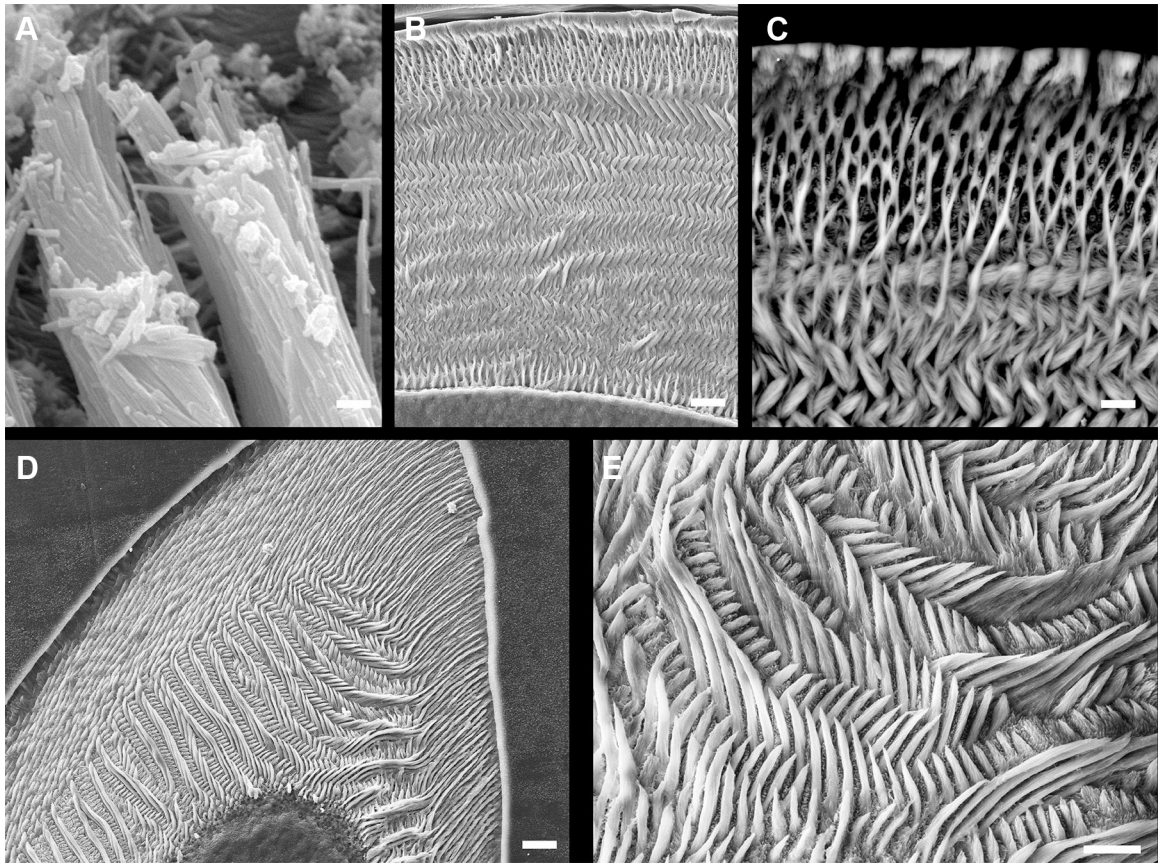


**FIGURE 6.** Scanning electron (SE) micrographs of mouse enamel. *A*: bundles of single Hap crystals can be seen forming tubular structures known as enamel prisms or enamel rods. Each ameloblast is responsible for the formation of one enamel rod. These rods are the basic structural units of enamel. The architectural patterning of the rods forms the microstructure. Scale = 2 $\mu$m. *B*: enamel microstructure in a cross section of a mouse incisor. Scale = 10 $\mu$m. *C*: close up of outer incisor enamel in back-scattered SE mode showing the change in organization of the rods as the Tomes' process is lost (top of image). At this point, the enamel microstructure loses the rod-interrod patterning. Scale = 2 $\mu$m. *D*: mouse molar enamel (same animal as in *A*) showing the complexity of its microstructure which reflects the movement of ameloblasts and how different tooth types may vary in microstructure. Inner enamel reflects strong decussation (crossing of ameloblasts along various planes as they move) but in the outer enamel (top of image) ameloblasts move in straight paths. Scale = 10 $\mu$m. *E*: close up of inner enamel showing the strong decussation of the enamel rods in this tooth. Scale = 10 $\mu$m. (All SE images by Timothy G. Bromage and Rodrigo S. Lacruz.)

phenotype (*Amtn*-null mice) (402) or no apparent phenotype (*Odam*-null mice) (623).

## B. Amelx Mutant Mice

Amelogenin (AMELX), first identified in 1983, has been the most studied of the enamel-specific proteins (553, 555). It was the first enamel-specific cDNA subclone to which a protein sequence could be identified (555), and specific antibodies against mouse Amelx were subsequently generated (537). AMELX assembles into multimeric units in vitro and possibly the extracellular space (151) that are widely referred to as "nanospheres" (51, 58, 79, 124, 136, 137, 148, 345, 493, 588). A number of three-dimensional models have been proposed for the assembly of amelogenin into nanospheres (124, 136, 138, 212, 389), and while these models vary in detail, all suggest that nanospheres are of the order of 20–30 nm in diameter and may contain ~12 (136) or more (124) amelogenin monomers.

A conventional targeted knockout approach produced *Amelx*-null mice, which had a dramatic phenotype limited to the enamel organ (178). While a thin layer of enamel was observed in these mutant mice, it lacked any prismatic architecture, and the thickness was ~20% (i.e., 1/5) that of normal enamel (177, 178). In addition, in the *Amelx*-null mice, the dimensions of individual enamel crystallites were smaller than in wild-type enamel (652).

Another feature of amelogenin gene products is the large number (>15) of alternatively spliced isoforms that have been identified based on mRNA profiling (26, 516, 528, 529, 653). Of these spliced isoforms, the most abundant in

**A**

MGTWILFACLLGAAFAMPLPPHPGSPGYINLSYEVLTPLKWYQSMIRQPYPSYGYEPMGGWLHHQI 65

"A" domain

IPVLSQQHPPSHTLQPHHHLPVVPAQQPVAPQQPMMPVPGHHSMTPTQHHQPNIPPSAQQPFQQPF 130

QPQAIPPQSHQPMQPQSPLHPMQPLAPQPPLPPLFSMQPLSPILPELPLEAWPATDKTKREEVD 196

"B" domain

**B**

MPLPPHPGSPGYINLSYEVLTPLKWYQSMIRQP#PLSPILPELPLEAWPATDKTKREEVD 59

**FIGURE 7.** Mouse amelogenin (Amelx) protein-protein interacting domains. The protein sequence of the most abundant Amelx isoform is shown in *A* (REFSEQ accession number NM_009666.4). The mature protein (after the signal peptide shown in red is removed) contains 180 amino acids and is frequently referred to as mouse M180 isoform. Domains A and B were defined using the yeast two-hybrid system. Interacting domains A and B are identified and underlined. The leucine-rich amelogenin peptide (LRAP) is the second most abundant amelogenin produced as a product from alternative splicing and is shown in *B* (without its signal peptide). This LRAP isoform contains the $NH_2$-terminal 33 amino acids and the COOH-terminal 26 amino acids of the sequence in *A*. This LRAP isoform has been referred to as either LRAP, or the mouse M59 isoform. The "#" indicates the spliced union of the $NH_2$- and COOH-terminal regions in LRAP.

mice is referred to as M180, followed by the leucine-rich amelogenin peptide (LRAP) (176, 179, 326, 391, 529, 656) **(FIGURE 7)**. Transgenic mice overexpressing either M180 or LRAP in the enamel organ have been generated and bred with the *Amelx*-null mice, and this has resulted in varying degrees of rescue of the enamel deficiencies, partially restoring both the prismatic architecture and crystallite dimensions (177, 652). M180 knockin mice show a normal enamel function and architecture as observed by electron microscopy (EM); however, the mechanical properties of the enamel were altered such that the hardness increased by 7%, and the fracture toughness decreased by 22% when analyzed by microhardness tests (556). Hardness has been considered as a surrogate for wear resistance, while toughness is a measure for fracture resistance (154, 556, 634). This M180 knockin mouse suggests that the inclusion of the other amelogenin spliced isoforms may contribute to the overall functional and structural properties of enamel under normal circumstances.

Additionally, a number of transgenic mouse lines have been created to study the disruption of amelogenin self-assembly. Prior studies using the yeast two-hybrid system have shown that the M180 amelogenin proteins self-assemble, thanks to the amino-terminal 42 residues (the so-called A domain) interacting either directly or indirectly with a 17-residue domain (the so-called B domain) in the carboxy region (427) **(FIGURE 7)**. Transgenic mice bearing mutant amelogenin transcripts that lack either the A or B domain show disruptions to the crystallite orientation and prismatic architecture (126, 425, 431).

The primary conclusion from all of the amelogenin mouse models is that while amelogenin is not responsible for hydroxyapatite (Hap) nucleation or growth, it is essential for normal and controlled enamel crystallite growth and crystallite orientation on the nanoscale, and rod/interrod or prismatic architecture on the microscale (652).

### C. Ambn Mutant Mice

Ameloblastin was first identified around 1996 by three independent research groups, and given the names ameloblastin (305), amelin (72), and sheathlin (227). Current nomenclature refers to this gene as ameloblastin (AMBN). An ameloblastin (Ambn) mutant animal model was generated in 2004, and at the time was thought to be a complete knockout/silencing of any ameloblastin expression (164). However, it was later shown that this line expressed only a truncated version of ameloblastin missing exons 5 and 6 (624). This mouse model did have a severe dental phenotype (164). The ameloblasts differentiated to polarized secretory ameloblasts but then quickly detached from the enamel matrix and lost their polarity, resulting in the termination of amelogenesis and the failure to produce any enamel. These data suggest that ameloblastin plays a role in cell-matrix attachment and the maintenance of the ameloblast differential state (164). These *Ambn*-mutant mice have been bred with a transgenic mouse that overexpresses ameloblastin in the enamel organ, and the resulting enamel appears normal (90), suggesting a complete or near-complete rescue of the enamel phenotype.

### D. Enam Mutant Mice

Enamelin was first identified in 1997 (226), and the first publication of the *Enam*-null mice, referred to as the *Enam* knockout NLS-lacZ knockin, was in 2008 (230). In addition to achieving a complete elimination of any Enam expression, the targeting vector included a lacZ ($\beta$-galactosi-

dase) reporter with a mouse nuclear localization signal (NLS) (229, 230). *Enam*$^{-/-}$ mice showed no "true enamel" (230) based on various imaging techniques (e.g., radiography, microcomputed tomography, and light and scanning electron microscopy); instead, a "thin, highly irregular, mineralized crust covered the dentin on erupted teeth" (230).

### E. Amtn Mutant Mice

Amelotin (AMTN) was first identified in 2005 (255). *Amtn*-null mice have also been generated and studied recently (402). In these *Amtn* mutant mice, the enamel prismatic structure appeared unaltered; however, enamel mineralization was delayed, resulting in hypomineralization of the inner enamel and structural defects in the outer enamel (402).

### F. Odam Mutant Mice

The odontogenic, ameloblast-associated gene (ODAM) was identified in 2006 and initially referred to as APin (385). *Odam*-null mice have recently been generated (623). This mutant line is a complete knockout with a functional insertion of the β-galactosidase gene with an amino-terminal nuclear localization signal (NLS-LacZ). In these mutant mice, the spatiotemporal expression of β-galactosidase relates directly to (i.e., copies) the Odam expression pattern, which is limited to late secretory-, transition-, and maturation-stage ameloblasts, and is also expressed in the cells of the dental junctional epithelium (JE) (386, 406, 623). The JE is the region where the oral epithelium unites with the tooth surface, thus forming a unique barrier or seal between the oral cavity and the underlying tissues (403, 407). These *Odam*-null mice have no observable enamel phenotype (623), but as they age there is an increased inflammatory infiltrate in the JE, and an apical down-growth of the JE typical of periodontal disease (407, 623). These findings suggest that ODAM expression in the dental JE helps maintain the integrity of the JE attachment (407, 623). It is therefore tempting to speculate that pathological mutations to Odam may increase the risk of periodontal disease.

## VI. ENAMEL MATRIX ASSEMBLY

### A. Amelogenin Self-Assemblies

The enamel matrix is composed primarily of three secreted structural proteins: AMELX, AMBN, and ENAM (359, 389, 430). AMELX has a single phosphorylated serine located at the amino-terminal region (149, 578). AMBN and ENAM are both glycoproteins (72, 153, 226, 305, 658) and likely account for reports indicating the existence of proteoglycans in the forming of the enamel matrix (77, 184, 190). Biglycan (BGN) has also been shown to be expressed in secretory ameloblasts, but at barely detectable levels (189). There have also been reports that phospholipids contribute to the enamel matrix (459, 514, 515). However, if these phospholipids are indeed extracellular (186), then it is unclear what role they play in amelogenesis.

Likely because amelogenin was the first enamel matrix protein cloned, and because of its abundance, most of the literature related to enamel matrix assembly has focused on amelogenin self-assembly properties (147, 148, 390, 423, 674). Transmission electron microscopy (TEM) of mouse, bovine, and hamster dental enamel tissues showed electron-lucent spherical structures/aggregates of (presumably) amelogenin that aligned with long axes of developing enamel crystallites (147, 148). In vitro studies confirmed the formation of amelogenin nanospheres with 10- to 15-nm radii (20–30 nm diameter) using native or recombinant amelogenins in aqueous solutions (150, 151). Further studies by Paine et al., using the yeast two-hybrid system and a series of systematic amino-terminal and carboxy-terminal deletions of a full-length Amelx, suggested that self-assembly of amelogenin occurs via two well-defined domains referred to as the amino-terminal "A" domain and the carboxy-region "B" domain (427, 431) **(FIGURE 7)**. Such Amelx-Amelx binding domains would allow for the formation of nanospheres containing clusters of amelogenins, and hydrophobic and hydrophilic constraints could help define their shape and size. It is because of these self-assembly properties of Amelx and its hydrophobic character that it is only sparingly soluble in physiological conditions, and requires extreme pH conditions to show significant dissolution (340, 427, 523). In vitro, using recombinant amelogenins, self-assembly into nanospheres is a phenomenon that can occur at physiological or near-physiological pH values (pH range of 7.2–7.7) (40, 630, 636), but only in the absence of $Ca^{2+}$ and $PO_4^{3-}$ (212, 361, 362, 493) **(FIGURE 8)**. Nanospheres disassemble in the presence of mineralizing ions and appear to attach to apatite surfaces as monomers or dimers (162, 212, 361, 362). It also seems that as soon as amelogenin is secreted into the extracellular space in vivo, it is processed by MMP20 into specific cleavage products with unknown functions. Ultimately amelogenin is severely hydrolyzed by KLK4 and the resulting peptide debris is removed from the enamel matrix through endocytosis (29, 348). There are reports that in vitro amelogenin may form microribbons a few micrometers in width and hundreds of micrometers long (124, 388, 389), although this remains controversial (123, 124).

While the general consensus has been that the supramolecular structures in the enamel matrix are critical to controlling the organization of apatite crystals in enamel (150, 338, 430, 431, 527), recent observations of nanoribbons developed from full-length AMELX proteins with the ability to self-organize challenge this paradigm **(FIGURE 8)**. Ameloge-

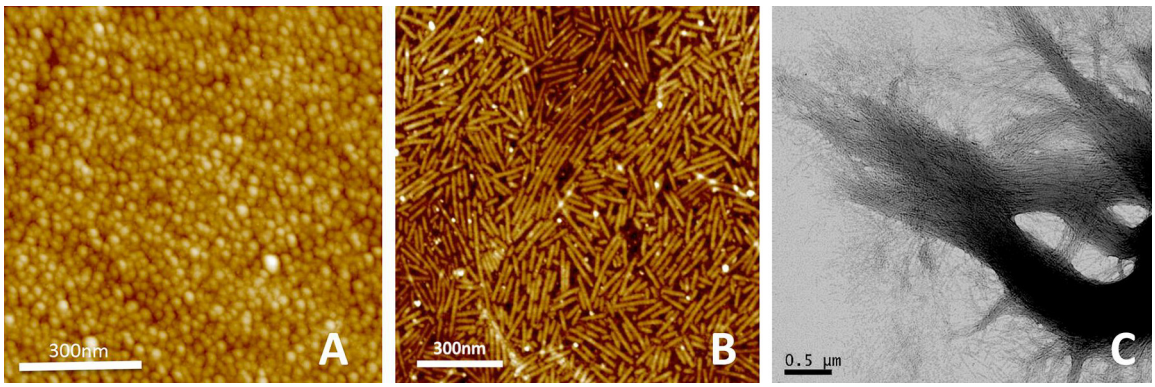


**FIGURE 8.** Micrographs of amelogenin assemblies. Micrographs of recombinant full-length amelogenin protein assembled in vitro without calcium and phosphate ions (*A*) and with addition of $Ca^{2+}$ (30 mM) (*B*) and $PO_4^{3-}$ (22 mM) (*C*). In the absence of mineralizing ions, amelogenin forms nanospheres with diameters between 15 and 30 nm (*A*). With the addition of calcium and phosphate ions, nanospheres disintegrate and at pH between 4.0 and 6.5 transform into nanoribbons over periods of days (*B*). Ribbons measure ~17 nm in width and are ~3–4 nm thick. The ribbons have a tendency to align themselves into parallel arrays and form bundles (*C*) that can reach several 10 s of micrometers in length. [*C* from Martinez-Avila et al. (361). Copyright 2012 American Chemical Society.]

nin nanoribbons from recombinant human proteins form over a period of days. They are ~17 nm wide and align parallel to each other, maintaining a 5- to 20-nm space between them (212, 361). Bundles of aligned AMELX nanoribbons up to 100 $\mu$m in length develop over a period of 1–3 wk, producing an organic scaffold that mimics the appearance of apatite nanofibers in an enamel rod (70, 361, 362). This suggests that aligned AMELX nanoribbons may be a precursor to enamel rods and provide a template for guided apatite crystal growth (198). Interestingly, self-assembly of AMELX into nanoribbons is dependent on $Ca^{2+}$ and $PO_4^{3-}$. These mineralizing ions build ion bridges between AMELX dimers and thus stabilize the formation of anti-parallel $\beta$-sheets comparable to amyloid fibers known from neurodegenerative diseases (70, 493). This in vitro observation is in agreement with X-ray diffraction analyses of developing enamel, showing evidence of cross-$\beta$ structures characteristic of amyloids (182, 266, 442, 446). The presence of a functional amyloid was further supported by positive staining for Congo Red in enamel of $Klk4^{-/-}$ mice (70). High-resolution images are often dominated by filamentous structures that have been attributed to the early apatite crystal ribbons that develop during secretory stage but remain present even when the specimen is demineralized (596).

A major difficulty in deciphering the exact mechanisms of protein-controlled mineralization lies in the transient nature of the enamel matrix, which is rapidly processed soon after secretion and is almost completely removed by the end of the mineralization process. Further analysis of the biological structures in the developing matrix and revision of current models of amelogenin-guided mineralization are warranted. Models of amelogenin nanosphere formation and nanosphere-crystallite interaction have been widely used in the enamel research community and have been reviewed by others (387). A comparison of the nanosphere model (662) to a model based on new data on in vitro nanoribbon assemblies and how they might guide crystallite growth is presented in **FIGURE 9**.

## B. Other Protein-Protein Interactions of the Enamel Matrix

Ameloblastin has been suggested to be a cell adhesion molecule that can influence ameloblast growth and differentiation (164). Observations from *Ambn*-mutant mice showed that in the absence of a fully functional Ambn protein, presecretory ameloblasts could differentiate into polarized secretory cells, but these cells quickly detached from the forming enamel matrix to form multicell layers that occasionally (~20% of mice) proceeded to form odontogenic tumors (164). Some reports have also suggested AMBN may act as a signaling molecule or a growth factor (38, 152, 587, 670). Using a bacterially generated recombinant human AMBN, Wald et al. (612) have shown that, similar to AMELX, AMBN under certain nonphysiological conditions can form flat ribbon-like supramolecular structures (width and thickness of ~18 nm and 0.34 nm, respectively) and of varying length. It should be noted that eukaryotic-generated AMBN is present as a glycosylated protein, but this naturally occurring glycoprotein cannot be produced from bacteria; the self-assembly property seen in vitro may not recapitulate in vivo events. Of note also is that earlier studies by Paine et al. (422), using the yeast two-hybrid system, suggested that a eukaryotic-generated mouse Ambn had no self-interacting properties, questioning further whether Ambn ribbons may be present in vivo. These data shed some light on the role of AMBN in enamel formation, but the exact role remains unclear. What we do know is that Ambn mutant mice fail to produce any enamel, or indeed

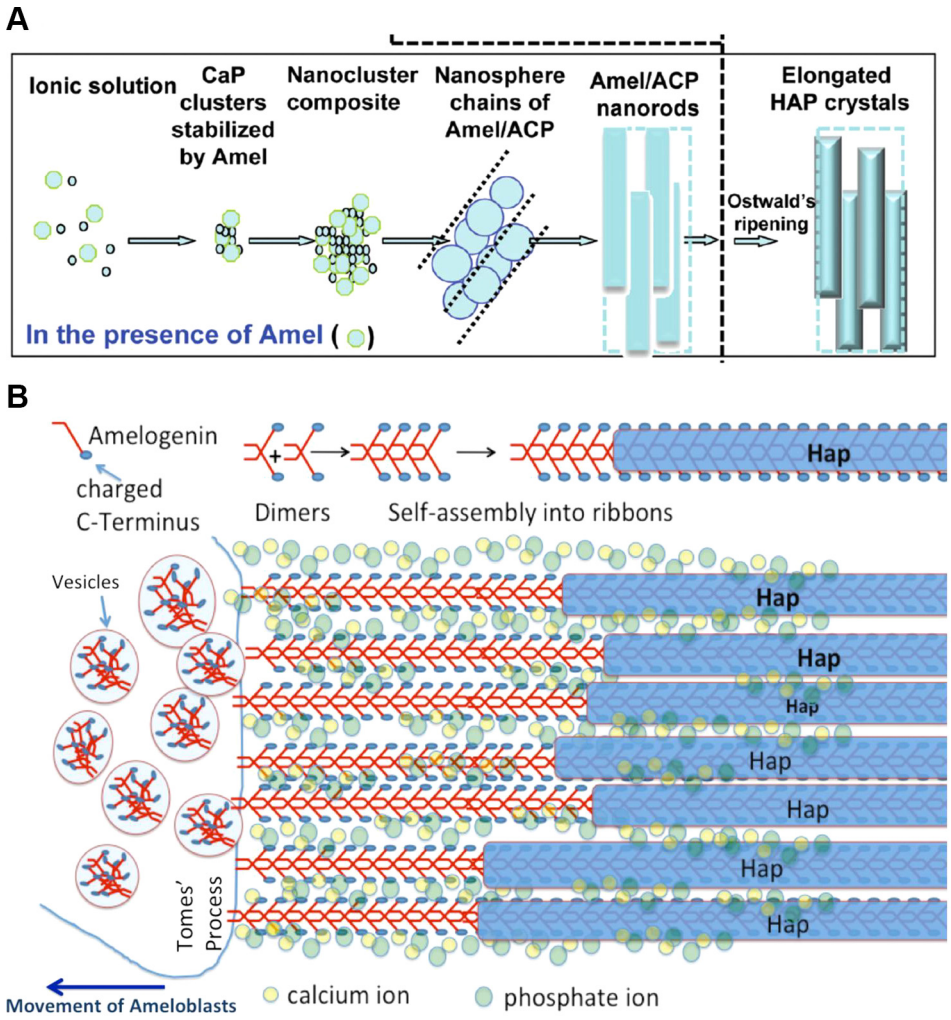


**FIGURE 9.** Proposed models of amelogenin-directed growth of apatite mineral during secretory stage of amelogenesis. Comparison of two models of amelogenin-directed growth of apatite mineral during secretory stage of amelogenesis. *A*: nanosphere model. Amelogenin protein is secreted into the extracellular space and assembles into nanospheres. Amelogenin stabilizes prenucelation clusters of calcium phosphates. Nanospheres align into chainlike structures along which amorphous calcium phosphate develops and through a ripening process transforms into crystalline Hap. Nanospheres act as spacers, as originally proposed by Fincham et al. (150). [*A* from Yang et al. (662), copyright 2010 American Chemical Society.] *B*: nanoribbon-directed crystal growth. Amelogenin is secreted from vesicles, possibly in the form of antiparallel dimers. Nanoribbon assembly is triggered by formation of ion bridges across dimers with $Ca^{2+}$ and $PO_4^{3-}$. Dimers are added to the existing amelogenin ribbons as soon as they are exocytosed and thus elongate the ribbons as the ameloblasts migrate away from the mineralization front. Hap mineral forms at a narrow distance from the cell membrane in form of thin ribbons that develop on the backbone of the protein ribbons. Full-length amelogenin does not induce mineral formation directly, and the mechanism of mineral nucleation is not known. Interaction with other non-amelogenin molecules and/or the processing by MMP20 may be required for guided growth of apatite onto amelogenin ribbons.

any mineralized tissue, from the enamel-producing cells (164).

A number of studies have investigated self-assembly properties of the different secreted enamel proteins and protein-protein interactions between them. As discussed above, using the yeast two-hybrid system, amelogenin-amelogenin interactions could be demonstrated (422) and interacting domains identified (427). In a paper by Holcroft and Ganss, also using the yeast two-hybrid system and cloned bovine enamel matrix protein sequences, it was shown that full-length AMTN could self-assemble, as could full-length ODAM, and ODAM could also interact directly with AMTN and AMELX (220). There is also one report, using in vivo-derived porcine enamel proteins, that suggested amelogenin interacts with the 32-kDa fragment of ENAM (659). *Enam*-null mice lack the formation of a mineralized layer, supporting the notion that ENAM may be critical to apatite nucleation (230). Similar to mineralizing collagen fibrils in bone and phosphoproteins in dentin, a mechanism of protein interaction can be suspected where an acidic or phosphorylated protein may act as a carrier, delivering min-

eral ions to nucleation sites on self-assembled protein scaffolds. In a similar fashion, ENAM may interact with AMELX supramolecular structures. However, work on the protein-protein interactions of the less abundant enamel matrix proteins remains in its infancy.

There have been two reports of either AMELX or ENAM interacting with members of the collagen family (111, 614), suggesting that AMELX interacts with COL1A1 (111) and COL5A3 (614), and that ENAM interacts with COL2A1 and COL5A1 (614). Collagens are a product of odontoblasts and present in dentin, while the amelogenins are a product of ameloblasts and found in the enamel. It has been shown that type IV collagen is expressed directly at the DEJ (371), and that type 1 collagen (341) and type VII (372) collagen pass from the dentin through the DEJ and into the enamel. The significance of such amelogenin-collagen or ENAM-collagen interactions, or the extension of dentin collagens into the inner enamel matrix, could help explain the significance and unusual structural and biomechanical properties of the DEJ (249, 371, 430, 633, 635). The DEJ is a unique structure of the tooth that functions to hold the enamel onto the dentin surface (34, 75, 166, 403, 635). While the DEJ is a critical component of the tooth, the biology and developmental mechanisms involved in its formation are not well understood and are beyond the scope of this review.

## VII. ENAMEL-SPECIFIC PROTEOLYTIC ENZYMES

### A. Overview

Although a number of proteinases have been described in amelogenesis, including matrix metallopeptidases 2, 3, and 4 (MMP2, MMP3, and MMP9) (187, 199), chymotrypsin C (CTRC) (322) and cathepsin C (CTSC, also known as dipeptidyl peptidase I) (601), most of the information on proteinase expression during amelogenesis relates to MMP20 (formerly known as enamelysin) and kallikrein-related peptidase 4 (KLK4) (27, 30, 235, 348). MMP20 expression dominates during the secretory stage (28, 29, 56, 233), and KLK4 expression during the maturation stage (29, 232, 233, 348). Two noteworthy reviews on enamel proteinases have been published (25, 348). Autosomal recessive forms of nonsyndromic amelogenesis imperfecta (AI) have been documented for mutations associated with both MMP20 and KLK4, and mutant animal models attest to the important role both enzymes play in amelogenesis.

### B. Mmp20 Mutant Mice

*Mmp20*-null mice were first reported in 2002 (71), and work on this animal model continues today (454, 521). These mice have a severe phenotype, with the enamel being hypoplastic and delaminating from the dentin soon after the tooth erupts into the oral cavity (71). The ameloblast morphology is clearly disrupted early during secretory-stage amelogenesis, and the normal rod-interrod pattern of fully formed enamel is also disturbed (71). Thus it is clear that MMP20 is critically important not just for proper enamel formation, but also for the integrity of the DEJ. Amelogenins form the bulk of the enamel matrix (29, 103, 428, 492); thus AMELX is seemingly an obvious substrate for MMP20 in the developing enamel. Multiple in vitro studies, using in vivo-derived or recombinant proteins, have confirmed that AMELX is indeed a major substrate of MMP20, suggesting this is also the case in vivo during amelogenesis (344, 488, 524, 656). MMP20 has also been shown to effectively cleave AMBN in vivo (91, 257). It is unclear today how the third major enamel protein, ENAM, is processed and degraded post-secretion (25, 657).

### C. Klk4 Mutant Mice

*Klk4*-null mice were first reported in 2009 (525) and showed an enamel hypomaturation phenotype (normal thickness but poorly mineralized) that, post-eruption, either quickly abrades, or fractures just above the DEJ (525). This suggests that KLK4 plays no role in the integrity of the DEJ. Although a rod-interrod morphology could be observed in *Klk4* mutant mice, individual enamel crystallites failed to pack tightly with neighboring crystallites, and gave the impression that they "spilled out" following controlled enamel fracture (525). KLK4 has broad substrate specificity and readily degrades the known enamel matrix proteins (348, 399). KLK4 expression in the mouse incisor starts during the transition stage and continues throughout the maturation stage; thus mice that do not express Klk4 retain much of the enamel organic matrix, resulting in hypomineralized enamel (525, 660).

## VIII. RESORPTIVE ACTIVITIES IN AMELOGENESIS

### A. Overview of Endocytotic and Other Resorptive Processes

Endocytosis can be either receptor mediated or fluid phase (4, 541), with receptor-mediated endocytosis most typically defined as a clathrin-dependent process (4). This is in part because the endocytotic cellular uptake of extracellular proteins frequently involves clathrin assemblies and clathrin adaptor protein (AP) complexes that are generally activated and assembled by a membrane-bound receptor-mediated event such as ligand binding. Fluid-phase endocytosis involves multiple, relatively low-energy and nonspecific, cellular activities that allow for the uptake of fluids from the extracellular environment, and do not appear to be initiated by receptor-ligand activities (9, 119, 291). Fluid-phase en-

docytosis involves a number of molecular activities of clathrin-independent pathways, including the CLIC/GEEC endocytotic pathway, the arf6-dependent pathway, flotillin-dependent endocytosis, micropinocytosis, circular doral ruffles, phagocytosis, and trans-endocytosis (119). As the molecular mechanisms for each of these fluid-phase activities are being better defined, it has become clear that they have some specificity as to what molecules and extracellular debris they each target for cellular uptake (9, 49, 119, 291, 327, 404).

## B. Early Concepts of Resorptive Activities of the Enamel Organ

Endocytotic activities in amelogenesis have not been extensively studied. However, on the basis of EM observations, papers of the late 1970s and early 1980s described coated pits and/or vesicles on the cytoplasmic surface of the apical pole of ameloblasts in both the secretory (160, 499, 500) and maturation stages [including both the smooth-ended (505) and ruffle-ended (498) phases] of amelogenesis. Clathrin was first discovered in 1976 associated with coated vesicles (443); thus the coated pits and vesicles described in these earlier enamel studies likely represent the clathrin-coated vesicles that are recognized today (313). Other earlier studies relating to the active and passive resorptive functions of ameloblasts have recently been discussed by Lacruz et al. (313), and the reader is referred to this paper for a historical perspective and relevant citations.

## C. Adaptor Protein Complex 2 (AP-2) Endocytosis in Amelogenesis

Earlier EM observations in the 1970s and 1980s of coated pits and/or vesicles forming on the inner surface of ameloblast cells (160, 498–500) were suggestive of clathrin-associated endocytotic activities being a feature of amelogenesis, and more recently published immunolocalization and real-time PCR data indicate the same conclusion (313). Lacruz et al. (313) clearly established that active, AP-2 mediated, clathrin-dependent endocytosis occurs during amelogenesis and that during amelogenesis the greatest expression of AP-2 and clathrin is noted at the apical poles of maturation ameloblasts.

AP-2-mediated endocytosis is a clathrin-dependent activity and is widely considered to be receptor-mediated (324, 584–586). Known receptors include transferrin receptor (Tfrc), the low-density lipoprotein receptor (Ldlr), and the epidermal growth factor receptor (Egfr) (50, 368, 394). When comparing the transcriptomes enamel organ cells in the rat incisor, it was noted that Tfrc transcripts increased significantly (~60-fold) from the maturation to the the secretory stage (319, 664). It has also been shown that the iron transport protein transferrin (Tf) is a potential protein binding partner of Enam (614). Although significantly more work is required in this field, it is reasonable to suggest that the removal of the enamel matrix debris could occur through direct protein-peptide interactions between Tf and the EMP debris, resulting in an EMP/Tf/Tfrc-initiated AP-2 endocytotic pathway (313). This scenario is feasible as multiple protein partners of Tf, in addition to enamelin, have already been identified; these include the GABA(A) receptor-associated protein (Gabarap) (195), leukocyte cell-derived chemotaxin 2 (Lect2) (82), insulin-like growth factor 1 and 2 (Igf1 and Igf2) (566), and insulin-like growth factor binding proteins 1–6 (Igfbp1-6) (629).

Lamp1, Lamp2, and Cd63 have individually and collectively been suggested as possible membrane-bound protein receptors initiating the AP endocytotic pathway by direct interaction with the various AP complexes (43, 50, 223, 444, 480, 483). LAMP-AP complex formation and the subsequent trafficking of Lamp1, Lamp2, and Cd63 from the cell membrane to the lysosome is initiated by a direct protein-protein interaction between a lysosomal targeting motif (GYXX∅; where X is any amino acid and ∅ is a bulky hydrophobic amino acid) located at the cytoplasmically contained carboxy terminus of all three LAMPs (Lamp1, Lamp2, and Cd63), and the mu/$\mu$ subunit of AP-2 (Ap2m1) (113, 223, 248, 324, 452, 483). Zou et al. (675) have previously shown that Amelx, through a proline-rich region (PLSPILPELPLEAW), interacts directly with Lamp1, Lamp2, and Cd63 through an extracellular 20-amino acid domain with high homology common to all three LAMP proteins. In Cd63 this binding domain is contained within the externalized "EC2" domain (675). This proline-rich Amelx binding region is hydrophobic, largely disordered, and accessible to the external environment (675). The externalized EC2 domain of Cd63 also interacts with full-length Enam and Ambn (614, 675); thus it is feasible that the LAMP proteins could act as ameloblast receptors for AP-2, clathrin-dependent endocytosis, but this needs further investigations. A schematic of the two scenarios presented for EMP initiated endocytosis is presented in **FIGURE 10**.

Another established pathway for the uptake of Tf located at the apical pole of some polarized epithelia (e.g., the small intestine, renal proximal tubule, visceral yolk sac, and placental cytotrophoblasts) is through the megalin-dependent cubilin-mediated endocytotic pathway (87, 88, 304, 384, 489), although to date there are no published data suggesting that this endocytotic pathway is active in the enamel forming cells (313, 318, 319).

## D. Summary

Recent data indicate that AP-2-mediated, clathrin-dependent endocytosis is a prominent feature of maturation-stage amelogenesis (313), and while other resorptive processes,

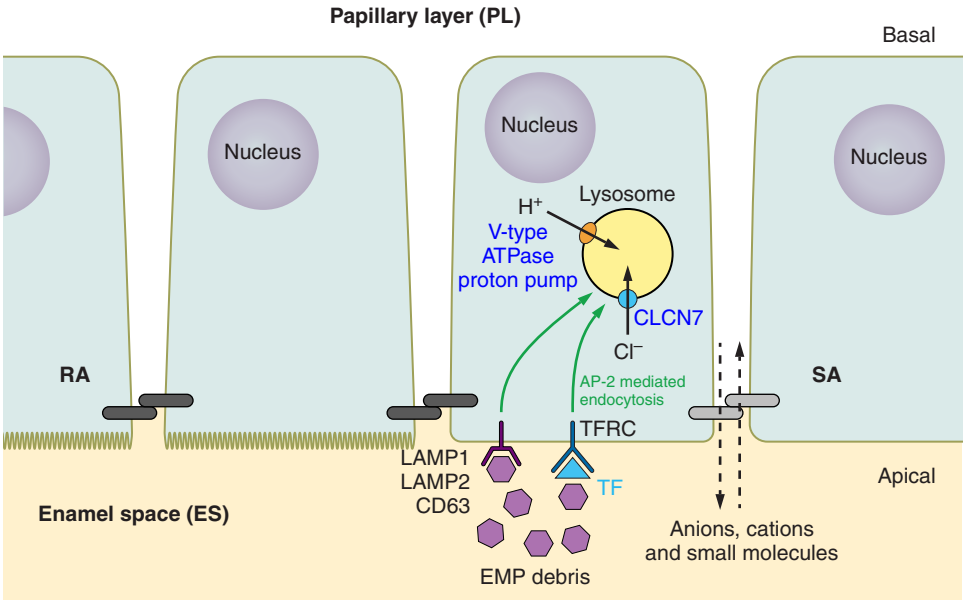


**FIGURE 10.** Hypothetical model for the initiation of AP-2, clathrin-mediated endocytosis of the degraded enamel matrix protein (EMP) debris in maturation ameloblasts. It is apparent that greater endocytotic activity is seen in the maturation ameloblasts, when compared with secretory ameloblasts. Endocytosis is likely a feature of both the ruffle-ended (RA) and smooth-ended (SA) ameloblasts. The figure illustrates that the endocytotic uptake may be initiated by direct receptor-ligand interaction, such as the EMP debris interacting directly with LAMP1, LAMP2, or CD63. Alternatively, EMP debris may bind to another EMP protein, such as TF, and then this complex may bind to the TFRC to initiate the uptake of the extracellular enamel matrix peptides. A dark gray double capsule represents a tight junctional complex at the apical region of RA, and a light gray double capsule represents a "leaky" junctional complex at the apical region of SA.

such as micropinocytosis, may also be active in amelogenesis, they are yet to be investigated at the molecular level. The process of enamel matrix removal is a significant topic worthy of investigation because the failure to properly remove the organic enamel matrix results in a hypomineralized enamel that is mechanically inferior and wears and fractures rapidly, as seen in *Mmp20*-null and *Klk4*-null mice (71, 525, 660).

## IX. IMPORTANCE OF pH MAINTENANCE

### A. Regulation of pH

Nucleation events leading to the development of enamel crystals require the formation of a stable cluster of ions that can organize and grow (127). For every unit cell of hydroxyapatite crystal, approximately eight $H^+$ protons are released into the extracellular environment, thus lowering the pH in the immediate surroundings (541). This calculation is based on the stoichiometric equation shown in *Equation 1* (above) (523, 541). To modulate the effects of these free protons, enamel cells use active bicarbonate ($HCO_3^-$) transport systems to regulate the extracellular pH (269, 316, 317, 429, 541, 542). Here we describe changes in pH during amelogenesis and review key components of the $HCO_3^-$ transport system.

### B. Changes in pH During Amelogenesis

Much of the available data on pH in enamel derive from chemical tools that in some cases are outdated. For example, injections of [$^{14}$C]dimethyl-oxazolidinedione (DMO), a compound that concentrates in areas of high pH, showed higher extracellular pH ~8.0–8.5 in the more matured areas of mouse enamel than in less mineralized areas where pH ~7.3–7.4 (352). This difference was associated with increased calcification as $Ca^{2+}$ binding to protein matrix generates high local pH, which in turn allows for the accumulation of $PO_4^{3-}$ and $OH^-$ ions enabling the initiation of crystal nucleation (352).

Using GBHA, Takano et al. (581) showed a pattern of red bands on the surface of matured enamel marking alkaline conditions. GBHA positively stained around bands of SA cells (581). More recently, Sasaki et al. (497) used three different pH indicator solutions to assess pH changes in unerupted whole bovine incisors after the removal of the enamel organ and showed alternating bands of acidic to neutral extracellular pH along the crown. These acidic and neutral zones were examined by suspension in distilled deionized water to measure pH using a glass-electrode pH meter. A number of halved incisors were stained with GBHA. Results from each technique were consistent showing extracellular pH conditions ranging from acidic (pH 5.5–6.0) to neutral zones (pH ~7.2) with the acidic zone located in the occlusal half of the crown. It was hypothesized that the acidic conditions observed related directly to the release of protons by the forming crystals (497).

Analysis of developing bovine incisors with the use of pH indicator solutions identified four different and alternating stages of acidic and neutral pH along the crown (577). The purified protein content from each stage showed that neutral zones of enamel were characterized by the presence of full-molecular-weight forms of AMELX and ENAM, whereas acidic zones showed low-molecular-weight forms of both proteins. The composition of crystals changed be-

tween the alternating acidic-neutral stages based on ratios ($Ca^{2+}$ + $Mg^{2+}$)/P with erupted enamel having a higher ratio than either the acidic or neutral unerupted enamel (577). Moreover, freeze-dried strips of rat incisor enamel organ isolated from various stages of amelogenesis were assessed based on a distance from the tooth apex (using a molar reference line) and provided relatively uniform pH during secretory stage with values clustering around ~7.23, whereas maturation stage samples showed greater variability in extracellular pH values ranging from near-neutral to weakly acidic conditions (pH values 6.2–7.2) (544). Recently, the immersion of rodent incisors with the enamel organ exposed in pH indicator solutions has become common practice to determine the presence of alternating bands of RA and SA cells. Low pH is associated with RA cells.

Taken together, these studies suggest that pH in enamel oscillates from neutral to acidic during maturation-stage amelogenesis, whereas in secretory stage the pH remains near the physiological levels.

## C. Regulation of Extracellular pH

Ameloblasts use a number of acid-base transport mechanisms to modulate extracellular pH. These include bicarbonate transporters, carbonic anhydrases, and chloride channels as well as other ion pumps and exchangers. As we have previously discussed (316), the acidification of the extracellular microenvironment associated with the release of $H^+$ is a complex event.

## D. Proteins Involved in pH Balance in Enamel

### *1. Bicarbonate transporters*

Two genes of the *SLC4* (solute carrier 4) gene family, the anion-exchanger (AE2) encoded by *SLC4A2* and the electrogenic bicarbonate cotransporter (NBCe1) encoded by *SLC4A4*, are expressed in enamel cells and associated with pH modulation (61, 258, 269, 317, 350, 429). Both are membrane proteins that play an important role in regulating intra- and extracellular pH in eukaryotic cells (460). In addition, five members of the SLC26A gene family (SLC26A1, SLC26A3, SLC26A4, SLC26A6, and SLC26A7), all membrane-bound ion exchangers (or $HCO_3^-/Cl^-$ exchangers), have recently been described as being expressed at the apical pole of maturation ameloblasts (60, 259, 665).

The first reports of AE2 and NBCe1 expression in enamel cells were by Paine et al. (429) and Lyaruu et al. (350). In the study by Paine et al. (429), NBCe1-B (the alternatively spliced B isoform of NBCe1) expression in ameloblasts was found primarily at the basolateral pole of maturation-stage ameloblasts, whereas AE2 showed a more apical distribution. Other reports have confirmed the localization of these proteins, albeit showing variation in the localization of the different NCBe1 isoforms, with some isoforms being found primarily in the adjacent enamel papillary layer cells (258, 269). It has also been suggested that NBCe1 expression might be associated with the developmental stage of ameloblasts (258). Paine et al. (429), using the immortalized ameloblasts-like cell line LS8, found that the mRNA expression levels of both NBCe1 and AE2 changed depending on extracellular pH.

Paine et al. (429) observed AE2 in the apical pole of secretory ameloblasts in frozen-unfixed tissues, while Lyaruu et al. (350) and Yin et al. (665) reported a basolateral localization in maturation ameloblasts, leaving open the question of AE2 function (527). If AE2 is localized at the basolateral pole rather than at the apical end of the cell, the latter being closest to the enamel-forming zone, the $HCO_3^-$ that has moved out of the basolateral cell membrane needs to find its way to the enamel across tight apical cell junctions to perform its putative pH buffering role. This path of movement is not necessary if AE2 is localized to the apical end (see below). However, a number of studies suggest that NBCe1 likely plays a role in mediating basolateral $HCO_3^-$ import with apical bicarbonate secretion mediated by AE2 or other $HCO_3^-$ export pumps/channels/exchangers, working in tandem to buffer the proton load generated by apatite formation (258, 269, 316, 320, 429). More recently, a number of members of the anion exchanger SLC26A gene family (SLC26A1, 3, 4, 6 and 7; $HCO_3^-/Cl^-$ exchangers) have been localized to the apical membrane of maturation ameloblasts (259, 665), and this large number of exchangers with similar or identical molecular activities ensures abundant opportunity for $HCO_3^-$ export to the enamel matrix during enamel maturation.

Mutations to *SLC4A2* and *SLC4A4* result in enamel abnormalities in humans and/or mice (117, 172, 251). Lyaruu et al. (350) showed that mice lacking two of the five AE2 spliced variants (AE2a/b) have abnormal enamel in incisors, but this defect is less severe in molar teeth. There are three variants of NBCe1 (NBCe1-A, NBCe1-B, and NBCe1-C) with mutations occurring in all variants. The incisors of mice lacking NBCe1 have a chalky white appearance and fracture easily (171, 317). In patients with loss of NBCe1 function, enamel defects have been described as showing white chalk-like spots (251). Mouse models deficient for AE2 or NBCe1 both showed decreased mineral content in their enamel (65, 317, 350).

The function and role of ameloblasts as $HCO_3^-$ transporting cells, and in particular that of the $Na^+/HCO_3^-$ cotransporter NBCe1, have been enhanced by in vitro studies using the ameloblast-like cell line HAT7 (52). In these studies, HAT7 cells were manipulated to form a polarized two-dimensional culture system from which transepithelial elec-

trical resistance, immunocytochemistry, and microfluorometry data could be collected. Polarized HAT7 cells expressed NBCe1, a number of anion exchangers already discussed (Slc4a2/AE2, Slc26a4/pendrin and Slc26a6/Pat1), and Cftr. Active transcellular vectorial basolateral-to-apical $HCO_3^-$ transport was recorded, and this vectorial movement of $HCO_3^-$ was dependent on $Na^+$ cotransport (52). One of the conclusions from this study was that "a basolateral $HCO_3^-$ transporter, most probably NBCe1/SLC4A4, has an important role in $HCO_3^-$ uptake." A similar conclusion was also published almost a decade earlier by Paine et al. (429) who, based on immunolocalization data, stated that "NBCe1 is expressed on the basolateral membrane of secretory ameloblasts" and that "AE2 and NBCe1 are expressed in ameloblasts in vivo in a polarized fashion, thereby providing a mechanism for ameloblast transcellular bicarbonate secretion in the process of enamel formation and maturation." Both studies by Bori et al. (52) and Paine et al. (429) strongly indicate that the basolaterally expressed $Na^+/HCO_3^-$ cotransporter NBCe1 is either fully or partially responsible for the import of $HCO_3^-$ into polarized ameloblasts, and is most active during maturation-stage amelogenesis (317, 318).

### 2. Chloride transport

Chloride transport in epithelial cells is an important regulator of salt and water (513). Chloride channels in the apical surface of the cells' plasma membrane allow the flow of $Cl^-$ across the cell membrane via an electrochemical gradient. In cystic fibrosis (CF), an autosomal recessive disease affecting 1 in ~3,000 births, the cystic fibrosis conductance transmembrane regulator protein (CFTR), which regulates water and chloride transport, is disrupted (122, 558, 564, 565). Chloride ($Cl^-$) therefore accumulates inside the cells, leading to abnormal and thick mucus secretion in the airways. Mutations to the CF gene also affect the dentition (21, 23, 63, 76, 96, 143, 445, 646, 650).

Mineralized enamel contains ~0.0065 mol/g of $Cl^-$, totaling 0.23% of enamel by dry weight (128). The role of $Cl^-$ in forming enamel crystals is poorly understood, but it has been suggested that it may act as a transmitter of charge (412) and as a regulator of pH (59). The first reports on abnormal enamel in CF patients were inconclusive of cause and effect as CF patients typically received heavy doses of antibiotics (such as tetracycline, which can disrupt amelogenesis), masking the etiology of these enamel defects (646, 650). Wright and co-workers reported a series of studies of enamel deficiencies in *Cftr*-deficient mice (21, 572, 646, 650), noting that during late secretion/early maturation, their ameloblasts become cuboidal cells and prematurely transition to a squamous epithelial stage (294). In *Cftr*-deficient mice, the microstructure and thickness of crystallites appeared normal but showed a more porous appearance in TEM, and overall, the enamel was softer and less mineralized with reduced $Cl^-$ levels compared with controls (21, 646, 650). The enamel defects of *Cftr*-deficient mice could result from a loss of the ameloblasts' capacity to process extracellular matrix proteins during the maturation stage. Incisors of *Cftr*-deficient mice showed yellow surface stainings when immersed in pH indicator solution, pointing to acidic pH in the transition and maturation zones of enamel (572). The enamel of the incisor teeth of *Cftr*-deficient mice wears rapidly (59). It should be noted that these data on enamel deficiencies of *Cftr*-null mice are derived from the analysis of incisors, whereas molar teeth from the same mice did not show alteration in enamel, a fact that remains unexplained (59, 572). A porcine model for CF was also studied by our group, reporting that molars of *CFTR*-null and *CFTR*-delta F508 mutant pigs showed hypomineralized enamel, with the most severe pathology in the *CFTR*-null pigs (76). The CFTR delta-F508 mutation is the most common one found in human CF patients.

Bronckers et al. (59) have shown that Cftr is localized to the apical end of maturation-stage ameloblasts. This localization pattern places Cftr in close proximity to the enamel zone and is thus consistent with a putative role as a modulator of enamel matrix pH, as noted above, buffering the protons released during crystal formation (63). Bronckers' group (63) and others (320) proposed that Cftr might be associated with releasing $Cl^-$ into the enamel zone as part of an electrogenic exchange for $HCO_3^-$. A number of exchangers could be involved in this process including anion exchanger 2 (AE2) and members of the SLC26A gene family, all of which can transport $HCO_3^-$ in exchange for $Cl^-$ (259, 665). It has been proposed that $K^+$ and $Na^+$ accumulate in enamel when $Cl^-$ is low, which suggests the possibility that $Na^+$-$K^+$- $Cl^-$ cotransporters (NKCCs) are also important during amelogenesis, although no direct evidence of NKCC expression in ameloblasts is currently available (61). Besides the presence of CFTR and its role in enamel formation, other $Cl^-$ channels have been identified in ameloblasts, including the $Ca^{2+}$-dependent $Cl^-$ channels (197, 313, 320, 631). In ameloblasts a number of $Cl^-$ channels are expressed, and in addition to $Cl^-$ export, likely play a role in endocytosis (313). For example, Clcn7/ClC7 is expressed on the lysosomal membrane in ameloblasts (313).

### 3. Carbonic anhydrases

Carbonic anhydrases (CAs) are enzymes that catalyze the reversible hydration of carbon dioxide to bicarbonate (*Equation 4*)

$$CO_2 + H_2O \overset{CA}{\leftrightarrow} HCO_3^- + H^+ \quad (4)$$

CAs also participate in pH homeostasis, $CO_2$ and $HCO_3^-$ transport, and bone resorption (539, 573). Many of the abundant CA isozymes are expressed in enamel cells but differ in cellular distribution (e.g., Refs. 315, 463). CA2 is the most widely expressed isozyme localized to the cyto-

plasm of many cells (316). Ameloblasts express CA2, as reported in a number of studies (118, 269, 298, 463). The earliest of these reports was made in cell homogenates from adult rat incisors (298), later confirmed by histochemical analysis of unerupted hamster molars which found CA2 signals in more mature ameloblasts (118). A similar expression pattern was later reported in rat incisors by Reibring et al. (463). RA cells were more strongly stained for CA2 than SA cells (269). The similar expression of $H^+$-ATPase prompted interpretations that RA cells pump $H^+$ ions into the enamel, acidifying the microenvironment in a similar fashion to that described in osteoclasts (269), but this remains untested.

Carbonic anhydrase CA6 appears to be the only CA isozyme that is secreted from cells (433, 441, 539). Complementary DNA (cDNA) library screens of rat incisor enamel-forming cells first identified a fragment that matched CA6, further characterized by RT-PCR and Northern blot analysis (549). We have since confirmed the high expression of CA6 in enamel cells (321), and a recent study found high expression of CA6 in maturation-stage ameloblasts (463). Smith et al. (549) have proposed that the function of CA6 in maturation might be associated with local buffering, supplying bicarbonate ions or recycling excess levels of carbonic acid.

In a survey of mRNA expression of all CA isozymes in mouse enamel cells, Lacruz et al. (315) identified that in addition to CA2 and CA6, other isozymes, notably Car11-15, were also expressed. More recently, Reibring et al. (463) investigated the localization of these isozymes and reported the expression of CA4, CA9, and the related isozyme CARP11 in the distal-ruffled border of RA cells, and a widespread localization in SA cells CA13 appears to be associated with the lysosomal pathway, as evidenced by similar punctate distribution of this protein with the lysosomal marker LAMP1 in ameloblasts. It should be pointed out, however, that presently human mutations or animal models deficient for CAs showing enamel defects are poorly described.

## E. Modeling pH Regulation in Enamel

It is widely recognized that during the formation of enamel Hap crystals, protons ($H^+$) are released in the microenvironment (523, 541); the export of protons at the apical ends of ameloblasts by the action of the V-type ATPase proton pump may contribute to this (269, 342, 495). Accumulation of $H^+$ may negatively impact the formation of additional crystals by lowering local pH, thus resulting in the dissolution of crystal surface structure. It has been shown that during the secretory stage of enamel formation, the extracellular pH values are close to neutral and crystal growth at this stage is limited (541, 544). This neutral pH value during secretory stage amelogenesis has been attributed to the abundance of matrix proteins which modulate and/or buffer against changes in pH (541). However, during the maturation stage, pH values are acidic, associated with increased expansion of crystals and concomitant release of $H^+$. Thus $H^+$ must be removed from the enamel zone to restore physiological pH conditions. It should be highlighted that a number of proteins associated with pH homeostasis increase in expression during the maturation stage; these include NBCe1, AE2, CFTR, multiple SLC26A gene family members, and many CAs (318, 664). This marked increase in gene and protein expression of certain ion exchangers, pumps, and enzymes has been linked to an increase in their activities to counteract the rise in $H^+$ observed during maturation stage amelogenesis.

A generalized model for pH maintenance in maturation stage must thus take into account the removal of $H^+$. Bicarbonate can perform this function by absorbing these $H^+$. In this model $HCO_3^-$ can be incorporated into the ameloblasts, via NBCe1 located at the basolateral membrane, and is released apically via exchange of $Cl^-$ facilitated by CFTR, AE2, and SLC26A family members. $HCO_3^-$ can also be produced via the function of CA6 in the extracellular domain combining $CO_2$ and $H_2O$. However, as previously highlighted by Simmer and Fincham (523), carbonic anhydrase activity is not an effective system as this chemical reaction, generating $HCO_3^-$ via CA enzymes, removes only one $H^+$ locally.

The cytosolic localization of CA2 suggests that $HCO_3^-$ can also be produced by the ameloblasts (269, 595). The removal of intracellular $H^+$ might be mediated by the antiporter NHE1, a $Na^+/H^+$ exchanger (269). NHE1 was expressed along the plasma membrane of secretory ameloblasts, as well as both RA and SA cells (269), likely removing $H^+$ into intercellular spaces. As noted earlier, if AE2 is localized along the lateral membrane, the transport of $HCO_3^-$ into that space might then buffer the removal of $H^+$ (61, 269). At the apical pole of RA cells, the V-type ATPase proton pump also moves $H^+$ into the enamel space, contributing to acidification of this region (269, 342, 495), and a number of anion exchangers of the SLC26A gene family (SLC26A1/SAT1, SLC26A3/DRA, SLC26A4/pendrin, and SLC26A6/PAT1) are also located at the apical pole of RA cells (259, 665). The coexpression of both the proton pump and bicarbonate channels responsible for the extrusion of $H^+$ and $HCO_3^-$ suggests extracellular pH is very strictly regulated during the process of enamel maturation (269). It is thus apparent that in enamel maturation ameloblasts use multiple mechanisms to lower and raise extracellular pH as needed.

The cyclical changes from RA to SA cell morphology also bear on the capacity to modulate pH as described above. While a number of proteins already discussed differ in expression profiles between these two stages, the functional

interpretation of these differences is still limited. However, it has been suggested that this cycle allows changes in crystallization conditions to occur, which would impact the stability of crystals so that only the more stable would pass through each cycle (269).

## X. ION TRANSPORT

### A. Overview

Enamel is an almost fully mineralized tissue composed of a substituted hydroxyapatite (Hap) of primarily calcium ($Ca^{2+}$) and inorganic phosphate ($P_i$). Disruptions to Hap formation can result in hypomineralized (soft) enamel, which is more prone to acid attack and caries (135, 335, 637). Recent reports suggest that $Ca^{2+}$ and $HCO_3^-$, originating from the circulation and largely diffusing across the papillary layer, are actively transported into polarized ameloblasts through ion exchangers and pumps located at their basolateral membrane (320, 429). While passive paracellular ion movement may occur during amelogenesis (403, 540), recent reports clearly suggest that the active transcellular ion transport dominates the process of enamel formation and maturation (52, 60, 269, 316, 317, 320, 321, 350). The differences between active and passive transport pathways are illustrated in **FIGURE 11**. Intracellular CAs are also present in ameloblasts such that $HCO_3^-$ is generated within the cytoplasm (315, 316, 320, 595). Calcium (see below for $Ca^{2+}$ uptake) and $HCO_3^-$ ions are then transported across ameloblasts (409) and eventually extruded through a different series of ion exchangers and pumps located at the apical membrane to be delivered to the enamel matrix (234, 416, 615). Mutations in many of the ion exchangers associated with $Ca^{2+}$ and $HCO_3^-$ transport result in enamel pathology (117, 125, 171, 251, 314, 317, 350). These findings suggest that the enamel organ epithelium and associated $Ca^{2+}$ and $HCO_3^-$ transporters are critically important to enamel mineralization. While recent studies are starting to define $Ca^{2+}$ and $HCO_3^-$ transcellular transport in amelogenesis, there is scant information related to $P_i$ transport associated with amelogenesis. As-yet-unidentified $P_i$ ion channels are likely to be located on ameloblast plasma membranes, thus allowing for the transcellular transport of $P_i$.

### B. Bicarbonate

#### 1. Overview

In 1998, Smith (541) published a review paper on enamel maturation clearly making the case that buffering is an essential part of the process, and that bicarbonate ($HCO_3^-$) was the main buffering system used by ameloblasts. This was based primarily on the knowledge that cytoplasmic carbonic anhydrase 2 (CA2) was highly expressed during maturation, and significant expression was noted at the apical ends of ruffle-ended ameloblasts (RA) (595). It was felt that if large quantities of $HCO_3^-$ were produced in the cytoplasm, then one would expect membrane-bound "carrier/transporter proteins" (i.e., ion transporters) to regulate both intracellular and extracellular pH (541). During this time Wright and co-workers were examining the enamel pathologies seen in the CFTR mutant mice (21, 572, 646, 650) and proposed that CFTR, working in conjunction with a chloride/bicarbonate exchanger, and both located at the apical ends of polarized ameloblasts, were responsible

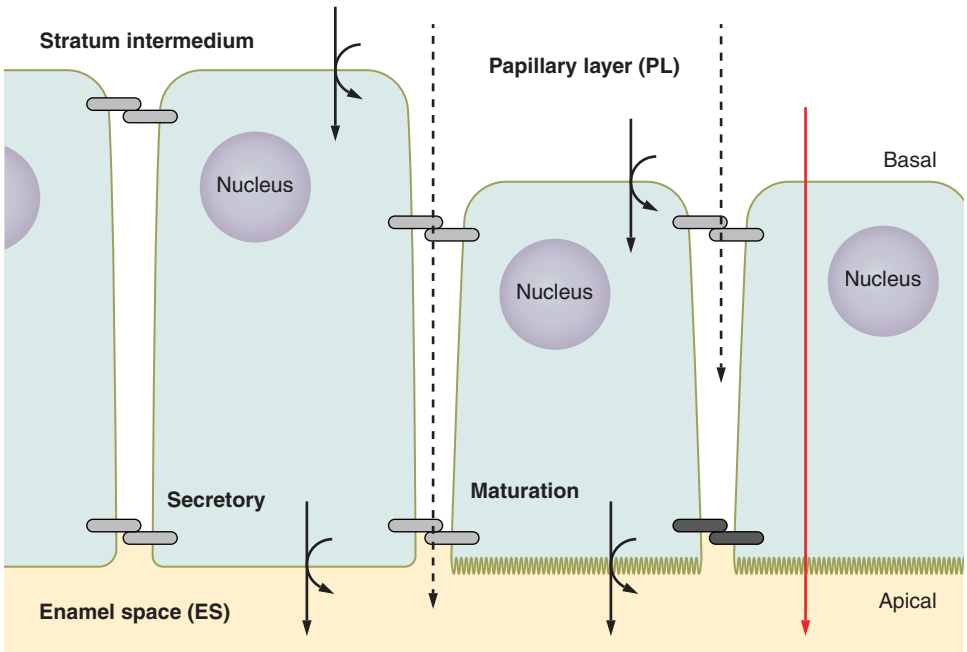


**FIGURE 11.** Modes of ion transport from the circulation at the basal (proximal) region to the enamel space beyond the apical (distal) pole of secretory and maturation ameloblasts. Black solid arrows indicate active transcellular transport involving ion transporters, channels, and pumps (curved arrows); black broken arrow indicates a passive paracellular/intercellular movement through "leaky" junctions (light gray double capsule) but not through tight junctions (dark gray double capsule); and a red arrow indicates a passive transcellular pathway. Dark gray double capsule indicates a tight junction at the apical region of maturation ameloblasts.

for the export of cytoplasmically generated or cytoplasmically located $HCO_3^-$ to the enamel matrix (572). Wright et al. (572) also suggested transcellular movements of $HCO_3^-$ were likely if a sodium bicarbonate cotransporter was located on the basolateral membrane of ameloblasts. In 2008, Paine et al. (429) identified the anion exchanger AE2 (SLC4A2) located at the apical ends of polarized ameloblasts, while the electrogenic sodium bicarbonate cotransporter NBCe1 (SLC4A4) could be identified at the basal pole of these same cells. More recent data however suggest AE2 is located on the basolateral membrane of maturation ameloblasts (269, 351, 665). The past decade has seen significant progress in identifying the genes and pathways involved in the buffering capabilities of ameloblasts and how $HCO_3^-$ enters the enamel space, summarized in **FIGURE 12**.

### *2. The enamel matrix buffering system*

The atomic structure of enamel crystals is a variation of a pure calcium/phosphate-based hydroxyapatite (Hap) lattice which incorporates other types of ions (i.e., carbonates); thus enamel can be referred to as a nonstoichiometric carbonated calcium Hap (188, 528, 668). Despite this clarification, enamel is most frequently identified as a Hap-based mineralized tissue, and as stated above, it has been calculated that approximately eight $H^+$ protons are released for every unit cell of Hap crystals formed in the extracellular environment. This generation of protons significantly lowers the enamel matrix pH (541, 544). These free protons may diffuse away from the matrix, but based on recently published data this seems unlikely. It appears that ameloblasts primarily use acid-base transport systems to regulate extracellular pH, with the bicarbonate buffer system being the primary (or perhaps the only) extracellular buffering mechanism that they employ (542). Neutralization of the increasingly acidic enamel environment is achieved with the generation of intracellular and extracellular $HCO_3^-$ through the action of CAs (see *Equation 4*) (118, 315, 316, 318, 523, 541, 549, 595), and by the active transport of blood-derived bicarbonate through specific ion channels (transcellular) (52, 259, 320, 350, 429, 665).

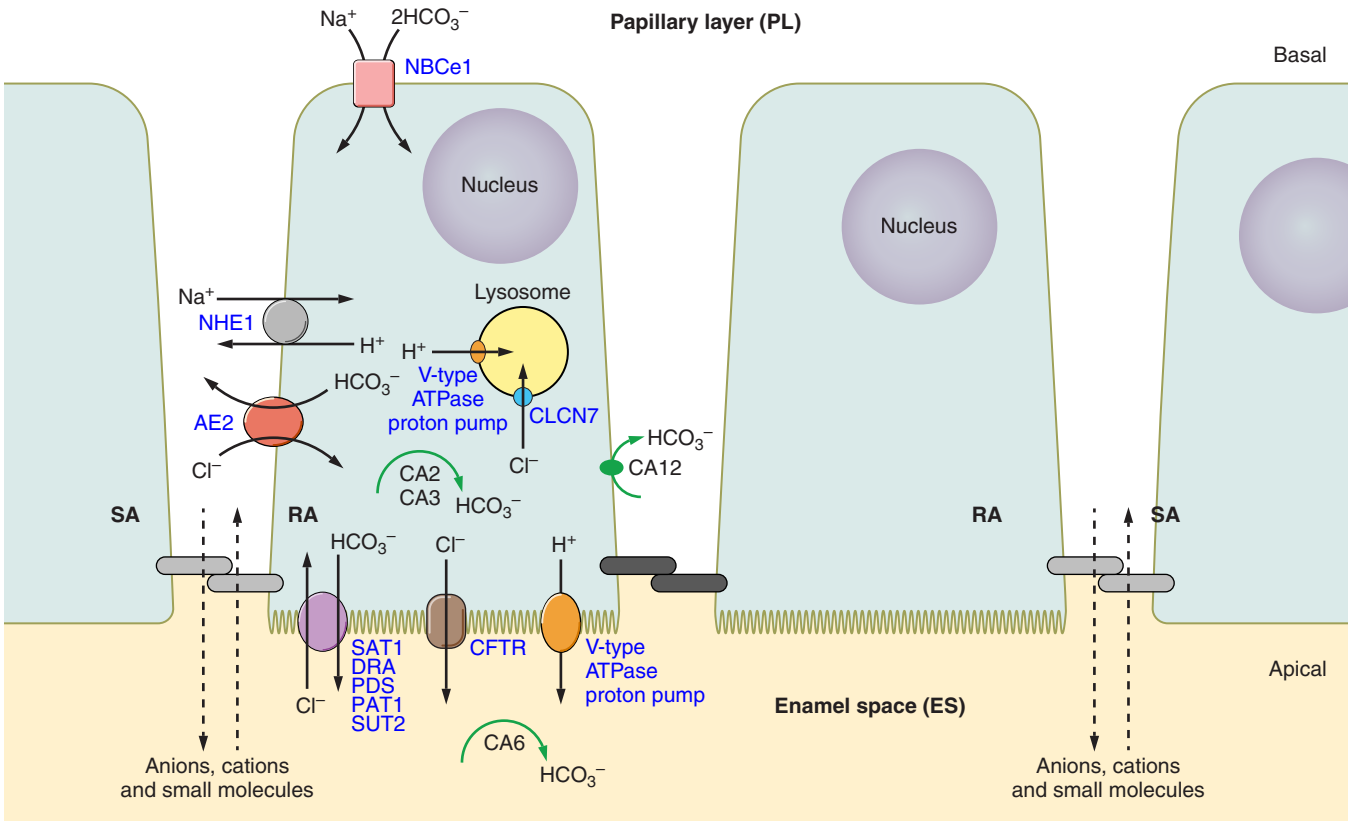


**FIGURE 12.** Generation and active transcellular movements of ameloblast-associated bicarbonate and associated ion movements during enamel formation. Ion transporters, channels, and pumps are identified either by their name or gene symbol. Nucleus (Nu) and lysosome (Ly) are identified. The transport pathways are identified in a ruffle-ended ameloblast (RA). Many of these channels have also been shown in secretory ameloblasts (not shown) and smooth-ended ameloblasts (SA) but at significantly lower levels of expression. A dark gray double capsule represents a tight junctional complex at the apical region of RA, and a light gray double capsule represents a "leaky" junctional complex at the apical region of SA. Black broken arrow indicates the movements of small molecules through leaky junctional complexes.

As described above, $HCO_3^-$ plays an important role in enamel formation (316). A number of CAs and $HCO_3^-$ transporters associated with enamel formation have been described recently. The most notable are CA2, CA3 (cytoplasmic), CA6 (secreted/extracellular), and CA12 (membrane bound) (118, 315, 316, 318, 549, 595). Membrane-bound CA12 is a type I membrane protein with a catalytically active enzyme domain located in the extracellular space (254, 598). Bicarbonate ion transporters identified in maturation-stage ameloblasts include the electrogenic sodium bicarbonate cotransporter SLC4A4 (NBCe1) and multiple anion exchangers; these are coded by the genes SLC4A2 (AE2), SLC26A1 (SAT1), SLC26A3 (DRA), SLC26A4 (pendrin), SLC26A6 (PAT1), and SLC26A7 (SUT1) (65, 258, 259, 350, 429, 665). The large number of molecules involved with either the synthesis or transport of $HCO_3^-$ in ameloblasts suggests that the entire process of pH regulation during enamel maturation is under tight molecular control.

### 3. The solute carrier (SLC) gene families

The solute carrier (SLC) gene series contains 52 families (SLC1 to SLC52) that include 395 unique transporter genes (214). SLC proteins transport a large number of solutes including both charged and uncharged organic molecules, in addition to inorganic molecules and gasses. The SLC proteins can be further classified as belonging to one of the following groups: facilitative transporters, secondary (coupled) active transporters, primary active transporters (requiring energy from ATPase hydrolysis), ion channels, and aquaporins. Many of the solute carriers are associated with genetic disease, and a significant number of these solute carriers are expressed in ameloblasts.

### 4. The SLC genes and CFTR in enamel mineralization

All of the anion exchangers identified in the enamel organ (i.e., SLC4A2 and SLC26A1, 3, 4, 6 and 7) are localized to either the apical or lateral membrane of polarized maturation-stage ameloblasts (259, 350, 429, 665), and this is a similar localization profile as CFTR in the same population of cells (59, 63, 665). Based on co-immunoprecipitation (Co-IP) data (665), there is evidence that physical interactions exist between CFTR and the SLC26A gene family members SLC26A1, SLC26A6, and SLC26A7 in maturation-stage ameloblasts (665). These functional complexes are likely localized to the apical membrane of ameloblasts where the expression of these genes is identified (665). The phenomenon of several ion transporters/exchangers, coupled to CFTR, with similar physiological functions and cellular localizations, interacting with one another to form united protein complexes, has been reported in multiple areas of biomedical research. In most cases when CFTR interacts with SLC26A family members, CFTR seems to serve as a hub for these potential interaction complexes (46, 78, 210, 216, 221, 531, 619). One example is that SLC26A3, SLC26A6, and SLC9A3R1 (the sodium/hydrogen exchanger regulatory factor or NHERF1) colocalize with CFTR in the midpiece of mouse sperm, and the protein complex formed by CFTR with SLC26A3, SLC26A6 and SLC9A3R1 functions primarily to mediate transmembrane transport of chloride, which is critical for sperm capacitation (i.e., the destabilization of the mammalian sperm head to allow for binding between the sperm head and oocyte) (78). In cochlear outer hair cells (OHCs), the physical interaction between CFTR and SLC26A5, which is localized to the lateral membrane of OHCs, has potential electrophysiological significance (221). Additionally, in human bronchial cell lines, functional CFTR contributes to the functions of SLC26A9 as an anion conductor (46). CFTR might also interact with a broader range of pH regulators, so pH regulation during enamel maturation might be achieved by the coordination of functional protein complexes that are far more sophisticated than expected. Thus the interactions noted between CFTR and members of the SLC26A family during amelogenesis warrant further investigation to determine their functional importance.

### 5. Carbonic anhydrases and bicarbonate transporter dysfunction and enamel pathologies

A) CARBONIC ANHYDRASES. There are 15 carbonic anhydrases isozymes/genes in the human genome (CA1-4, 5A, 5B, and 6–14) and 16 in the mouse genome (Ca1-4, 5a, 5b, and 6–15) (315, 573, 574). However, the isoforms CA8, 10, and 11 (also Ca8, Ca10, and Ca11) do not contain one or more of the required histidine residues of the catalytic domain that binds a zinc ion; thus these three isozymes are devoid of any catalytic activity. Because of this, CA8, 10, and 11 are sometimes classified as CA-related proteins, or CA-RPs. Referencing the Online Mendelian Inheritance in Man website (www.OMIM.org), disease states for humans or rodents have been described for only CA2 (cytosolic), CA5A (mitochondrial), CA8 (573), and CA12 (membrane bound). To the knowledge of the authors, dental defects have only been associated with mutations to CA2 in humans and include abnormal teeth and malocclusion (22, 55, 398, 567); however, dental anomalies in the *Ca2*-null mice were not reported (57).

B) SLC4A2. The bicarbonate/chloride anion exchanger SLC4A2/AE2 is expressed widely, being localized on the basolateral membranes of most epithelial cells (481). The functional role of AE2 is notable in many cell types, including gastric parietal cells (568), choroid-plexus epithelial cells (6), surface enterocytes in colon (5), and renal collecting duct cells (7, 569). In humans, primary biliary cirrhosis has been described for SLC4A2 mutations (3, 270, 375). However, because of the wide distribution of expression of AE2, it is surprising that a greater number of human pathologies have not been linked to SLC4A2; this suggests that

many mutations that impact AE2 function may be early embryonic lethal.

Mice null for *Slc4a2* display a changed immune response and achlorhydria (172, 491), and squamous metaplasia of the epididymal epithelium leaves the male mutants infertile (376). *Slc4a2*-null mice also have significant dental pathology limited to the enamel organ (350). AE2 is most highly expressed along the lateral membranes of maturation ameloblasts (65, 269, 321, 350, 665), although our earlier reports showed a more apical expression pattern related to secretory ameloblasts (429). Gene expression array and real-time PCR data from the enamel organ show that a significant increase in *Slc4a2* mRNA expression from secretory ameloblasts to maturation ameloblasts (318, 321), and it may be that this transition from secretory to maturation stage results in a redistribution of AE2 localization (i.e., from the apical to lateral membranes). However, in the maturation stage, data from Lyaruu et al. (350), Josephsen et al. (269), and Yin et al. (665) clearly show AE2 expression along the lateral/basolateral membranes. These data are also most consistent with the basolateral localization of AE2 seen for most other epithelial cell types (481). The enamel of *Slc4a2*-null mice had a disorganized prismatic architecture and wore significantly more quickly than that of normal control mice, while the dentin (dentin-producing cells are of mesenchymal origin) was unaffected (350).

C) SLC4A4. Mutations to *SLC4A4*/NBCe1 can result in complex disease in humans and mice including proximal renal tubular acidosis (pRTA), growth delay, heart failure, mental retardation, as well as ocular and dental enamel defects; all these pathological states clearly impact on morbidity and mortality (105, 117, 246, 247, 251, 292, 436, 481). Similar disease states have been shown in the *Slc4a4*-null mice (171). *Slc4a4*-null mice died soon after birth (mean age of ~12 days), attributed to severe metabolic acidosis with blood $HCO_3^-$ concentrations of 4.0–7.6 mM and pH values of 6.80–6.93 (171).

NBCe1 is expressed at the basal pole of polarized ameloblast cells (317, 429), and it is upregulated by three- to fourfold as ameloblasts transition from secretory to maturation stage (318, 321). During maturation stage, significant NBCe1 expression is also noted in the papillary layer cells (269). The gross appearance of the dentition of *Slc4a4* null mice was of a hypomineralized enamel (i.e., chalky white and opaque), while an electron microscopic examination showed that the enamel had a pitted surface, had lost its prismatic structure, and was both hypoplastic and hypomineralized (317). The dentin of these NBCe1 mutant mice was normal (317). These data highlight the importance of NBCe1 activity in amelogenesis (320, 604).

D) SLC26A3. In humans, mutations to *SLC26A3*/DRA result in congenital chloride diarrhea and can be associated with hypokalemia, increased serum bicarbonate, and high aldosterone (86, 217–219, 357). The *Slc26a3*/Dra-deficient mouse displays a similar pathology to humans (511). In mice, Slc26a3 is expressed at the apical pole of maturation ameloblasts (259). To the authors' knowledge there have been no reports of dental pathologies related to human or mouse *SLC26A3* mutations.

E) SLC26A4. Pendred syndrome, which involves sensorineural hearing loss and goiter, results from mutations to SLC26A4/Pendrin/PEN (2, 85, 93, 134, 253, 300, 301, 365, 605, 606). Although a case report does identify a patient with Pendred syndrome as having dental disease (periodontal attachment loss and hypercementosis) (517), enamel defects have not been reported with Pendred syndrome or with any of the known *SLC26A4* mutations. With the use of a normal mouse model, it has been shown that, as is the case with Slc26a3, Slc26a4 is expressed at the apical pole of maturation-stage ameloblasts (60, 259). While Slc26a4 mutant mouse models have been developed and studied (121, 133), dental pathologies have not been reported in the mice.

F) SLC26A6. Referencing the Online Mendelian Inheritance in Man website (OMIM.org), disease states for human SLC26A6 mutations have not been documented, although an in silico analysis suggests that certain single nucleotide polymorphisms (SNPs) in SLC26A6 may be a risk factor for kidney stones (347). *Slc26a6*/Pat1 mutant mice form calcium oxalate urolithiasis, with this being the only noticeable pathology (265); however, in a second Slc26a6 mouse mutant model, changes in the physiology of $Cl^-$/base exchange in the kidney proximal tubules and oxalate stimulated NaCl absorption of the duodenum were noted (620).

## C. Calcium

### 1. Overview

In mineralized enamel, $Ca^{2+}$ is the most abundant ion and can be incorporated rapidly into the enamel zone from blood (541). $Ca^{2+}$ represents ~36% of enamel by weight, about twice as much as the next ion represented (392). $Ca^{2+}$ is largely incorporated during the maturation stage, with ~86% of the $Ca^{2+}$ found in enamel entering the tissue during this stage (541). During the secretory stage, the concentration of calcium measured in pig enamel fluid was ~$5 \times 10^{-4}$ M, lower than in the serum (~$3 \times 10^{-3}$ M), suggesting that the enamel zone represents a specialized micro-compartment (17) and also pointing to the presence of an active transport system. However, the cyclical nature of morphological changes from RA to SA in maturation may indicate that both passive and active transport systems are available to these cells (see below) (541).

$Ca^{2+}$ is also important to ameloblasts during the secretory stage. The bulk of $Ca^{2+}$ in the enamel fluid in the secretory

stage is bound, likely to 11- to 13-kDa amelogenin-derived fragments (392, 475). Amelogenin-$Ca^{2+}$ binding can potentially be a $Ca^{2+}$ reservoir, acting as a regulator of mineralization in particular at the secretory stage as there are limited adsorption sites for $Ca^{2+}$ giving a smaller crystal size (17). It is estimated that one molecule of amelogenin can bind ~6.4 $Ca^{2+}$ (328). Reith and Boyde (469) suggested that the binding of $Ca^{2+}$ to amelogenins provides a route for the diffusion of $Ca^{2+}$ into the deeper layers of enamel; however, this might seem paradoxical because of the increased bulk of an amelogenin-$Ca^{2+}$ complex compared with $Ca^{2+}$ alone. Saturation of the enamel fluid and precipitation of the mineral phase appears to be largely determined by the concentration of $Ca^{2+}$ (392, 523).

The mechanisms associated with the transport of $Ca^{2+}$ by the enamel organ have been the subject of a number of important reviews; however, much of our previous understanding of $Ca^{2+}$ transport is currently being challenged and redefined (32, 240, 541, 579).

### 2. Classic hypotheses for $Ca^{2+}$ transport

$Ca^{2+}$ travels across the barrier formed by ameloblasts in the basolateral to apical direction into the enamel, rather than from the underlying dentin (469). Transport of $Ca^{2+}$ is considered to proceed largely via a transcellular route rather than a paracellular or passive route as secretory and maturation stage ameloblasts form tight cell cohorts bound by junctional complexes (502). Perfusion studies using lanthanum observed that this tracer leaked across the proximal but not the distal intercellular junctions of secretory ameloblasts (580). In RA, tight junctions are only found near the basolateral pole, but in SA, these junctions can be found at the apical pole (268). It was found that lanthanum and horseradish peroxidase (HRP) did not leak across the distal junctions of RA or the proximal junctions of SA (579, 580, 583). The cyclic nature of RA and SA indicates that during the smooth phase, intercellular spaces are opened to the enamel area, allowing fluids to move passively in a proximal direction, but remaining in that intercellular space until the RA stage, when fluids can move towards the papillary layer area and be cleared via the vascular system. About 70% of all maturation-stage ameloblasts are ruffle-ended, limiting the passive movement of $Ca^{2+}$ (268, 541). Studies using radiolabelled $Ca^{2+}$ ($^{45}Ca$) suggest that $Ca^{2+}$ is incorporated through the RA (467, 582).

Considering the transcellular transport of $Ca^{2+}$, most prior studies have suggested that $Ca^{2+}$ entry into ameloblasts is passive (32, 579). Influx occurred at the basolateral pole via concentration gradient differences between the lower intracellular [$Ca^{2+}$] and higher [$Ca^{2+}$] in the extracellular compartment (32). Leaked $Ca^{2+}$ into the basal pole increased intracellular [$Ca^{2+}$], exposing cells to potentially toxic $Ca^{2+}$ levels. To prevent this while enabling transfer across the cytosolic compartment towards the apical pole, it was proposed that ameloblasts use a number of common cytosolic $Ca^{2+}$ buffers (32, 541, 579) including parvalbumin and calretinin, as well as others with lower binding capacity acting also as $Ca^{2+}$ sensors, including calmodulin and calcineurin (98, 239, 241). The most abundant buffers are the $Ca^{2+}$-binding proteins known as calbindins (members of the *S100* gene family). Calbindin 9kD/S100, calbindin 28kD/CALB1, and calbindin 30/CALB2 have been the subject of a number of studies (41, 42, 238, 239, 241, 243, 312, 330, 599). Binding of $Ca^{2+}$ to buffers occurs on the subsecond scale and thus is a key process to maintaining intracellular $Ca^{2+}$ homeostasis. The role of mobile buffers was considered to be of importance as it was postulated that cytosolic [$Ca^{2+}$] near the apical pole is lower than at the basal pole so that calbindins can safely transfer bound $Ca^{2+}$ across the cell (240). In addition to cytosolic buffers, Hubbard's group also identified the expression of the sarco/endoplasmic $Ca^{2+}$-ATPase (SERCA) (161) whose main function is to pump cytosolic $Ca^{2+}$ into the lumen of the endoplasmic reticulum (ER), thus playing a role in $Ca^{2+}$ homeostasis. Moreover, ER luminal buffers including calreticulin/CALR, endoplasmin/HSP90B1, and ERp72/PDIA4 were also identified in enamel cells (238, 242). The safe transit of $Ca^{2+}$ also involves transport via secretory vesicles and along the inner leaflet of the plasma membrane through phospholipids (469).

Concerning $Ca^{2+}$ extrusion, the plasma membrane $Ca^{2+}$-ATPases (PMCA) were considered the main clearing mechanism (32). Four genes code for PMCA proteins: ATP2B1-4. PMCAs, which exchange protons for one $Ca^{2+}$ in each ATP hydrolysis, were identified throughout the membrane of secretory-stage ameloblasts. In maturation stage these pumps were predominantly localized to the ruffled border of RA cells (579), thus suitably positioned to extrude $Ca^{2+}$ while removing protons from the enamel area and indirectly participating in pH regulation (63).

Hubbard proposed a revised version of the $Ca^{2+}$ transport system by the enamel epithelium largely based on his group's findings that the ER played a role in transiting $Ca^{2+}$ across the cell (238, 240). In addition to the findings of SERCA in enamel cells, Hubbard (238) also identified the expression of inositol receptors ($IP_3R$) which enable the release of ER $Ca^{2+}$ pools. These findings and others related to protein buffers in the ER allowed Hubbard to put forth a model he termed the "transcytosis hypothesis," which gained traction in the literature as a potential model for $Ca^{2+}$ transport in enamel epithelium (238). Considering that mouse models deficient for the two calbindins found in enamel and mentioned above showed no abnormal enamel phenotypes (243, 599), the ER-based transcytosis model proposed that $Ca^{2+}$ remained buffered within the ER lumen where it was moved across the cell to be extruded by PMCA pumps at

the apical pole (240). This model, however, also envisioned that $Ca^{2+}$ entry was likely a passive process (e.g., Refs. 32, 579). This is a key point revised in recent publications showing that this passive influx of $Ca^{2+}$ is not a likely scenario (318, 409, 411).

### 3. Current ideas on calcium influx during amelogenesis

A) CALCIUM INFLUX. A genome-wide study which compared rat enamel organ cells from maturation and secretory stages identified *Stim1* and *Stim2* transcripts as being upregulated in maturation, which was also supported by Western blot analysis (318). STIM1 and its homolog STIM2 are single-pass proteins with an ER lumen amino terminus and a cytosolic carboxy terminus. They are key components of a mechanism involved in $Ca^{2+}$influx in many cell types known as store-operated $Ca^{2+}$ entry (SOCE), of which the $Ca^{2+}$ release-activated $Ca^{2+}$ (CRAC) channels is the best characterized. STIM proteins are largely localized to the ER membrane, acting as sensors of changes in luminal ER [$Ca^{2+}$]. When the [$Ca^{2+}$] in the ER lumen decreases, $Ca^{2+}$ dissociates from the EF-hand motif in the amino terminus, promoting the oligomerization of STIM (146). STIM1 oligomers directly interact with the plasma membrane pore subunit of the channel known as ORAI1, resulting in sustained $Ca^{2+}$ entry (146). ORAI is a plasma membrane-bound protein with three homologs in mammals (ORAI1-3), but human mutations impacting on SOCE are only known for *ORAI1* (314). Patients with mutations in the *STIM1* and *ORAI* genes present with amelogenesis imperfecta (AI) (163, 314, 370, 615), linking CRAC channel function with enamel formation.

Nurbaeva et al. (411) recently demonstrated that CRAC channels are functional in enamel cells. Using the ameloblast-like LS8 cells (494), a murine enamel organ-derived immortalized cell line, we adapted protocols used in many other cell types to modulate CRAC channel function using thapsigargin to inhibit SERCA pumps, thus passively depleting the [$Ca^{2+}$] in the ER to activate SOCE (411). Readdition of extracellular $Ca^{2+}$ showed a marked rise in cytosolic [$Ca^{2+}$] demonstrating that SOCE is expressed in LS8 cells (411). Some cells were exposed to inhibitors that have been previously used to block CRAC channels (i.e., Synta-66, BTP2, 2-APB), all of which hampered $Ca^{2+}$ entry, thus demonstrating that $Ca^{2+}$ uptake in LS8 cells is via CRAC channels (411).

This research was extended to primary enamel cells, taking advantage of the fact that enamel organs can be isolated from the secretory and maturation stages using commonly accepted protocols (547). STIM1 and STIM2 and all three ORAI homologs were detected in ameloblasts with high expression (409). STIM1 and ORAI1 showed cytosolic and plasma membrane localization, respectively (409). Stimulation of isolated enamel organ cells from secretory and maturation stage with thapsigargin showed that both cell types are equipped with SOCE. In primary cells pretreated with the CRAC channel inhibitor Synta-66, $Ca^{2+}$ entry was significantly impaired, demonstrating that CRAC channels are functional in primary enamel cells (409). These measurements were carried out using a Flexstation-3 which records the average fluorescence of a pool of cells. A schematic model for the entry (and exit) of $Ca^{2+}$ in enamel cells is presented in **FIGURE 13**.

B) EVIDENCE FOR $CA^{2+}$ SIGNALING IN ENAMEL CELLS. It is well known that a rise in cytosolic [$Ca^{2+}$] has important signaling effects over a wide range of processes (461). It has been shown that stimulation of the enamel cell line PABSo with different concentrations of extracellular $Ca^{2+}$ resulted in an increase in cytosolic [$Ca^{2+}$] measured by fura-2 ratios (363). The expression of the $Ca^{2+}$ sensing receptor (CaR/CASR) in these cells was linked to this process (363). A later study investigated the effects of exposing primary enamel organ cells to external $Ca^{2+}$ and found that media containing concentrations of 0.1–0.3 mM $Ca^{2+}$ resulted in mRNA increase of *AMELX* and *AMTN*, suggesting that $Ca^{2+}$ played a role in modulating their expression (83). More recently, the effects of $Ca^{2+}$ were investigated more directly by stimulating the murine cell line LS8 with thapsigargin to induce SOCE (411). Stimulation of LS8 cells for 0.5 h resulted in a marked increase of *Amelx*, *Ambn*, and *Enam* mRNA levels but not when cells were pretreated with the CRAC channel inhibitor Synta-66 (411). These data indicate that SOCE-mediated $Ca^{2+}$ entry is important in regulating enamel gene expression in LS8 cells. A similar result was found in primary enamel cells dissected from mouse enamel organs after stimulation with thapsigargin (411). As this effect was in response to a decrease in ER $Ca^{2+}$ stores, it suggests that SOCE mediates the expression of enamel genes. Protein changes analyzed by Western blot showed that Ambn expression increased in primary cells after only 1 h following stimulation with thapsigargin, supporting the relatively fast action of SOCE and enamel protein expression.

C) CALCIUM EXTRUSION: ROLES OF NCX1, NCX3, AND NCKX4. Two families of exchangers expressed in enamel cells have helped redefine $Ca^{2+}$ extrusion in ameloblasts. The first of these reports focused on the bidirectional $Na^+/Ca^{2+}$ exchanger family NCX (416) which exchange one $Ca^{2+}$ for three $Na^+$. The second family is the $Na^+/K^+/Ca^{2+}$ (NCKX) exchanger, bidirectionally cotransporting one $K^+$ and one $Ca^{2+}$ inwardly and four $Na^+$ outwardly. In most cells, [$Na^+$] and [$Ca^{2+}$] are higher outside the cell while [$K^+$] is higher inside.

NCX1 and NCX3 are expressed in ameloblasts with an apical or apicolateral distribution with NCX1 also showing basal staining (416), and based on the histological analyses, it appears both secretory and maturation ameloblasts ex-

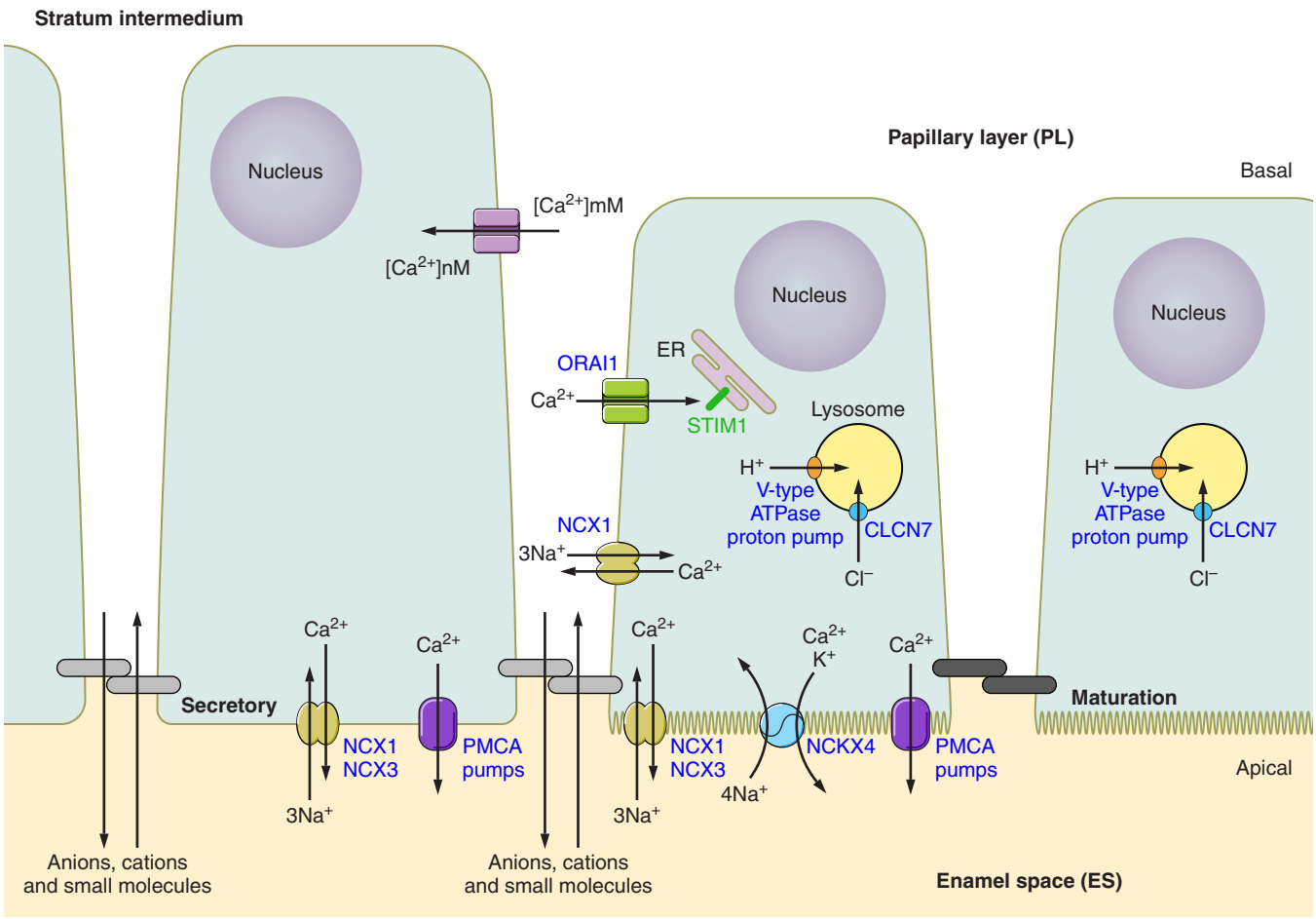


**FIGURE 13.** Proposed model for $Ca^{2+}$ handling by ameloblasts. Secretory ameloblasts (Sec.) have either passive and/or SOCE for $Ca^{2+}$ uptake. Extrusion at this stage is mediated largely by plasma membrane $Ca^{2+}$-ATPases (PMCAs) or sodium/calcium exchangers (NCXs). $Ca^{2+}$ uptake in maturation (Mat.) stage RA occurs largely via SOCE. STIM1 has a wide distribution throughout the endoplasmic reticulum (ER), and ORAI1 is found in the plasma membrane of RA. Sarco/endoplasmic reticulum SERCA2 pumps sequester cytosolic $Ca^{2+}$ into the ER lumen, whereas inositol 1,4,5-trisphosphate receptors ($IP_3R$) might be the main ER $Ca^{2+}$ release channels although ryanodine receptors (RyR) have also been identified. As $Ca^{2+}$ pools are depleted in the ER, STIM1 clusters enable $Ca^{2+}$ entry via the ORAI1 channel. Extrusion in RA is mediated principally by NCKX4, with NCX1, NCX3, and PMCA also playing a lesser role. In SA cells, STIM1 is nearly absent, and the localization of NCKX4 changes becoming internalized which is predicted to alter $Ca^{2+}$ transport during SA phase. A dark gray double capsule represents a tight junctional complex at the apical region of RA, and a light gray double capsule represents a "leaky" junctional complex at the apical region of SA.

press NCX1 and NCX3 at similar levels (416). Electrophysiological analysis of whole cell recordings and pharmacological inhibitors for NCX further demonstrated NCX activity in $Ca^{2+}$ transport (416). More recently, Lacruz et al. (321) assessed by RT-PCR expression of NCX1 and NCX3 during amelogenesis and showed that neither of these genes increased expression during the maturation stage, supporting the data that both genes are expressed at similar levels during both the secretory and maturation stages of amelogenesis.

Results from a genome-wide study comparing secretory- and maturation-stage enamel organ cells found that NCKX4 was upregulated in maturation (318). There are six NCKX gene family members, NCKX1-6, coded by genes *SLC24A1-6*, respectively. RT-PCR analysis identified all members of the NCKX family in both secretory and maturation stages, but NCKX4 was the most highly upregulated, suggesting an important role for NCKX4 in enamel formation (234, 615). NCKX4 is localized to the apical end of maturation stage ameloblasts and thus likely associated with $Ca^{2+}$ extrusion (234, 320). Subsequent reports identified severe enamel defects in patients and in mouse models with mutations to *SLC24A4* (439, 615), strengthening the link between NCKX4 and enamel formation.

D) CALCIUM EXTRUSION: PLASMA MEMBRANE $CA^{2+}$-ATPASES. Borke and co-workers (53, 54, 669) have reported the presence of plasma membrane $Ca^{2+}$ pump (PMCA) proteins in the enamel organ cells, and further investigation is warranted based on the current interest in ion transport and amelogenesis. The PMCA proteins are coded by four unique

genes: the ATPase plasma membrane transporting genes 1–4 (*ATP2B1, ATP2B2, ATP2B3*, and *ATP2B4*). Borke and co-workers used antibodies that recognized the PMCA proteins, but it is unclear if they could distinguish between the four gene products/isoforms. The majority of the staining was located at the apical membrane of both secretory- and maturation-stage ameloblasts, with the greatest reactivity seen in early maturation (669). Expression was also evident in the papillary layer cells (669). In situ hybridization showed that both Atp2b1 and Atp2b4 were expressed in ameloblasts, with the highest signal being noted during early maturation (54). With the exception of a single paper looking at the expression of Atp2b1 in zebrafish bone and teeth (183), no other papers could be identified that have extended the prior work on the role of PMCA proteins in amelogenesis.

Taking the above studies together, a number of calcium exchangers and pumps have been identified primarily on the apical membrane (and occasionally the lateral membranes) of secretory- and maturation-stage ameloblasts, with these being NCX1, NCX3, and the PMCA proteins. Expression of the NCKX4 is restricted to the apical membrane of maturation-stage ameloblasts. A summary schematic of these calcium extruding exchangers and pumps is shown above (**FIGURE 13**).

#### *4. A revised model for $Ca^{2+}$ influx/efflux in enamel organ cells.*

Current evidence suggests that $Ca^{2+}$ entry into enamel cells is modulated by CRAC channel proteins STIM1 and ORAI1 (314, 409). Stimulation of CRAC channels in most cells is mediated by the action of an agonist binding to a cell surface receptor, which results in intracellular production of phospholipase C (PLC) and inositol 1,4,5-trisphosphate ($IP_3$) (455). $IP_3$ binds to its receptor in the ER membrane, releasing $Ca^{2+}$ into the cytosol and activating SOCE (158, 435). Given that $IP_3$ receptors ($IP_3Rs$) are highly expressed in ameloblasts (409) and that $IP_3R$ expression predominates in nonexcitable cells (559), it is likely that this receptor family is associated with SOCE in enamel cells (409). The increase in cytosolic [$Ca^{2+}$] resulting from SOCE activation is buffered via a number of cytosolic proteins, although it is as yet unclear whether these buffers, in particular the calbindins, can move $Ca^{2+}$ safely across ameloblasts or whether the extensive tubular network of the ER mediates this process (240). $Ca^{2+}$ homeostasis can also be monitored by $Ca^{2+}$-ATPases, SERCA2, and exchangers extruding $Ca^{2+}$ including NCX1, NCX3, NCKX4, and PMCAs (32, 234, 416) (see **FIGURE 13**).

Overall differences between secretory- and maturation-stage ameloblasts in the expression of these proteins tend to suggest that all of them are expressed in both stages, but during maturation many of them show increased expression. These data are in keeping with the increased transport of $Ca^{2+}$ during maturation reported by others (240, 541), so the expectation would be that as $Ca^{2+}$ mineral uptake increases in maturation, the $Ca^{2+}$ handling machinery is also upregulated (318).

The contribution of SA cells to $Ca^{2+}$ transport in enamel cells during the maturation stage remains unclear. While tracer analyses ($^{45}Ca$) indicate rapid movement of $Ca^{2+}$ from blood to the enamel area in ways that would seem more appropriate to a passive (intercellular) movement of $Ca^{2+}$ (541), it can also be speculated that injection of $^{45}Ca$ might overload the active system associated with RA cells, facilitating rapid and perhaps artificial passive diffusion across the leaky SA cells. Until the functional differences between these two cells types are more clearly explored, this will remain unresolved. However, as pointed out by Smith (541), it is also a strong possibility that ameloblasts use the RA-to-SA modulation to enhance $Ca^{2+}$ transport so that a constant supply is maintained regardless of the cell type involved.

### D. Phosphate

#### *1. Overview*

At least two studies have used a $^{32}P_i$-labeled pulse (following intraperitoneal injection) to investigate $P_i$ incorporation into enamel (279, 477). Labeled $^{32}P_i$ in the enamel matrix was observed within 10 min, with a greater incorporation found in the secretory-stage enamel matrix when compared with maturation stage. While the data presented by Robinson et al. (477) show a very complex pattern of $P_i$ movements into the enamel matrix, when viewed over 24 h there seems to be a peak of $^{32}P_i$ inclusion at ~4 h (times examined from the initial injection were 10 min and 2, 4, 8, and 24 h), again with the majority of $P_i$ moving into the secretory-stage matrix. Similarly rapid (minutes) radiolabeled $Ca^{2+}$ uptake into the enamel space has also been shown (202, 396, 602). The incorporation of $P_i$ from the circulation to the enamel matrix in as little as 10 min suggests the possibility of a paracellular/intercellular route, but as discussed in a prior review paper (541), while $P_i$ (and $Ca^{2+}$) movement from the circulation to the enamel space occurs quickly, likely via intercellular spaces, there does appear to be a level of cellular control and facilitated movement offered by ameloblasts (541).

Lacruz et al. (318) and Yin et al. (664) have recently performed a whole-genome array analysis for rat incisor secretory-stage and maturation-stage enamel organ cells and identified that sodium-dependent $P_i$ transporters (cellular transporters for the coupled import of $Na^+$ and $HPO_4^{2-}$ or $H_2PO_4^-$) feature prominently in amelogenesis. Our array data indicate that *Slc20a1* and *Slc20a2* are expressed at high levels throughout amelogenesis, while *Slc34a2* in-

creases ~30- to 60-fold as enamel organ cells transition from secretory stage to maturation stage (318, 664). This is of particular interest because the expression of *Slc34a2* is pH sensitive (156, 382, 610), being upregulated at lower pH, which is known to characterize the enamel environment during maturation (316, 318, 544, 664). The SLC20 gene family comprises *SLC20A1* and *SLC20A2*, which code for the proteins referred to as PiT-1 and PiT-2, respectively (157). PiT-1 and PiT-2 are ubiquitously expressed in all tissues and are thought of as "housekeeping" transport proteins, although differences in function in various tissues are noted (157).

### 2. Sodium-dependent phosphate ($P_i$) transporters of the solute carrier (SLC) class of genes

The sodium-dependent (or sodium-coupled) phosphate ($P_i$) transporters are members of the SLC17A (*SLC17A1-4*), SLC20A (*SLC20A1-2*), and SLC34A (*SLC34A1-3*) gene families. In an initial genome-wide array analysis of the enamel organ cells (318), the expression levels of all of the SLC17 gene family members were negligible while members of both the SLC20 and SLC34 families were expressed at high levels, as was the alkaline phosphatase (*Alpl*) gene (318). SLC20A and SLC34A are known classically as electrogenic transmembrane proteins that cotransport $P_i$ and $Na^+$ from the extracellular space/fluid into the cell (157, 174). SLC20A moves two $Na^+$ and one $H_2PO_4^-$ across the cell membrane, while SLC34A moves three $Na^+$ and one $HPO_4^{2-}$ (157, 174, 508).

### 3. Phosphate export in amelogenesis

There are no published data that add to our understanding of $P_i$ export to the enamel matrix once it is internalized in the enamel-forming cells. Once $P_i$ is internalized in ameloblasts it then may be transported by an as-yet-unknown mechanism to the mitochondria and stored as polyphosphates, as has been proposed for bone cells (418, 419). From the mitochondria, the polyphosphates would then need to be transported in specialized secretory vesicles to the plasma membrane to be released to the extracellular matrix as needed (418, 419). Polyphosphates would then be enzymatically cleaved into orthophosphates allowing for Hap formation. For such an activity to occur, the expression of alkaline phosphatase (ALPL) would be required, and it has been shown previously that ALPL activity is expressed at the apical pole of polarized ameloblasts, both during secretion and maturation (311).

### 4. SLC20 and SLC34 gene families and their roles in health and disease

The SLC20 gene family comprises *SLC20A1* and *SLC20A2*, which code for the proteins referred to as PiT-1 and PiT-2, respectively (157). PiT-1 and PiT-2 are ubiquitously expressed in all tissues and are thought of as "housekeeping" transport proteins, although differences in function in the various tissues are noted (157). For example, PiT-1 is involved with bone $P_i$ homeostasis and is under the regulation of bone-specific signaling factors such as IGF-1 and BMP2 (155, 381). Pit-1 is essential for liver development (35), and in cell culture Pit-1 has been shown to play a role in cell proliferation, cell cycle regulation, mitosis, and cytokinesis (36). *Slc20a1* knockout mice are embryonic lethal (35), and to date, no mutations in *SLC20A1* have been linked to human disease. Humans with mutations to *SLC20A2* (613) and mice null for *Slc20a2* are viable and in both species show a similar neurological pathology limited to basal ganglia calcifications (261). The function of the SLC20 gene family members has not been investigated in dental tissues.

The SLC34 gene family is composed of three members, *SLC34A1-3*, which code for proteins NaPi-IIa, NaPi-IIb, and NaPi-IIc, respectively. Expression of NaPi-IIa and NaPi-IIc is somewhat limited to the kidney proximal tubules (155, 405). NaPi-IIb is not expressed in the kidney and mediates $P_i$ absorption in the gut (155, 405). SLC34A2 is also expressed in lungs, testes, salivary glands, thyroid, liver, and mammary glands (405). In humans, mutations in *SLC34A1* are linked to nephrolithiasis and osteoporosis (457), autosomal recessive Fanconi syndrome, hypophosphatemic rickets (356), nephrocalcinosis, and hypercalcemia (290). *SLC34A2* mutations are linked to alveolar and testicular microlithiasis (381), and *SLC34A3* mutations are linked to hypophosphatemic rickets and hypercalciuria (44).

Several mutant mouse models have been studied for *Slc34a1* (593), *Slc34a2* (413), and *Slc34a3* (593) and generally bear nonlethal phenotypes similar to those noted in humans. In enamel organ tissues, levels of Slc34a1 and Slc34a3 mRNA are negligible (318). The levels of Slc34a2/NaPi-IIb mRNA are negligible in the secretory-stage enamel organ cells, and significantly upregulated during maturation-stage amelogenesis (318, 664). A recent paper in the dental literature shows, using immunolocalization with two distinct antibodies against mouse Slc34a2/NaPi-IIb, expression is limited to the apical pole of maturation ameloblasts (61). The authors suggest that $NaP_i$-IIb may secrete/export $P_i$ and $Na^+$ into the enamel space (61). This would require that NaPi-IIb flip such that the amino terminus and carboxy terminus, normally located in the cystoplasm, relocate to the enamel space. This would be a novel functional role for NaPi-IIb in cells; however, based on the localization data presented by Bronckers et al. (61), this positioning of NaPi-IIb at the apical membrane of maturation ameloblasts is worth investigating further.

## E. Fluoride

Fluoride is incorporated into the developing enamel crystallites during enamel formation, and also after the enamel is completely formed. During amelogenesis, fluoride ions ($F^-$) can substitute randomly for hydroxide ions ($OH^-$) or carbonate ions ($CO_3^{2-}$), usually at very low levels, in the hydroxyapatite (Hap) crystallite structure (15, 16, 45, 62, 107, 131, 476, 523). Some dental researchers thus refer to dental enamel as a fluorohydroxyapatite-based structure (99, 329, 523). The inclusion of low levels of $F^-$ enhances crystal growth rates and makes the resulting enamel more stable than pure Hap (523), thus improving its resistance to dental caries by decreasing its acid solubility (141, 487, 597). This property has made fluoride a staple of modern dental health care. Nevertheless, if fluoride were absent during amelogenesis, teeth would form without any significant deficiencies, pathologies, or changes in morphology and function.

Once a tooth erupts, $F^-$ can still be incorporated into the enamel crystallites, but $F^-$ must diffuse into the enamel from the enamel surface to substitute or replace $OH^-$ that may be lost, for example, as a consequence of demineralization during the process of dental caries. In an incipient carious lesion, demineralization is initially seen just below the enamel surface (20, 89, 252), and the chemical events that contribute to the demineralization/remineralization process result from the effusion and infusion of ions to restore the damaged Hap-based enamel. Topical fluorides are an effective approach to prevent early carious lesions from progressing and hasten the remineralization process (1, 14, 224).

Excessive exposure to $F^-$ during enamel formation can result in dental fluorosis or mottled enamel (11, 13, 62), which is hypomineralized. Fluorosed enamel has a greater amount of retained matrix proteins (62, 108, 110, 476, 643); thus some researchers have speculated that $F^-$, above a certain concentration, may have a negative impact on the function and activity of the secreted enamel proteinases such as MMP20 and KLK4 (15, 62, 107). However, recent studies suggest this may not be the case, given that a high concentration of fluoride ions does not impact the enzymatic activities of either MMP20 or KLK4 in vitro (173, 600). In vitro, excess levels of $F^-$ have been shown to decrease MMP20 expression, but not the expression of AMELX (673). There is, however, an in vivo-based (rodent) study showing that increases in ingested $F^-$, to levels that cause dental fluorosis, result in a decrease in TGF-$\beta$1/Tgfb1 expression in enamel cells and this in turn inhibits Klk4 expression (575). These data may suggest that decreased Klk4 activity results in retained protein matrix in surface enamel that is visualized as dental fluorosis (or white spot lesions) (575). Some of the most current research on dental fluorosis and amelogenesis suggest that there is a connection between high levels of $F^-$ and the initiation of both oxidative and ER stress pathways (306, 518, 522, 576). It has been shown in ameloblasts and other cell lineages that both oxidative and ER stress result in a decrease in overall protein synthesis and secretion (215, 306, 309, 310, 346, 628), including the enamel proteinases (522). However, secretion of the major enamel structural proteins (i.e., AMELX) during secretory-stage amelogenesis appears relatively unaffected to exposure of high levels of $F^-$ (62). Thus one likely cause of hypomineralization as it relates to fluorosis appears to result from lesser quantities of secreted enamel proteinases acting on a "normal" quantity of enamel protein substrates, rather than decreased kinetic activity in the presence of a normal quantity of proteinases (106, 110, 522).

While there has been extensive research directed at discovering the pathogenic mechanism behind dental fluorosis, and much of this work has been done either using cultured human enamel cells, or using mice or rats exposed to various levels of $F^-$, there needs to be caution translating these findings to humans. In rats and mice, long-term exposure to $F^-$ at 25–30 ppm in the drinking water would be required to produce visible sign of enamel fluorosis (12, 109), while $F^-$ at 100 ppm is a typically used dose to induce dental fluorosis in both rats and mice (62, 576, 607, 608). This dose is high when compared with the dose of ~6 ppm that would result in enamel fluorosis (with most individuals being severely affected) in close to 100% of the human population (see below).

While work continues on the biological, physical, and chemical properties of $F^-$ inclusion in dental enamel, the pathways that import and export $F^-$ in ameloblasts remain unknown. Some researchers believe $F^-$ itself is unable to diffuse across the plasma cell membrane, but can readily pass through the membrane in the form of hydrofluoric acid (HF) (522). To the authors' knowledge, ion channels that selectively transport $F^-$ in mammalian cells have not been described; however, in bacteria, yeast, and some plant cells, a number of ion channels have been described that effectively transport $F^-$ (264, 323, 551, 563). For example, in bacteria, members of the voltage-sensitive chloride channel (ClC) superfamily have been shown to transport $F^-$ (323, 339, 562). It should be noted that mammalian cells express nine members of this ClC family (Clcn1-7, plus Clcnka and Clcnkb) (37, 313); thus future studies may make a connection between the role of certain chloride channels and/or pumps, or even channels specific to fluoride, and the transmembrane movements of $F^-$ in mammalian cells, including ameloblasts.

## F. Iron

Iron is seen at its highest concentrations at the labial surface or rodent incisors and gives the surface of these teeth a yellowish appearance (374, 632). Over a century ago, it was

noted that hypoparathyroidism resulted in loss of pigment in rat incisors (130). Early studies have led to differing conclusions regarding the role of iron in surface enamel. Stein and Boyle (560) suggested that iron pigmentation does not impact enamel structural properties based on the observation that, after surgically destroying the pigment-containing part of the enamel organ, the integrity of the underlying enamel is not affected. In contrast, Prime et al. (458) showed that an extended deficiency in dietary iron caused loss of pigmentation, resulting in enamel hypoplasia and aplasia, suggesting that an iron deficiency was associated with severe enamel structural defects.

Iron is essential to all living organisms. The most abundant iron-containing proteins are hemoproteins that are involved in oxygen transport and delivery. The ability of iron to shuttle between ferric iron ($Fe^{3+}$) and ferrous iron ($Fe^{2+}$) makes it especially useful in electron transport and enzyme catalysis. However, unregulated fluctuations in iron concentration can cause cellular damage by catalyzing reactions leading to the production of toxic oxygen radicals (10, 181). Excess iron that is not for immediate use is stored in ferritin, a shell-like protein structure with a central cavity containing $Fe^{3+}$. Mammalian ferritins are 24-subunit heteropolymers made of two different subunit types, a heavy and light chain, coded by the *FTH* and *FTL* genes, respectively. The early embryonic lethality in *Fth* knockout mice suggests a critical role for ferritin during development (144). The expression of FTH and FTL is influenced by iron concentrations in the immediate environment (206).

Iron is actively involved in numerous biological functions by serving as a cofactor for many proteins, including catalases and peroxidases in oxygen metabolism, hemoglobins in oxygen binding and transport, cytochromes in oxidative phosphorylation and in electron transport (434). Energy-requiring events, such as active ion transport, and water and matrix protein removal from the maturing enamel, demand a high level of ATP production through mitochondrial oxidative phosphorylation (414). It is therefore conceivable that iron is required by maturation-stage ameloblasts to assist in cellular energy production.

Rodent incisors are characterized by yellowish pigmentation on the labial side due to an iron content of ~0.030% in the whole upper incisor and 0.027% in the whole lower incisor (449). Electron microscopy has shown that iron is found primarily in the region of the enamel organ associated with maturation (465). The functional significance of iron in rodent incisor enamel is not understood, but it has been proposed that iron can decrease the solubility of crystallized Hap because iron density positively correlates with acid resistance of outer enamel (415). In addition, many knockout or transgenic animals targeting the silencing or overexpression of enamel gene products result in an enamel with a chalky white appearance and structural defects (230, 237, 317, 525, 526, 646, 650), suggesting the incorporation of iron into enamel is linked to the normal process of enamel formation (424, 666). Given the high iron content in mature enamel, not surprisingly, *Fth* has been identified as one of the genes most highly upregulated in maturation ameloblasts when compared with secretory ameloblasts (318, 319).

To date, published reports on the presence of iron and ferritin in teeth have been primarily limited to observations in ameloblasts and in the enamel of rodent incisors (383, 465, 632); however, limited iron uptake in developing rat molars has also been observed using autoradiographic (33) and immunolocalization approaches (632). Data from Wen and Paine (632) indicate that iron is present in ameloblasts of continuously growing incisors, and also evident in ameloblasts of molars (albeit at significantly lower levels), and favor the idea that iron is an integral component for enamel formation. Iron is not released from the ameloblasts and deposited into the enamel until the $Ca^{2+}$ and phosphorus contents of the enamel have reached a maximum level (201). In addition, there is an inverse relationship between the iron and $Ca^{2+}$ content in the outer enamel layer (303). One hypothesis proposed by Halse and Selvig (201) is that enamel mineralization advances only to a point, leaving room for subsequent incorporation of iron accompanied by removal of $Ca^{2+}$. Therefore, iron incorporation may represent the final refinement of surface enamel mineralization to provide extra strength or acid resistance. This would help explain the wear pattern of rodent incisors, where the surface enamel wears less than underlying enamel, resulting in "bladelike" occlusal surfaces that allow for gnawing of hard foods.

### G. The "Other" Ions: Magnesium, Sodium, and Potassium

Mineralized enamel contains, in addition to the main components $Ca^{2+}$, $PO_4^{3-}$, $OH^-$, and $Cl^-$, a small amount of various trace elements including $Mg^{2+}$, $Na^+$, and $K^+$. These elements are represented in different concentrations across the enamel layer; variation exists across species and even across individuals. This individual variation is associated with external factors such as diet and the chemistry of the water consumed during tooth formation. Young (668) reported concentrations (as percentage by weight) for these elements in mineralized enamel as follows: $Mg^{2+}$ (0.22%), $Na^+$ (0.70%), and $K^+$ (0.03%), which are far lower than the values reported for $Ca^{2+}$ (36.6%) or $P_i$ (18%). The millimolar concentrations for $Mg^{2+}$ and $Na^+$ measured by Aoba and Moreno (17) in the enamel fluid just adjacent to the apical pole of ameloblasts were lower than in serum, whereas $K^+$ was higher, suggesting that there is a system at the apical pole modulating the movement of these ions.

$Mg^{2+}$ concentration in mineralized enamel increases from the outer enamel towards the deeper layers near the dentin (519). Being a divalent cation like $Ca^{2+}$, it sometimes competes with the latter for space in the crystal structure (19). However, $Mg^{2+}$ has a smaller atomic radius than $Ca^{2+}$ as well as a greater affinity for water molecules, which limit its incorporation into the enamel crystals (523). In many cells, cytosolic $Mg^{2+}$ concentration is higher than extracellular levels. Transcellular transport of $Mg^{2+}$ in enamel has been poorly understood until recently as only $Ca^{2+}$-$Mg^{2+}$-ATPases had been implicated in enamel physiology (490). More recently, it was reported that mutations in the cyclin and cystathionine-beta-synthase (CBS) domain divalent metal cation transport mediator 4 (*CNNM4*) gene associated with Jalili syndrome also showed enamel deficiencies (438). Patients with *CNNM4* mutations are characterized by ocular deficiencies associated with retinal dystrophy and also present hypomineralized, thin enamel. The enamel from patients with *CNNM4* mutations showed lower $Ca^{2+}$ but increased $Mg^{2+}$ in enamel than that from healthy patients (349). In ameloblasts, CNNM4 is found at the basolateral pole and has been linked to $Mg^{2+}$ extrusion (661). Patients with hypomagnesemia also present with dental defects (hypoplasias), adding to the relevance of $Mg^{2+}$ in enamel formation (73).

$Mg^{2+}$-deficient enamel phenotypes are also associated with the ion channel for divalent metal cations, TRPM7, which has been shown to play a critical role in enamel mineralization (401). TRPM7 is upregulated during maturation stage and expressed in maturation-stage ameloblasts (401, 672). *Trpm7* mutant mice show an enamel phenotype that is very similar to the *Alpl*-null mice, with severe hypomineralization, which suggested that the activity of one protein may be influenced by the other (373, 401). Prior studies have shown that $Mg^{2+}$ enhances the activity of ALPL (102, 213, 470). The hypomineralized enamel phenotype seen in the *Trpm7* mutant mice could be rescued with supplemental dietary $Mg^{2+}$, indicating that in amelogenesis, TRPM7 allows for the inward passage of $Mg^{2+}$ in ameloblasts which in turn enhances the activity of ALPL (401).

In 2009 Beniash et al. (39) identified that, in newly forming enamel, the presence of amorphous calcium phosphate (ACP) is a precursor for the formation of the Hap crystals. Despite the fact that the presence of ACP in newly forming enamel had been suggested many years earlier (e.g., Refs. 48, 114, 474), the data presented by Beniash et al., showing that ACP could be detected in structures with similar shape and dimensions as more mature Hap crystals (39), were a paradigm shift in how dental researchers viewed initial enamel crystallite growth. In mature enamel, $Mg^{2+}$, in a Mg-substituted ACP (Mg-ACP), can be detected at its highest levels at the boundaries of individual enamel crystals (192, 193), suggesting $Mg^{2+}$ may play a role in ACP stabilization (116), or that Mg-ACP could play a significant role in the dynamic demineralization/remineralization properties of enamel, for example, as seen in initial carious lesions or the incorporation of $F^-$ after the tooth has erupted (192, 193).

The amount of $Na^+$ in enamel, like that of $Mg^{2+}$, increases towards the deeper enamel layer, whereas that of $K^+$ appears to be steadily represented throughout (519). There has been a renewed interest in $Na^+$ transport in ameloblasts because of the recent identification of a number of exchangers and contransporters that move $Na^+$ in and out of these cells (61, 234, 317, 318, 320, 416). The critical role of these proteins in enamel is evidenced by the severity of the abnormal dental phenotypes found in patients with mutations to some of these exchangers (NCKX4) and cotransporters (NBCe1), as discussed in the previous sections. NCKX4 exchanges one $K^+$ and one $Ca^{2+}$ for four $Na^+$. The similar exchange of $K^+$ and $Ca^{2+}$ and the much higher abundance of the latter in enamel suggests that there is likely a rapid removal of $K^+$ soon after secretion (61). The exact roles of $Na^+$ and $K^+$ in forming enamel crystals are poorly understood.

## XI. FLUORIDE AND DENTAL HEALTH

Dental caries is a disease caused by biofilm on the tooth surface metabolizing carbohydrates and generating acids that dissolve the tooth mineral. As noted above, incorporation of fluoride into enamel occurs during development and enamel mineralization, and also after the dental crown is fully formed and has erupted into the mouth due to continued environmental exposure (250, 626). Reduced enamel solubility due to fluoride incorporation is one of the mechanisms whereby fluoride helps reduce the risk for developing dental caries. Fluoride ions are incorporated into the hydroxyapatite (Hap) molecular structure through substitution for hydroxide or carbonate ions creating fluoride-enriched Hap (45). Fluoride is not uniformly distributed throughout the dental crown and is most abundant in the outer layers of enamel compared with the enamel closer to the dentin (625). As the fluoride level in enamel increases and the carbonate level decreases, the enamel becomes less acid soluble.

Another caries prevention mechanism for fluoride occurs through exposure of partially demineralized and damaged enamel crystallites to $F^-$, $Ca^{2+}$, and $PO_4^{3-}$ (200). Fluorine is highly reactive, allowing fluoride ions to attach to the partially demineralized enamel crystallites and then react with $Ca^{2+}$ and $PO_4^{3-}$ ions that are present in saliva or provided via therapeutic agents designed to control dental caries. Through this process, known as remineralization, fluoride is able to help repair the damaged crystallites and assist in replacing mineral content lost during acid exposure or demineralization (140).

Because of these properties, the acquisition of fluoride in the diet of pregnant and nursing mothers, and young children up to the time when enamel is fully formed on all permanent teeth except the third molars (circa 8 yr of age), is widely recommended by dentists and pediatricians. Fluoride is often present in, or added to, drinking water. Natural concentrations vary depending on the ground water aquifer, but the current optimal recommended level in the United States is 0.7 ppm or 0.7 mg/liter (8, 69, 139, 277, 426). If fluoride is not present in the drinking water, or present at suboptimal levels, fluoride can be given as a dietary supplement in the form of sodium fluoride salt, with the dosage (0.25–1.0mg $F^-$/day or 0.55–2.2mg NaF/day) being predicated on factors such as risk for developing dental caries, the individual's age and stage of tooth development, and consideration of their overall fluoride exposure (69).

The inverse relationship of fluoride exposure in drinking water to dental caries prevalence was discovered by evaluating populations exposed to naturally occurring variations in drinking water fluoride concentrations (101). These early epidemiological studies led to community water fluoridation studies that confirmed the reduction in tooth decay when water had 0.7–1 ppm fluoride ions compared with no fluoride. Epidemiological studies also revealed that exposure to fluoride levels in excess of 1 ppm during enamel formation increased the risk of developing dental fluorosis (142). The inverse relationship between dental caries and dental fluorosis with respect to drinking water fluoride content is illustrated in **FIGURE 14**. As stated above, in the United States, the Department of Health and Human Services recommends community drinking water have an optimal fluoride level of 0.7 ppm. Worldwide most dentists recommend that everyone, throughout their lifetime, continuously expose their teeth to fluoride from sources such as fluoride-containing drinking water (at 0.7 ppm) and fluoride-containing toothpastes.

Enamel fluorosis is an irreversible pathological condition characterized by hypomineralization of the enamel due to excessive exposure to fluoride during enamel development/mineralization. The level of hypomineralization and clinical appearance of the fluorotic enamel varies from mild to severe **(FIGURE 15)** and is partially determined by the amount of fluoride in the individual's serum (471). Individuals have differing risk and resistance to developing dental fluorosis based on their genetic makeup and health. Studies indicate there are likely multiple genes that are important in defining variance for dental fluorosis risk (132). Fluoride has a variety of actions that contribute to the development of dental fluorosis including direct effects on the ameloblasts, the developing matrix, and processing of the matrix, altering the proton release during mineralization and how these protons are handled during pH regulation (18, 24, 106, 351). The combined effects on these processes during amelogenesis cause a dose-dependent response to excessive fluoride that results in changes in the enamel crystallite morphology and packing, presenting ultimately as decreased enamel mineral content.

## XII. DEVELOPMENTAL ANOMALIES IMPACTING ENAMEL

Enamel development can be perturbed by many different environmental influences and genetic alterations. Amelogenesis is a highly regulated process and can be negatively influenced by pathological/medical conditions such as fever, infection, trauma, changes in oxygen saturation, antibiotics, and many other factors **(TABLE 1)** (397, 571). The enamel phenotype resulting from different types of insults during amelogenesis will vary depending on the type of stress as well as duration and intensity of the influence. In general, the resulting enamel defects can be classified as defects in the amount of enamel (hypoplasia) or deficiencies in the mineral content (hypomineralization). Enamel hypoplasia can be generalized throughout the dentition or it can be localized. Environmental stressors that are of short duration (e.g., fever) often cause localized defects, whereas

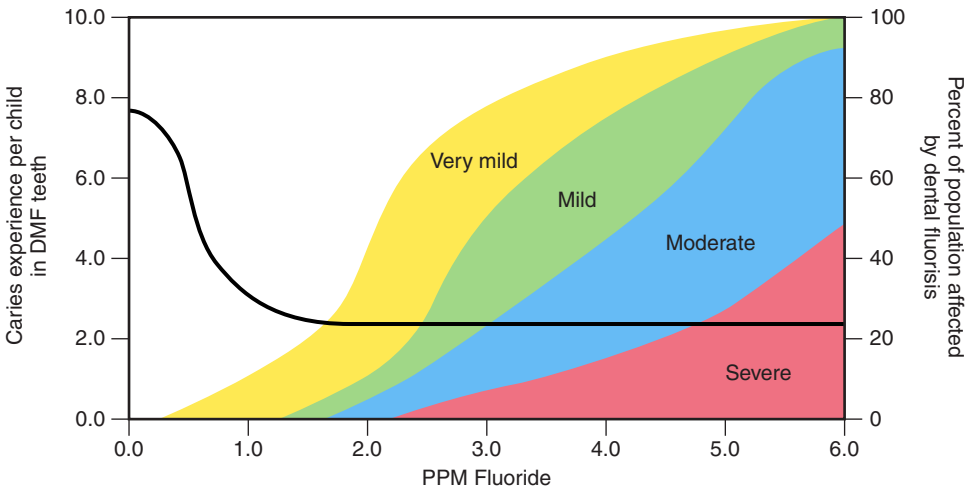


**FIGURE 14.** This graph shows that the level of dental caries, as measured by Decayed, Missing and Filled (DMF) Teeth (shown on *left y*-axis), increases as the drinking water fluoride level decreases from 6 ppm to 0 ppm as shown on the *x*-axis. Conversely, the prevalence of dental fluorosis increases in the population from ~0% affected individuals when there is no fluoride in the water to ~100% of individuals being affected when the drinking water fluoride concentration is 6 ppm. The severity of fluorosis increases as the drinking water fluoride concentration increases.

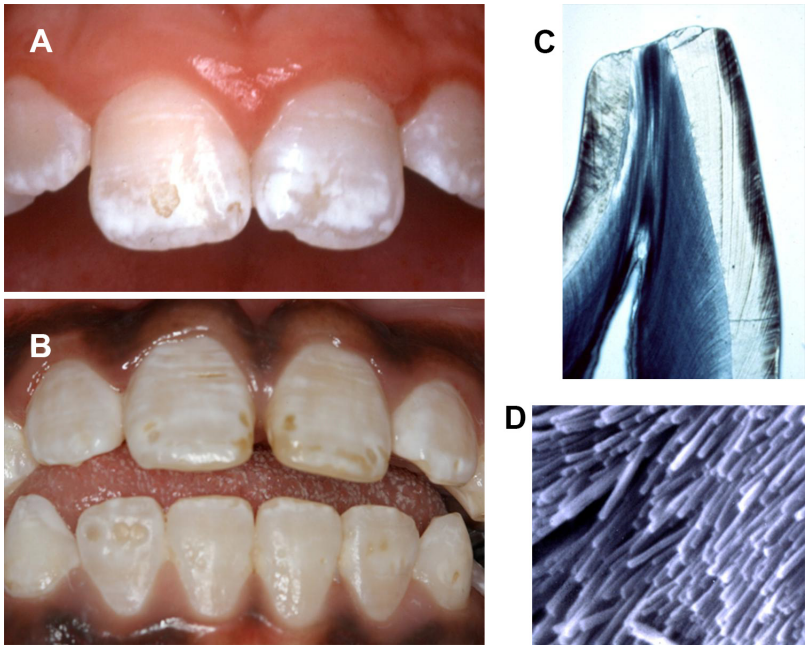


**FIGURE 15.** Clinical appearance of hypomineralized teeth resulting from high fluoride exposure during development. In milder cases, the enamel has an opaque white appearance (*A*) while in moderate to severe cases the enamel will be yellow brown in color and have areas that break or wear away from the tooth, often leaving round "punched-out" areas (*B*). These changes in enamel color and strength as a result of hypomineralization are seen in this thin section of a tooth viewed with light microscopy that shows the outer opaque hypomineralized enamel in contrast to the more normal translucent enamel (*C*). Changes in enamel crystallite morphology and packing (i.e., increased spacing) resulting from dental fluorosis are illustrated in this high-resolution electron micrograph of a fractured enamel sample with no etching before imaging (SE 80,000K) (*D*).

chronic stressors (e.g., elevated fluoride exposure) are more likely to be associated with generalized defects **(TABLE 1)**.

Enamel defects are common in the general population, with reports suggesting that between 20 and 80% of the world's population have enamel defects (538, 570). The broad range of reported enamel defect prevalence is largely due to inclusion criteria for what constitutes an enamel defect (e.g., actual hypoplasia or a deficiency in the amount of enamel vs. a color change indicating hypomineralization). Not all teeth, or even all surfaces of teeth, are affected equally by enamel defects even though they form at the same time. Children having more frequent and serious illnesses are more likely to have enamel defects.

Not uncommonly, children (2–15%) have enamel defects of the facial or front surface of their primary canine teeth (395, 535). It has been hypothesized that these lesions occur due to the thin or often fenestrated bone over the developing canine teeth during infancy that predisposes them to minor trauma, leading to enamel defects (535). Another common enamel defect involves any or all of the first permanent molars (prevalence range from 5 to 25% of children) and can vary markedly in severity of hypomineralization (168, 627). The more severely hypomineralized the molars, the more likely it is that there will be defects of the permanent incisor enamel as well. This condition is called molar incisor hypomineralization (MIH); in its mildest form the enamel shows only a minor color change and altered opacity, while in the severe forms the enamel breaks away from the tooth during eruption, leading to loss of the enamel and not uncommonly the tooth **(FIGURE 16)**. Teeth affected by MIH are often very sensitive to thermal or chemical stimulation as they do not have an adequately mineralized enamel-insulating layer. The etiology of MIH is not fully understood, but it is known to be more prevalent in children that have had more significant illness (609). There is some evidence that there could be a genetic predisposition or increased sensitivity to certain environmental stressors (308). The af-

**Table 1.** *Environmental influences on enamel formation*

| Condition | Enamel Phenotype |
|---|---|
| Fever | Hypomineralization to marked hypoplasia |
| Starvation | Enamel hypoplasia |
| Excess fluoride exposure | Hypomineralization |
| Trauma | Hypomineralization to marked hypoplasia |
| Hypoxia (e.g., severe cardiac defect) | Hypomineralization to marked hypoplasia |
| Infection (congenital syphilis, cytomegalo virus, congenital rubella) | Hypomineralization to marked hypoplasia |
| Tetracycline | Hypoplasia |
| Low birth weight | Hypoplasia |


**FIGURE 16.** Molar incisor hypomineralization (MIH). The first permanent molar (*A*) has a creamy yellow brown coloration that is mostly contained on the biting occlusal surface and has not resulted in any enamel loss in this mild to moderate case. In contrast, this first permanent molar (*B*) from the same individual has severe enamel loss over much of the tooth. This child had a relatively marked enamel phenotype of the permanent central incisors (*C*) while the permanent lateral incisor (left area of the panel) appears normal.

fected areas of enamel have an increased protein content and decreased mineral content.

## XIII. GENETIC DISEASES IMPACTING ENAMEL

There are thousands of genes expressed by ameloblasts (318, 664) and ~100 different hereditary conditions associated with an enamel phenotype (642). The majority of hereditary conditions affecting enamel formation are syndromes that have more generalized clinical manifestations and phenotypes extending beyond the dental enamel. Many of these conditions are caused by genes that have a known function in ameloblasts. The pathophysiology resulting from these genetic alterations and ameloblast dysfunction most commonly results in a hypoplastic enamel phenotype. For example, junctional epidermolysis bullosa is caused by mutations in genes that are expressed by ameloblasts and are important in cell-to-cell adhesion (e.g., COL17A1, LAMB3, IGTA6, and ITGB4) (645). The abnormal proteins produced from these genes result in fragile skin that blisters. In ameloblasts, abnormal function of these proteins results in cells that do not adhere to each other or to the stratum intermedium, resulting in cell separation and enamel hypoplasia **(FIGURE 17)**. Interestingly, some mutation in genes such as LAMB3 can be associated with a syndrome such as epidermolysis bullosa or can result in only an enamel phenotype (296, 453, 618).

A review of the known hereditary conditions associated with enamel defects, identifying mutations in genes coding for transcription factors, growth factors, matrix proteins, ion channels, and proteinases, has been presented by Wright et al. (642). For example, mutations in the *DLX3* homeobox gene, which functions as a transcription factor, cause the tricho-dento-osseous syndrome that is associated with kinky curly hair at birth, dense-thick bone, generalized thin and or pitted enamel, and large pulp chambers (651). Mutations in the *p63* gene, which is important in cell growth, cause a variety of ectodermal dysplasia syndromes (e.g., Rapp Hodkins syndrome, ectrodactyly, ectodermal dysplasia cleft syndrome), all of which can have enamel defects (302). Many of the genes known to be critical for enamel formation were first identified by determining the molecular basis of hereditary conditions that had associated

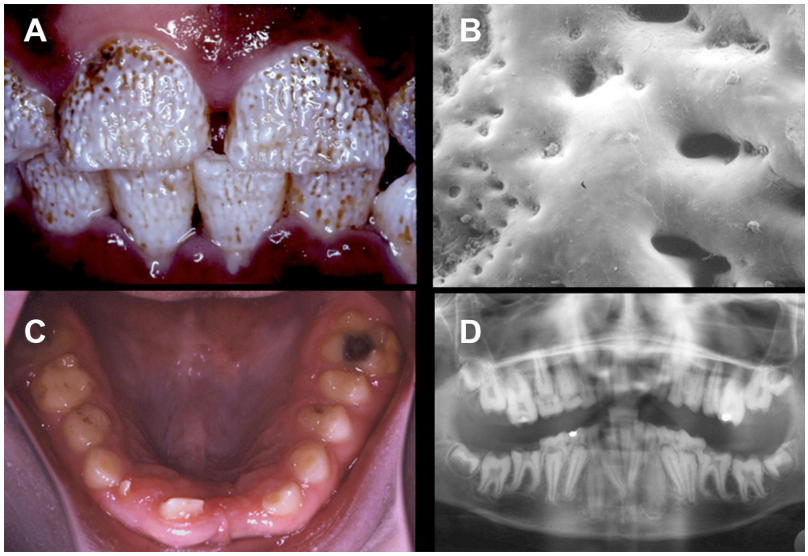


**FIGURE 17.** Abnormal enamel resulting from junctional epidermolysis bullosa. Mutations in genes associated with cell-to-cell adhesion, such as LAMA3, LAMB3, LAMC2, and COL17A1, can result in junctional epidermolysis bullosa and abnormal enamel formation. The clinical phenotype resulting from mutations in these genes is a deficiency in amount of enamel that can be localized in the form of pitting (*A*). The variation in size of the pits is thought to be a reflection of the numbers or groups of ameloblasts that are lacking appropriate cell-to-cell attachment (*B*). [*B* from Wright et al. (649a), with permission from Elsevier.] In other cases the phenotype presents as a generalized thinning of the enamel, as seen in the teeth of this individual with the Herlitz form of junctional epidermolysis bullosa (*C*). This individual also had failure of tooth eruption of the permanent dentition as seen in their panographic radiograph (*D*). This is illustrative that the developing tooth epithelium plays a role in tooth eruption as well as enamel formation.

enamel phenotypes. A recent example of this was identification of the *ROGDI* gene that is associated with Kohlschütter-Tönz syndrome (510). This syndrome has a distinct phenotype where all teeth exhibit a yellow-brown discoloration of the enamel and a decreased level of mineralization. The *ROGDI* gene was not known to be critical for enamel formation before this discovery. This gene is thought to code for a leucine-zipper protein that is highly expressed in the brain and spinal cord. Leucine zipper motifs are a structural feature common to transcription factors and other types of proteins implicated as negative transcription regulators. Another interesting association occurs in Jalili syndrome where affected individuals have cone-rod dystrophy in the eyes and enamel that has a brown appearance and is hypomineralized. This condition is caused by mutations in the cyclin and CBS domain divalent metal cation transport mediator 4 gene (*CNNM4*) that may play a role in metal ion transport (438). Cystic fibrosis (CF) is caused by mutations in the *CFTR* gene that is involved in regulating ion movement and pH regulation. Clinical evaluation of humans with CF found a high percentage of affected individuals had associated enamel defects of varying severity. In the CF mouse model (*Cftr* knockout), the incisors had an opaque-white hypomineralized phenotype that was 100% penetrant (59, 572, 646). This led to the discovery that the *Cftr* gene was expressed by and important in the regulation of pH in the developing mouse enamel organ and provided a likely explanation for the enamel defects seen in people with CF (63, 572). Other genes involved in ion transport associated with hereditary conditions resulting in immune dysfunction include the members of the $Ca^{2+}$ release-activated $Ca^{2+}$ channels STIM1 and ORAI1 (145, 447). Mutations in the $Na^{+}/K^{+}/Ca^{2+}$ exchanger NCKX4 (coded by *SLC24A4*) are directly linked with AI, but less is known about other disorders caused by mutations to *SLC24A4* that include heart disease (222, 439).

Hereditary nonsyndromic conditions primarily affecting the enamel are referred to as AI (639). The prevalence of AI varies around world and is thought to occur in ~1/8,000 people, although there has only been one epidemiological study ever conducted in the United States (638). AI describes a variety of disorders that have been classified based on their clinical phenotype and mode of inheritance, as well as based on the perceived mechanism leading to the enamel defect, i.e., deficient matrix formation leading to hypoplasia, deficient crystal growth and mineralization during the maturation stage causing a decreased level of maturation and mineralization, or abnormal initiation of the enamel crystallites with subsequent abnormal mineralization or hypocalcification (639). Both hypomaturation and hypocalcification are characterized by the predominant phenotype of decreased enamel mineral or hypomineralization (see **FIGURE 18**). Enamel affected by these types of AI has greater amounts of protein present compared with normal enamel (647).

The first gene to be associated with these conditions was *AMELX*, which codes for the most abundant enamel matrix protein, amelogenin (552–555). There are now known to be many allelic mutations in the AMELX gene that cause different alterations in the protein and result in different phenotypes (648). Missense mutations resulting in single amino acid changes are often associated with a hypomineralized enamel phenotype. Mutations causing a loss of the carboxy terminus of the amelogenin protein all result in a hypoplastic enamel phenotype. This is presumably due to the critical functionality of the carboxy terminus in amelogenin aggregation and orientation to the developing enamel crystallites. These genotype-phenotype associations result from changes in the protein function due to the alteration of specific functional domains with importance in cellular processes such as protein

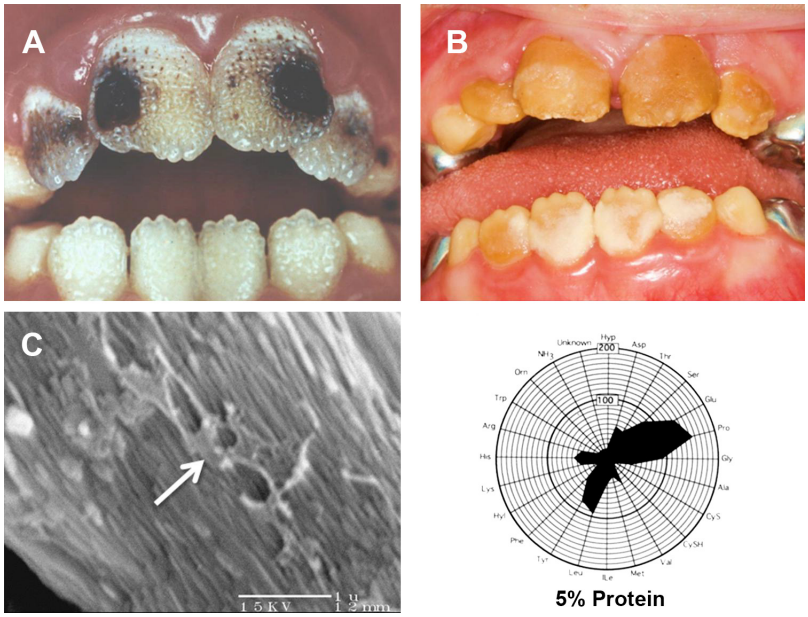


**FIGURE 18.** Amelogenesis imperfecta. Amelogenesis imperfecta (AI) is caused by mutations in numerous genes that lead to deficiencies in the amount of enamel and a hypoplastic (*A*) and/or hypomineralized enamel phenotype (*B*). [*A* from Nusier et al. (411a), with permission from Elsevier.] The hypomineralized forms typically have retained protein in the enamel, such as seen in this defective fractured enamel resulting from a FAM83H mutation (*C*), that is not normally seen in sound enamel. Lacy protein (arrow) is seen on top of the enamel crystallites that make up the underlying enamel prism or rod. In the hypomaturation AI types, the amino acid content in the retained protein resembles that of amelogenin having a high percentage of proline residues, as seen in this enamel affected with AI caused by a C4orf 26 mutation (*D*).

self-assembly, protein-mineral interactions, and changes in proteolytic processing of the mutant protein (423, 520).

Mutations causing AI have been identified in many of the known enamel extracellular matrix proteins and proteinases, along with a number of other genes **(TABLE 2)**, and there will likely be additional AI-associated genes identified in the future. The phenotypes are quite diverse, with some causing more localized enamel defects, while others are associated with generalized phenotypes affecting all the teeth and areas of enamel (641). Variability in phenotypes associated with some AI types is thought to result from mutations causing proteins to have a dominant negative effect while others cause haploinsufficiency. This is the case with mutations in the *ENAM* gene that can result in generalized thin enamel hypoplasia (dominant negative effect) or bands of pitted enamel (haploinsufficiency) (208, 293, 358). When *Enam* is knocked out in the mouse, there is a complete absence of any organized and mineralized enamel layer (229). This is thought to be illustrative of the critical role the enamelin protein plays in growth of the enamel crystallites along the C-axis.

The protein functions for several of the more recently identified causative genes (e.g., *C4ORF26*, *WDR72*, *FAM83H*) are not fully understood, and their involvement in enamel formation was discovered by evaluation of families having AI **(TABLE 2)**. *FAM83H* mutations cause autosomal dominant hypocalcified AI that is thought to be the most common type of AI in North America (295). Phenotypes associated with *FAM83H* mutations also can vary from generalized to localized enamel defects depending on the location and type of mutation and, presumably, the altered function of the resulting protein (644). FAM83H interacts with casein kinase 1 (CK1) and is thought to play a role in keratin cytoskeleton organization and desmosomes in ameloblasts (307). Mutations of the *WDR72*

**Table 2.** *Amelogenesis imperfecta: OMIM designations, genes, and phenotypes*

| Amelogenesis Imperfecta | Gene/Locus | Enamel Phenotype | Mode of Inheritance |
|---|---|---|---|
| #301200, Amelogenesis imperfecta, type IE; AI1E | *AMELX* | Hypoplasia/hypomaturation depending on mutation and protein effect | X-linked |
| #301201, Amelogenesis imperfecta, hypoplastic/hypomaturation, X-linked 2 | *Xq22-q28* | Hypoplastic and/or hypomaturation | X-linked |
| #104500, Amelogenesis imperfecta, type IB; AI1B | *ENAM* | Localized hypoplastic/generalized hypoplastic | Autosomal dominant |
| #204650, Amelogenesis imperfecta, type IC; AI1C | *ENAM* | Generalized hypoplastic | Autosomal recessive |
| #204700, Amelogenesis imperfecta, hypomaturation type, IIA1; AI2A1 | *KLK4* | Normal enamel thickness: hypomineralized orange brown color | Autosomal recessive |
| #612529, Amelogenesis imperfecta, hypomaturation type, IIA2; AI2A2 | *MMP20* | Normal enamel thickness: hypomineralized orange brown color | Autosomal recessive |
| #130900, Amelogenesis imperfecta, type III; AI3 | *FAM83H* | Localized or generalized hypomineralized enamel | Autosomal dominant |
| #613211, Amelogenesis imperfecta, hypomaturation type, IIA3; AI2A3 | *WDR72* | Hypomaturation: creamier/opaque enamel upon eruption, discoloration and loss of tissue posteruption | Autosomal recessive |
| #104510, Amelogenesis imperfecta, type IV; AI4 | *DLX3* | TDO-thin pitted hypoplastic | Autosomal dominant |
| #614253, Amelogenesis imperfecta AND gingival fibromatosis syndrome; AIGFS | *FAM20A* | Generalized hypoplastic and failure of tooth eruption, gingival hypertrophy | Autosomal recessive |
| #104530, Amelogenesis imperfecta, hypoplastic type IA, AI1A | *LAMB3* | Hypoplastic: failure to erupt and calcification of pulp | Autosomal dominant |
| #614832, Amelogenesis imperfecta, hypomaturaltion type, IIA4; AI2A4 | *C4ORF26* | Hypomaturation AI | Autosomal recessive |
| #616270, Amelogenesis imperfecta, hypoplastic type, IF, AI1F | *AMBN* | Generalized hypoplastic | Autosomal recessive |
| #615887, Amelogenesis imperfecta, hypomaturation type, IIA5, AI2A5 | *SLC24A4* | Hypomineralized: mottled appearance | Autosomal recessive |
| #Not listed, amelogenesis imperfecta, hypomaturation type | *AMTN* | Hypomineralized | Autosomal dominant |
| #Not listed, amelogenesis imperfecta, hypomaturation type | *ACPT* | Generalized hypoplastic | Autosomal recessive |
| #Not listed, amelogenesis imperfecta, hypomaturation type | *GPR68* | Hypomaturation | Autosomal recessive |

gene result in hypomaturation defects of the enamel that are thought to be caused by abnormal endocytic vesicle trafficking of matrix proteins and subsequent enamel mineralization (278, 616). The *C4orf26* gene is now thought to be tooth-specific but not enamel-specific, and it may play a role in Hap nucleation through its phosphorylated carboxy terminus (437).

Mutations in genes coding for the enamel proteinases MMP20 and KLK4 both result in hypomineralized enamel that has an orange to brown discoloration (207, 421). Abnormal function of these proteinases results in an increased retention of protein in the affected enamel, as is common to most of the hypomineralized forms of AI (647). Diminished processing and removal of the enamel matrix proteins, such and AMELX, AMBN, and ENAM, results in abnormal crystallite growth and a decreased final mineral content of the enamel (649).

As can be appreciated by the reader, discovering new genes, and identifying genotype/phenotype relationships, is ongoing. During the writing of this review paper three additional genes were been associated with AI **(TABLE 2)**. These are mutations to amelotin (*Amtn*) (546), a protein expresses exclusively during maturation-stage amelogenesis (255, 402), the pH-sensing G protein-coupled receptor *GPR68* (440), and the testicular acid phosphatase *ACPT* (512) **(TABLE 2)**.

## XIV. ENAMEL BIOMIMETICS

While enamel cannot regenerate itself or remodel like most bones do, it is nevertheless an ideal candidate to apply novel materials chemistry without the use of biology for its regeneration as it is completely acellular. Conventional restorative methods in dentistry use artificial materials like composites, ceramics, and amalgam to restore functional properties and are not discussed here. There are, however, a series of approaches available or currently being tested in the laboratory that can rebuild lost enamel structure through remineralization (92). These so-called biomimetic methods are designed to rebuild the intricate apatite crystallite structure by application of calcium phosphate chemistry that stimulates the regrowth of the natural tissue and ideally restores the mechanical and optical properties of enamel. Due to the high organization and alignment of fibrous apatite crystallites, enamel almost acts like a single crystal. It reflects only a portion of visible light and is therefore translucent (267). To mimic the translucency of enamel, the restorative process will need to rebuild the highly organized structure of enamel to perfectly blend in with the surrounding healthy tissue (267).

Initial damage on the enamel surface is often observed as "white spots" which illustrate that the organized mineral layer in enamel has been altered by a demineralization/remineralization process that most likely has been triggered by cariogenic acids produced by bacteria in the oral environment (20, 456). White spot lesions or incipient caries consist of a demineralized zone that is covered by a superficial mineral layer often comprised of larger apatite crystals, which reflect light and therefore appears white. The common treatment for those lesions is the use of fluoride, often in the form of an acidulated gel or dentifrice (68, 334, 360, 426, 589, 590). The mildly acidic composition of the delivery system will dissolve the surface mineral layer and allow fluoride ions to penetrate into the demineralized zone, which leads to an increase in saturation levels towards apatite. The reaction of this fluoride with calcium and phosphate ions then leads to the nucleation of flouroapatite crystals (191). The growing apatite crystals rebuild the structure of dental enamel fairly successfully and often fully restore its mechanical and optical properties. The simple chemistry of this approach, however, only works well on shallow lesions that are in the order of tens of micrometers deep (334, 353). Deeper lesions, and lesions that are infected with bacteria or result from secondary caries underneath a restoration, require a more sophisticated approach for recovery of form and function by the reintroduction of apatite mineral. A number of studies are currently exploring novel methods for biomimetic remineralization of such lesions (92, 337).

A fundamental difficulty with the clinical application of remineralization systems is the low solubility of calcium phosphates, particularly in the presence of fluoride ions, which makes it difficult to remineralize deeper lesions (478). In saturated solutions, mineral will precipitate randomly and thus not rebuild the enamel structure. Therefore, stabilizing agents have been developed to extend the lifetime of calcium and phosphate ions in solution (417) and thus allow for a controlled mineralization of apatite ideally through epitaxial growth of mineral onto the damaged crystalline structure in carious enamel (337). Casein, a protein present in milk, is such a stabilizing agent that facilitates the formation of ACP (95). The casein phosphopeptide-ACP complex has successfully been used for the remineralization of white spot lesions and is recommended to treat deeper lesions when a restorative treatment is not desired (408). Its success is based on the delivery of casein-stabilized ACP droplets that transform into apatite crystallites when in contact with enamel crystallites (95). Based on these studies, a number of other natural proteins, peptides, and synthetic molecules have been developed that are able to stabilize the saturated solutions and thus prevent heterogeneous nucleation while promoting homogeneous nucleation (84, 92).

The delivery of such stabilizing agents is challenging in a clinical setting as aqueous solutions will be washed out of the site and saliva can interfere with the remineralization process. The development of gels or cements that provide

sustained release of mineralizing agents is desirable. A chitosan gel has been explored that has shown great ability to crystallize apatite nanofibers with similar orientation to that observed in natural enamel (486). The ability of the gel was further enhanced when amelogenin protein was added as the thickness of the rebuilt enamel layer increased in in vitro tests, taking advantage of the growth-promoting effect of amelogenin (484, 486).

In addition to these methods that attempt to regenerate enamel on decayed teeth, there are numerous studies that emphasize the generation of enamel or an enamel-like tissue in vitro and de novo (485, 654). These approaches promote oriented crystal growth of fibrous apatite that mimics the structure of enamel. EDTA is known as a chelating agent and has been used to stabilize high concentrations of calcium phosphate ions that upon water evaporation produce a layer of nanometer-sized apatite crystals with high alignment, mimicking the structure of nonprismatic dental enamel very well (80, 81). Clinical studies are currently underway to explore this method by direct application to demineralized teeth (617). A common challenge in testing and evaluating these systems, however, is the lack of suitable standards of evaluation that allow for systematic comparison between the various approaches in vitro, leaving the ultimate litmus test to the clinical trial which requires a large number of subjects for statistical validation (353).

## XV. CONCLUSIONS

In mammals, in nonpathological conditions, dental enamel is the only epithelial-derived tissue that mineralizes. Ameloblasts are primarily responsible for the formation of enamel, which is essentially a Hap-based material containing less than 5% organic material by weight. It is because of its cellular origins that an extracellular matrix has evolved, comprised of proteins with little homology to any other animal proteins, to be capable of guiding the formation of a unique hierarchical structure with a highly ordered and very repetitive patterning. In normal situations, enamel's distinctive biomechanical properties allow it to function for the entire lifespan of an animal, despite the amount of wear resulting from mastication, clenching and grinding, and disease such as caries. Ameloblasts have a very short lifespan, relative to the life of the organism, to produce the avascular enamel that, once formed, has no reparative abilities. Amelogenesis involves a large number of activities including the formation of a temporary proteinaceous matrix conducive to mineralization followed by the removal of this matrix by endocytosis, ion transport and pH regulation, and apoptosis. Failure during any one of these stages of amelogenesis may result in pathologies impacting enamel health. We have summarized the literature related to amelogenesis, with a greater emphasis on mineralization events occurring largely during the maturation stage. We have also reviewed enamel pathologies that have been linked to known genes and discussed the role of fluoride-based and biomimetic approaches to enamel repair and conservation.

There are, however, many voids in our understanding of amelogenesis. There is an increasing need to define experimentally the transport and movement of ions in the enamel organ and to gain a deeper understanding of key functions as they relate to amelogenesis. For example, phosphate transport activities and molecular mechanisms responsible for pH regulation remain poorly understood. There is also limited information to explain ameloblast movements that result in enamel's remarkable prismatic architecture, although recent studies partly attribute this to the extensive remodeling of ameloblast junctional complexes during amelogenesis (31). It is also unknown if the small amounts of protein retained in mature enamel are ordered or not, and a recent paper has provided evidence that individual enamel crystals occlude some matrix protein (454), which may also contribute to enamel's unique biomechanical properties. It appears reasonable to suggest that remnant proteins help to achieve stiffness and hardness required for the longevity of the tooth (198). Finally, there is current interest in generating an enamel biomimetic for future dental clinical applications, with some of this work investigating amelogenin-based peptides in mineralizing solutions (194, 203, 260, 387, 432, 485). Future research in these areas will have an immensely positive impact on understanding enamel biology and disease.

## ACKNOWLEDGMENTS

We thank Daniel Ezra Johnson and Bridget Samuels for help in the preparation of this manuscript. We acknowledge the two anonymous reviewers for helpful comments that have helped improve the paper. We also acknowledge all our collaborators, co-authors, and colleagues over the past decades for the invaluable insights related to the biology of enamel, which truly is a uniquely engineered and inspiring biomaterial. In particular, we acknowledge Alan Boyde, Timothy G. Bromage, Michael J. Hubbard, Stefan Feske, Ira Kurtz, Antonio Nanci, Charles E. Smith, and Malcolm L. Snead for past and future collaborations and outstanding mentorship, for without their invaluable and novel insights into ion transport, pH regulation, and biomineralization as it relates to enamel formation this review paper would not have been possible.

Present addresses: S. Habelitz, Dept. of Preventive and Restorative Dental Sciences, Univ. of California, San Francisco, San Francisco, CA; J. T. Wright, School of Dentistry, Department of Pediatric Dentistry, University of North Carolina, Chapel Hill, NC.

Address for reprint requests and other correspondence: R. S. Lacruz, College of Dentistry, Dept. of Basic Science and Craniofacial Biology, New York University, New York, NY (e-mail: rodrigo.lacruz@nyu.edu) and M. L.

Paine, Herman Ostrow School of Dentistry, Center for Craniofacial Molecular Biology, Univ. of Southern California, Los Angeles, CA 90033 (e-mail: paine@usc.edu).

## GRANTS

This work was supported by National Institute of Dental and Craniofacial Research Grants R00 DE022799 and R01 DE025639 (to R. S. Lacruz), R01 DE025709 (to S. Habelitz), R01 DE016079 (to J. T. Wright), and R01 DE019629 and R21 DE024704 (to M. L. Paine).

## DISCLOSURES

No conflicts of interest, financial or otherwise, are declared by the authors.

## REFERENCES

1. Conference Papers. NIH Consensus Development Conference on Diagnosis and Management of Dental Caries Throughout Life. Bethesda, MD, March 26-28, 2001. *J Dent Educ* 65: 935–1179, 2001.

2. Abe S, Usami S, Hoover DM, Cohn E, Shinkawa H, Kimberling WJ. Fluctuating sensorineural hearing loss associated with enlarged vestibular aqueduct maps to 7q31, the region containing the Pendred gene. *Am J Med Genet* 82: 322–328, 1999. doi:10.1002/(SICI)1096-8628(19990212)82:4<322::AID-AJMG9>3.0.CO;2-0.

3. Aiba Y, Nakamura M, Joshita S, Inamine T, Komori A, Yoshizawa K, Umemura T, Horie H, Migita K, Yatsuhashi H, Nakamuta M, Fukushima N, Saoshiro T, Hayashi S, Kouno H, Ota H, Muro T, Watanabe Y, Nakamura Y, Komeda T, Shimada M, Masaki N, Komatsu T, Yagura M, Sugi K, Koga M, Tsukamoto K, Tanaka E, Ishibashi H; PBC Study Group in NHOSLJ. Genetic polymorphisms in CTLA4 and SLC4A2 are differentially associated with the pathogenesis of primary biliary cirrhosis in Japanese patients. *J Gastroenterol* 46: 1203–1212, 2011. doi:10.1007/s00535-011-0417-7.

4. Alberts B, Johnson A, Lewis J, Raff M, Roberts K, Walter P. *Molecular Biology of the Cell*. New York: Garland, 2002.

5. Alper SL, Rossmann H, Wilhelm S, Stuart-Tilley AK, Shmukler BE, Seidler U. Expression of AE2 anion exchanger in mouse intestine. *Am J Physiol Gastrointest Liver Physiol* 277: G321–G332, 1999.

6. Alper SL, Stuart-Tilley A, Simmons CF, Brown D, Drenckhahn D. The fodrin-ankyrin cytoskeleton of choroid plexus preferentially colocalizes with apical Na+K+-ATPase rather than with basolateral anion exchanger AE2. *J Clin Invest* 93: 1430–1438, 1994. doi:10.1172/JCI117120.

7. Alper SL, Stuart-Tilley AK, Biemesderfer D, Shmukler BE, Brown D. Immunolocalization of AE2 anion exchanger in rat kidney. *Am J Physiol Renal Fluid Electrolyte Physiol* 273: F601–F614, 1997.

8. American Academy of Pediatric Dentistry. Liaison with Other Groups Committee. Guideline on fluoride therapy. *Pediatr Dent* 34: 166–169, 2012.

9. Amyere M, Mettlen M, Van Der Smissen P, Platek A, Payrastre B, Veithen A, Courtoy PJ. Origin, originality, functions, subversions and molecular signalling of macropinocytosis. *Int J Med Microbiol* 291: 487–494, 2002. doi:10.1078/1438-4221-00157.

10. Anderson GJ, Vulpe CD. Mammalian iron transport. *Cell Mol Life Sci* 66: 3241–3261, 2009. doi:10.1007/s00018-009-0051-1.

11. Angmar-Månsson B, Ericsson Y, Ekberg O. Plasma fluoride and enamel fluorosis. *Calcif Tissue Res* 22: 77–84, 1976. doi:10.1007/BF02010348.

12. Angmar-Månsson B, Whitford GM. Enamel fluorosis related to plasma F levels in the rat. *Caries Res* 18: 25–32, 1984. doi:10.1159/000260743.

13. Angmar-Månsson B, Whitford GM. Single fluoride doses and enamel fluorosis in the rat. *Caries Res* 19: 145–152, 1985. doi:10.1159/000260841.

14. Anusavice KJ. Present and future approaches for the control of caries. *J Dent Educ* 69: 538–554, 2005.

15. Aoba T. The effect of fluoride on apatite structure and growth. *Crit Rev Oral Biol Med* 8: 136–153, 1997. doi:10.1177/10454411970080020301.

16. Aoba T, Fejerskov O. Dental fluorosis: chemistry and biology. *Crit Rev Oral Biol Med* 13: 155–170, 2002. doi:10.1177/154411130201300206.

17. Aoba T, Moreno EC. The enamel fluid in the early secretory stage of porcine amelogenesis: chemical composition and saturation with respect to enamel mineral. *Calcif Tissue Int* 41: 86–94, 1987. doi:10.1007/BF02555250.

18. Aoba T, Moreno EC, Tanabe T, Fukae M. Effects of fluoride on matrix proteins and their properties in rat secretory enamel. *J Dent Res* 69: 1248–1255, 1990. doi:10.1177/00220345900690060501.

19. Aoba T, Shimoda S, Moreno EC. Labile or surface pools of magnesium, sodium, and potassium in developing porcine enamel mineral. *J Dent Res* 71: 1826–1831, 1992. doi:10.1177/00220345920710111201.

20. Arends J, Christoffersen J. The nature of early caries lesions in enamel. *J Dent Res* 65: 2–11, 1986. doi:10.1177/00220345860650010201.

21. Arquitt CK, Boyd C, Wright JT. Cystic fibrosis transmembrane regulator gene (CFTR) is associated with abnormal enamel formation. *J Dent Res* 81: 492–496, 2002. doi:10.1177/154405910208100712.

22. Awad M, Al-Ashwal AA, Sakati N, Al-Abbad AA, Bin-Abbas BS. Long-term follow up of carbonic anhydrase II deficiency syndrome. *Saudi Med J* 23: 25–29, 2002.

23. Azevedo TD, Feijó GC, Bezerra AC. Presence of developmental defects of enamel in cystic fibrosis patients. *J Dent Child (Chic)* 73: 159–163, 2006.

24. Ba Y, Zhang H, Wang G, Wen S, Yang Y, Zhu J, Ren L, Yang R, Zhu C, Li H, Cheng X, Cui L. Association of dental fluorosis with polymorphisms of estrogen receptor gene in Chinese children. *Biol Trace Elem Res* 143: 87–96, 2011. doi:10.1007/s12011-010-8848-1.

25. Bartlett JD. Dental enamel development: proteinases and their enamel matrix substrates. *ISRN Dent* 2013: 684607, 2013. doi:10.1155/2013/684607.

26. Bartlett JD, Ball RL, Kawai T, Tye CE, Tsuchiya M, Simmer JP. Origin, splicing, and expression of rodent amelogenin exon 8. *J Dent Res* 85: 894–899, 2006. doi:10.1177/154405910608501004.

27. Bartlett JD, Ganss B, Goldberg M, Moradian-Oldak J, Paine ML, Snead ML, Wen X, White SN, Zhou YL. 3. Protein-protein interactions of the developing enamel matrix. *Curr Top Dev Biol* 74: 57–115, 2006. doi:10.1016/S0070-2153(06)74003-0.

28. Bartlett JD, Ryu OH, Xue J, Simmer JP, Margolis HC. Enamelysin mRNA displays a developmentally defined pattern of expression and encodes a protein which degrades amelogenin. *Connect Tissue Res* 39: 101–109, 1998. doi:10.3109/03008209809023916.

29. Bartlett JD, Simmer JP. Proteinases in developing dental enamel. *Crit Rev Oral Biol Med* 10: 425–441, 1999. doi:10.1177/10454411990100040101.

30. Bartlett JD, Simmer JP, Xue J, Margolis HC, Moreno EC. Molecular cloning and mRNA tissue distribution of a novel matrix metalloproteinase isolated from porcine enamel organ. *Gene* 183: 123–128, 1996. doi:10.1016/S0378-1119(96)00525-2.

31. Bartlett JD, Smith CE. Modulation of cell-cell junctional complexes by matrix metalloproteinases. *J Dent Res* 92: 10–17, 2013. doi:10.1177/0022034512463397.

32. Bawden JW. Calcium transport during mineralization. *Anat Rec* 224: 226–233, 1989. doi:10.1002/ar.1092240212.

33. Bawden JW, Wennberg A, Hammarström L. In vivo and in vitro study of 59Fe uptake in developing rat molars. *Acta Odontol Scand* 36: 271–277, 1978. doi:10.3109/00016357809029077.

34. Bechtle S, Fett T, Rizzi G, Habelitz S, Klocke A, Schneider GA. Crack arrest within teeth at the dentinoenamel junction caused by elastic modulus mismatch. *Biomaterials* 31: 4238–4247, 2010. doi:10.1016/j.biomaterials.2010.01.127.

35. Beck L, Leroy C, Beck-Cormier S, Forand A, Salaün C, Paris N, Bernier A, Ureña-Torres P, Prié D, Ollero M, Coulombel L, Friedlander G. The phosphate transporter PiT1 (Slc20a1) revealed as a new essential gene for mouse liver development. *PLoS One* 5: e9148, 2010. doi:10.1371/journal.pone.0009148.

36. Beck L, Leroy C, Salaün C, Margall-Ducos G, Desdouets C, Friedlander G. Identification of a novel function of PiT1 critical for cell proliferation and independent of its phosphate transport activity. *J Biol Chem* 284: 31363–31374, 2009. doi:10.1074/jbc.M109.053132.

37. Begenisich T, Melvin JE. Regulation of chloride channels in secretory epithelia. *J Membr Biol* 163: 77–85, 1998. doi:10.1007/s002329900372.

38. Bègue-Kirn C, Krebsbach PH, Bartlett JD, Butler WT. Dentin sialoprotein, dentin phosphoprotein, enamelysin and ameloblastin: tooth-specific molecules that are distinctively expressed during murine dental differentiation. *Eur J Oral Sci* 106: 963–970, 1998. doi:10.1046/j.0909-8836.1998.eos106510.x.

39. Beniash E, Metzler RA, Lam RS, Gilbert PU. Transient amorphous calcium phosphate in forming enamel. *J Struct Biol* 166: 133–143, 2009. doi:10.1016/j.jsb.2009.02.001.

40. Beniash E, Simmer JP, Margolis HC. Structural changes in amelogenin upon self-assembly and mineral interactions. *J Dent Res* 91: 967–972, 2012. doi:10.1177/0022034512457371.

41. Berdal A, Hotton D, Pike JW, Mathieu H, Dupret JM. Cell- and stage-specific expression of vitamin D receptor and calbindin genes in rat incisor: regulation by 1,25-dihydroxyvitamin $D_3$. *Dev Biol* 155: 172–179, 1993. doi:10.1006/dbio.1993.1016.

42. Berdal A, Hotton D, Saffar JL, Thomasset M, Nanci A. Calbindin-D9k and calbindin-D28k expression in rat mineralized tissues in vivo. *J Bone Miner Res* 11: 768–779, 1996. doi:10.1002/jbmr.5650110608.

43. Berditchevski F, Odintsova E. Tetraspanins as regulators of protein trafficking. *Traffic* 8: 89–96, 2007. doi:10.1111/j.1600-0854.2006.00515.x.

44. Bergwitz C, Roslin NM, Tieder M, Loredo-Osti JC, Bastepe M, Abu-Zahra H, Frappier D, Burkett K, Carpenter TO, Anderson D, Garabedian M, Sermet I, Fujiwara TM, Morgan K, Tenenhouse HS, Juppner H. SLC34A3 mutations in patients with hereditary hypophosphatemic rickets with hypercalciuria predict a key role for the sodium-phosphate cotransporter NaPi-IIc in maintaining phosphate homeostasis. *Am J Hum Genet* 78: 179–192, 2006. doi:10.1086/499409.

45. Bertoni E, Bigi A, Cojazzi G, Gandolfi M, Panzavolta S, Roveri N. Nanocrystals of magnesium and fluoride substituted hydroxyapatite. *J Inorg Biochem* 72: 29–35, 1998. doi:10.1016/S0162-0134(98)10058-2.

46. Bertrand CA, Zhang R, Pilewski JM, Frizzell RA. SLC26A9 is a constitutively active, CFTR-regulated anion conductance in human bronchial epithelia. *J Gen Physiol* 133: 421–438, 2009. doi:10.1085/jgp.200810097.

47. Biehs B, Hu JK, Strauli NB, Sangiorgi E, Jung H, Heber RP, Ho S, Goodwin AF, Dasen JS, Capecchi MR, Klein OD. BMI1 represses Ink4a/Arf and Hox genes to regulate stem cells in the rodent incisor. *Nat Cell Biol* 15: 846–852, 2013. doi:10.1038/ncb2766.

48. Bodier-Houllé P, Steuer P, Meyer JM, Bigeard L, Cuisinier FJ. High-resolution electron-microscopic study of the relationship between human enamel and dentin crystals at the dentinoenamel junction. *Cell Tissue Res* 301: 389–395, 2000. doi:10.1007/s004410000241.

49. Bohdanowicz M, Grinstein S. Role of phospholipids in endocytosis, phagocytosis, and macropinocytosis. *Physiol Rev* 93: 69–106, 2013. doi:10.1152/physrev.00002.2012.

50. Boll W, Ohno H, Songyang Z, Rapoport I, Cantley LC, Bonifacino JS, Kirchhausen T. Sequence requirements for the recognition of tyrosine-based endocytic signals by clathrin AP-2 complexes. *EMBO J* 15: 5789–5795, 1996.

51. Bonde J, Bülow L. Random mutagenesis of amelogenin for engineering protein nanoparticles. *Biotechnol Bioeng* 112: 1319–1326, 2015. doi:10.1002/bit.25556.

52. Bori E, Guo J, Rácz R, Burghardt B, Földes A, Kerémi B, Harada H, Steward MC, Den Besten P, Bronckers AL, Varga G. Evidence for bicarbonate secretion by ameloblasts in a novel cellular model. *J Dent Res* 95: 588–596, 2016. doi:10.1177/0022034515625939.

53. Borke JL, Zaki AE, Eisenmann DR, Ashrafi SH, Ashrafi SS, Penniston JT. Expression of plasma membrane $Ca^{2+}$ pump epitopes parallels the progression of enamel and dentin mineralization in rat incisor. *J Histochem Cytochem* 41: 175–181, 1993. doi:10.1177/41.2.7678268.

54. Borke JL, Eisenmann DR, Zaki AE-M, Mednieks MI. Localization of plasma membrane $Ca^{2+}$ pump mRNA and protein in human ameloblasts by in situ hybridization and immunohistochemistry. *Connect Tissue Res* 33: 139–144, 1995. doi:10.3109/03008209509016993.

55. Bosley TM, Salih MA, Alorainy IA, Islam MZ, Oystreck DT, Suliman OS, Malki S, Suhaibani AH, Khiari H, Beckers S, van Wesenbeeck L, Perdu B, AlDrees A, Elmalik SA, Van Hul W, Abu-Amero KK. The neurology of carbonic anhydrase type II deficiency syndrome. *Brain* 134: 3502–3515, 2011. doi:10.1093/brain/awr302.

56. Bourd-Boittin K, Septier D, Hall R, Goldberg M, Menashi S. Immunolocalization of enamelysin (matrix metalloproteinase-20) in the forming rat incisor. *J Histochem Cytochem* 52: 437–445, 2004. doi:10.1177/002215540405200402.

57. Breton S, Alper SL, Gluck SL, Sly WS, Barker JE, Brown D. Depletion of intercalated cells from collecting ducts of carbonic anhydrase II-deficient (CAR2 null) mice. *Am J Physiol Renal Fluid Electrolyte Physiol* 269: F761–F774, 1995.

58. Bromley KM, Lakshminarayanan R, Lei YP, Snead ML, Moradian-Oldak J. Folding, assembly, and aggregation of recombinant murine amelogenins with T21I and P41T point mutations. *Cells Tissues Organs* 194: 284–290, 2011. doi:10.1159/000324342.

59. Bronckers A, Kalogeraki L, Jorna HJ, Wilke M, Bervoets TJ, Lyaruu DM, Zandieh-Doulabi B, DenBesten P, de Jonge H. The cystic fibrosis transmembrane conductance regulator (CFTR) is expressed in maturation stage ameloblasts, odontoblasts and bone cells. *Bone* 46: 1188–1196, 2010. doi:10.1016/j.bone.2009.12.002.

60. Bronckers AL, Guo J, Zandieh-Doulabi B, Bervoets TJ, Lyaruu DM, Li X, Wangemann P, DenBesten P. Developmental expression of solute carrier family 26A member 4 (SLC26A4/pendrin) during amelogenesis in developing rodent teeth. *Eur J Oral Sci* 119, Suppl 1: 185–192, 2011. doi:10.1111/j.1600-0722.2011.00901.x.

61. Bronckers AL, Lyaruu D, Jalali R, Medina JF, Zandieh-Doulabi B, DenBesten PK. Ameloblast modulation and transport of $Cl^-$, $Na^+$, and $K^+$ during amelogenesis. *J Dent Res* 94: 1740–1747, 2015. doi:10.1177/0022034515606900.

62. Bronckers AL, Lyaruu DM, DenBesten PK. The impact of fluoride on ameloblasts and the mechanisms of enamel fluorosis. *J Dent Res* 88: 877–893, 2009. doi:10.1177/0022034509343280.

63. Bronckers AL, Lyaruu DM, Guo J, Bijvelds MJ, Bervoets TJ, Zandieh-Doulabi B, Medina JF, Li Z, Zhang Y, DenBesten PK. Composition of mineralizing incisor enamel in cystic fibrosis transmembrane conductance regulator-deficient mice. *Eur J Oral Sci* 123: 9–16, 2015. doi:10.1111/eos.12163.

64. Bronckers AL, Lyaruu DM, Jalali R, DenBesten PK. Buffering of protons released by mineral formation during amelogenesis in mice. *Eur J Oral Sci* 124: 415–425, 2016. doi:10.1111/eos.12287.

65. Bronckers AL, Lyaruu DM, Jansen ID, Medina JF, Kellokumpu S, Hoeben KA, Gawenis LR, Oude-Elferink RP, Everts V. Localization and function of the anion exchanger Ae2 in developing teeth and orofacial bone in rodents. *J Exp Zool B Mol Dev Evol* 312B: 375–387, 2009. doi:10.1002/jez.b.21267.

66. Brookes SJ, Lyngstadaas SP, Robinson C, Shore RC, Wood SR, Kirkham J. Enamelin compartmentalization in developing porcine enamel. *Connect Tissue Res* 43: 477–481, 2002. doi:10.1080/03008200290000862.

67. Brookes SJ, Robinson C, Kirkham J, Bonass WA. Biochemistry and molecular biology of amelogenin proteins of developing dental enamel. *Arch Oral Biol* 40: 1–14, 1995. doi:10.1016/0003-9969(94)00135-X.

68. Buzalaf MA, Pessan JP, Honório HM, ten Cate JM. Mechanisms of action of fluoride for caries control. *Monogr Oral Sci* 22: 97–114, 2011. doi:10.1159/000325151.

69. Carey CM. Focus on fluorides: update on the use of fluoride for the prevention of dental caries. *J Evid Based Dent Pract* 14, Suppl: 95–102, 2014. doi:10.1016/j.jebdp.2014.02.004.

70. Carneiro KM, Zhai H, Zhu L, Horst JA, Sitlin M, Nguyen M, Wagner M, Simpliciano C, Milder M, Chen CL, Ashby P, Bonde J, Li W, Habelitz S. Amyloid-like ribbons of amelogenins in enamel mineralization. *Sci Rep* 6: 23105, 2016. doi:10.1038/srep23105.

71. Caterina JJ, Skobe Z, Shi J, Ding Y, Simmer JP, Birkedal-Hansen H, Bartlett JD. Enamelysin (matrix metalloproteinase-20) deficient mice display an amelogenesis imperfecta phenotype. *J Biol Chem* 277: 49598–49604, 2002. doi:10.1074/jbc.M209100200.

72. Cerný R, Slaby I, Hammarström L, Wurtz T. A novel gene expressed in rat ameloblasts codes for proteins with cell binding domains. *J Bone Miner Res* 11: 883–891, 1996. doi:10.1002/jbmr.5650110703.

73. Cetrullo N, Guadagni MG, Piana G. Two cases of familial hypomagnesemia with hypercalciuria and nephrocalcinosis: dental findings. *Eur J Paediatr Dent* 7: 146–150, 2006.

74. Chai Y, Jiang X, Ito Y, Bringas P Jr, Han J, Rowitch DH, Soriano P, McMahon AP, Sucov HM. Fate of the mammalian cranial neural crest during tooth and mandibular morphogenesis. *Development* 127: 1671–1679, 2000.

75. Chan YL, Ngan AH, King NM. Nano-scale structure and mechanical properties of the human dentine-enamel junction. *J Mech Behav Biomed Mater* 4: 785–795, 2011. doi:10.1016/j.jmbbm.2010.09.003.

76. Chang EH, Lacruz RS, Bromage TG, Bringas P Jr, Welsh MJ, Zabner J, Paine ML. Enamel pathology resulting from loss of function in the cystic fibrosis transmembrane conductance regulator in a porcine animal model. *Cells Tissues Organs* 194: 249–254, 2011. doi:10.1159/000324248.

77. Chardin H, Septier D, Goldberg M. Immunolocalization of a 110 kD molecule and a 150 kD molecule in rat incisor and mandibular bone. *J Biol Buccale* 19: 99–105, 1991.

78. Chávez JC, Hernández-González EO, Wertheimer E, Visconti PE, Darszon A, Treviño CL. Participation of the Cl-/HCO(3)- exchangers SLC26A3 and SLC26A6, the Cl- channel CFTR, and the regulatory factor SLC9A3R1 in mouse sperm capacitation. *Biol Reprod* 86: 1–14, 2012. doi:10.1095/biolreprod.111.094037.

79. Chen CL, Bromley KM, Moradian-Oldak J, DeYoreo JJ. In situ AFM study of amelogenin assembly and disassembly dynamics on charged surfaces provides insights on matrix protein self-assembly. *J Am Chem Soc* 133: 17406–17413, 2011. doi:10.1021/ja206849c.

80. Chen H, Clarkson BH, Sun K, Mansfield JF. Self-assembly of synthetic hydroxyapatite nanorods into an enamel prism-like structure. *J Colloid Interface Sci* 288: 97–103, 2005. doi:10.1016/j.jcis.2005.02.064.

81. Chen H, Tang Z, Liu J, Sun K, Chang SR, Peters MC, Mansfield JF, Czajka-Jakubowska A, Clarkson BH. Acellular synthesis of a human enamel-like microstructure. *Adv Mater* 18: 1846–1851, 2006. doi:10.1002/adma.200502401.

82. Chen J, Yang HY, Shi YH, Li MY. An interaction between leukocyte cell-derived chemotaxin 2 and transferrin of ayu, *Plecoglossus altivelis*. *Fish Shellfish Immunol* 26: 536–542, 2009. doi:10.1016/j.fsi.2009.02.010.

83. Chen J, Zhang Y, Mendoza J, DenBesten P. Calcium-mediated differentiation of ameloblast lineage cells in vitro. *J Exp Zool B Mol Dev Evol* 312B: 458–464, 2009. doi:10.1002/jez.b.21279.

84. Chen L, Yuan H, Tang B, Liang K, Li J. Biomimetic remineralization of human enamel in the presence of polyamidoamine dendrimers in vitro. *Caries Res* 49: 282–290, 2015. doi:10.1159/000375376.

85. Choi BY, Muskett J, King KA, Zalewski CK, Shawker T, Reynolds JC, Butman JA, Brewer CC, Stewart AK, Alper SL, Griffith AJ. Hereditary hearing loss with thyroid abnormalities. *Adv Otorhinolaryngol* 70: 43–49, 2011. doi:10.1159/000322469.

86. Choi M, Scholl UI, Ji W, Liu T, Tikhonova IR, Zumbo P, Nayir A, Bakkaloğlu A, Ozen S, Sanjad S, Nelson-Williams C, Farhi A, Mane S, Lifton RP. Genetic diagnosis by whole exome capture and massively parallel DNA sequencing. *Proc Natl Acad Sci USA* 106: 19096–19101, 2009. doi:10.1073/pnas.0910672106.

87. Christensen EI, Birn H. Megalin and cubilin: multifunctional endocytic receptors. *Nat Rev Mol Cell Biol* 3: 258–266, 2002. doi:10.1038/nrm778.

88. Christensen EI, Verroust PJ. Megalin and cubilin, role in proximal tubule function and during development. *Pediatr Nephrol* 17: 993–999, 2002. doi:10.1007/s00467-002-0956-5.

89. Christoffersen J, Arends J. [Early stages of caries lesions in enamel]. *Tandlaegebladet* 90: 765–767, 1986.

90. Chun YH, Lu Y, Hu Y, Krebsbach PH, Yamada Y, Hu JC, Simmer JP. Transgenic rescue of enamel phenotype in Ambn null mice. *J Dent Res* 89: 1414–1420, 2010. doi:10.1177/0022034510379223.

91. Chun YH, Yamakoshi Y, Yamakoshi F, Fukae M, Hu JC, Bartlett JD, Simmer JP. Cleavage site specificity of MMP-20 for secretory-stage ameloblastin. *J Dent Res* 89: 785–790, 2010. doi:10.1177/0022034510366903.

92. Cochrane NJ, Cai F, Huq NL, Burrow MF, Reynolds EC. New approaches to enhanced remineralization of tooth enamel. *J Dent Res* 89: 1187–1197, 2010. doi:10.1177/0022034510376046.

93. Coyle B, Reardon W, Herbrick JA, Tsui LC, Gausden E, Lee J, Coffey R, Grueters A, Grossman A IV, Phelps PD, Luxon L, Kendall-Taylor P, Scherer SW, Trembath RC. Molecular analysis of the PDS gene in Pendred syndrome. *Hum Mol Genet* 7: 1105–1112, 1998. doi:10.1093/hmg/7.7.1105.

94. Crawford PJ, Aldred M, Bloch-Zupan A. Amelogenesis imperfecta. *Orphanet J Rare Dis* 2: 17, 2007. doi:10.1186/1750-1172-2-17.

95. Cross KJ, Huq NL, Reynolds EC. Casein phosphopeptides in oral health--chemistry and clinical applications. *Curr Pharm Des* 13: 793–800, 2007. doi:10.2174/138161207780363086.

96. Cua FT. Calcium and phosphorous in teeth from children with and without cystic fibrosis. *Biol Trace Elem Res* 30: 277–289, 1991. doi:10.1007/BF02991422.

97. Cuisinier FJ, Steuer P, Senger B, Voegel JC, Frank RM. Human amelogenesis. I: High resolution electron microscopy study of ribbon-like crystals. *Calcif Tissue Int* 51: 259–268, 1992. doi:10.1007/BF00334485.

98. Davideau JL, Celio MR, Hotton D, Berdal A. Developmental pattern and subcellular localization of parvalbumin in the rat tooth germ. *Arch Oral Biol* 38: 707–715, 1993. doi:10.1016/0003-9969(93)90011-A.

99. Dawes C, Weatherell JA. Kinetics of fluoride in the oral fluids. *J Dent Res* 69, Suppl 2: 638–644, 1990. doi:10.1177/00220345900690S125.

100. Deakins M, Volker JF. Amount of organic matter in enamel from several types of human teeth. *J Dent Res* 20: 117–121, 1941. doi:10.1177/00220345410200020201.

101. Dean HT. The investigation of physiological effects by the epidemiological method. In: *Fluorine and Dental Health*, edited by Moulton FR. Washington, DC: AAAS, 1942, p. 23–33.

102. Dean RL. Kinetic studies with alkaline phosphatase in the presence and absence of inhibitors and divalent cations. *Biochem Mol Biol Educ* 30: 401–407, 2002. doi:10.1002/bmb.2002.494030060138.

103. Delgado S, Vidal N, Veron G, Sire JY. Amelogenin, the major protein of tooth enamel: a new phylogenetic marker for ordinal mammal relationships. *Mol Phylogenet Evol* 47: 865–869, 2008. doi:10.1016/j.ympev.2008.01.025.

104. Delsuc F, Gasse B, Sire JY. Evolutionary analysis of selective constraints identifies ameloblastin (AMBN) as a potential candidate for amelogenesis imperfecta. *BMC Evol Biol* 15: 148, 2015. doi:10.1186/s12862-015-0431-0.

105. Demirci FY, Chang MH, Mah TS, Romero MF, Gorin MB. Proximal renal tubular acidosis and ocular pathology: a novel missense mutation in the gene (SLC4A4) for sodium bicarbonate cotransporter protein (NBCe1). *Mol Vis* 12: 324–330, 2006.

106. DenBesten PK. Effects of fluoride on protein secretion and removal during enamel development in the rat. *J Dent Res* 65: 1272–1277, 1986. doi:10.1177/00220345860650101401.

107. DenBesten PK. Mechanism and timing of fluoride effects on developing enamel. *J Public Health Dent* 59: 247–251, 1999. doi:10.1111/j.1752-7325.1999.tb03277.x.

108. DenBesten PK, Crenshaw MA. The effects of chronic high fluoride levels on forming enamel in the rat. *Arch Oral Biol* 29: 675–679, 1984. doi:10.1016/0003-9969(84)90171-7.

109. DenBesten PK, Crenshaw MA, Wilson MH. Changes in the fluoride-induced modulation of maturation stage ameloblasts of rats. *J Dent Res* 64: 1365–1370, 1985. doi:10.1177/00220345850640120701.

110. DenBesten PK, Heffernan LM. Enamel proteases in secretory and maturation enamel of rats ingesting 0 and 100 PPM fluoride in drinking water. *Adv Dent Res* 3: 199–202, 1989. doi:10.1177/08959374890030022001.

111. Deshpande AS, Fang PA, Simmer JP, Margolis HC, Beniash E. Amelogenin-collagen interactions regulate calcium phosphate mineralization in vitro. *J Biol Chem* 285: 19277–19287, 2010. doi:10.1074/jbc.M109.079939.

112. Deutsch D, Haze-Filderman A, Blumenfeld A, Dafni L, Leiser Y, Shay B, Gruenbaum-Cohen Y, Rosenfeld E, Fermon E, Zimmermann B, Haegewald S, Bernimoulin JP, Taylor AL. Amelogenin, a major structural protein in mineralizing enamel, is also expressed in soft tissues: brain and cells of the hematopoietic system. *Eur J Oral Sci* 114, Suppl 1: 183–189, 2006. doi:10.1111/j.1600-0722.2006.00301.x.

113. Di Pietro SM, Dell'Angelica EC. The cell biology of Hermansky-Pudlak syndrome: recent advances. *Traffic* 6: 525–533, 2005. doi:10.1111/j.1600-0854.2005.00299.x.

114. Diekwisch TG. Subunit compartments of secretory stage enamel matrix. *Connect Tissue Res* 38: 101–111, 1998. doi:10.3109/03008209809017026.

115. Diekwisch TGH, Berman BJ, Gentner S, Slavkin HC. Initial enamel crystals are not spatially associated with mineralized dentine. *Cell Tissue Res* 279: 149–167, 1995. doi:10.1007/BF00300701.

116. Ding H, Pan H, Xu X, Tang R. Toward a detailed understanding of magnesium ions on hydroxyapatite inhibition. *Cryst Growth Des* 14: 763–769, 2014. doi:10.1021/cg401619s.

117. Dinour D, Chang MH, Satoh J, Smith BL, Angle N, Knecht A, Serban I, Holtzman EJ, Romero MF. A novel missense mutation in the sodium bicarbonate cotransporter (NBCe1/SLC4A4) causes proximal tubular acidosis and glaucoma through ion transport defects. *J Biol Chem* 279: 52238–52246, 2004. doi:10.1074/jbc.M406591200.

118. Dogterom AA, Bronckers AL. Carbonic anhydrase in developing hamster molars. *J Dent Res* 62: 789–791, 1983. doi:10.1177/00220345830620070201.

119. Doherty GJ, McMahon HT. Mechanisms of endocytosis. *Annu Rev Biochem* 78: 857–902, 2009. doi:10.1146/annurev.biochem.78.081307.110540.

120. Dorozhkin SV, Epple M. Biological and medical significance of calcium phosphates. *Angew Chem Int Ed Engl* 41: 3130–3146, 2002. doi:10.1002/1521-3773(20020902)41:17<3130::AID-ANIE3130>3.0.CO;2-1.

121. Dror AA, Politi Y, Shahin H, Lenz DR, Dossena S, Nofziger C, Fuchs H, Hrabé de Angelis M, Paulmichl M, Weiner S, Avraham KB. Calcium oxalate stone formation in the inner ear as a result of an Slc26a4 mutation. *J Biol Chem* 285: 21724–21735, 2010. doi:10.1074/jbc.M110.120188.

122. Drumm ML, Collins FS. Molecular biology of cystic fibrosis. *Mol Genet Med* 3: 33–68, 1993. doi:10.1016/B978-0-12-462003-2.50006-7.

123. Du C, Falini G, Fermani S, Abbott C, Moradian-Oldak J. Corrections and Clarifications: Supramolecular assembly of amelogenin nanospheres into birefringent microribbons. *Science* 309: 2166b, 2005. doi:10.1126/science.309.5744.2166b.

124. Du C, Falini G, Fermani S, Abbott C, Moradian-Oldak J. Supramolecular assembly of amelogenin nanospheres into birefringent microribbons. *Science* 307: 1450–1454, 2005. doi:10.1126/science.1105675.

125. Duan X. Ion channels, channelopathies, and tooth formation. *J Dent Res* 93: 117–125, 2014. doi:10.1177/0022034513507066.

126. Dunglas C, Septier D, Paine ML, Zhu DH, Snead ML, Goldberg M. Ultrastructure of forming enamel in mouse bearing a transgene that disrupts the amelogenin self-assembly domains. *Calcif Tissue Int* 71: 155–166, 2002. doi:10.1007/s00223-001-2116-5.

127. Eanes ED. Dynamics of calcium phosphate precipitation. In: *Calcification in Biological Systems*, edited by Bonucci E. Boca Raton, FL: CRC, 1991, p. 1–18.

128. Eanes ED. Enamel apatite: chemistry, structure and properties. *J Dent Res* 58, Suppl 2: 829–836, 1979. doi:10.1177/00220345790580023501.

129. Eng B, Ainsworth P, Waye JS. Anomalous migration of PCR products using nondenaturing polyacrylamide gel electrophoresis: the amelogenin sex-typing system. *J Forensic Sci* 39: 1356–1359, 1994. doi:10.1520/JFS13724J.

130. Erdheim J. Zur Kenntnis der parathyreopriven dentinveranderungen. *Frankf Z Pathol* 7: 238–248, 1911.

131. Everett ET. Fluoride's effects on the formation of teeth and bones, and the influence of genetics. *J Dent Res* 90: 552–560, 2011. doi:10.1177/0022034510384626.

132. Everett ET, Yin Z, Yan D, Zou F. Fine mapping of dental fluorosis quantitative trait loci in mice. *Eur J Oral Sci* 119, Suppl 1: 8–12, 2011. doi:10.1111/j.1600-0722.2011.00868.x.

133. Everett LA, Belyantseva IA, Noben-Trauth K, Cantos R, Chen A, Thakkar SI, Hoogstraten-Miller SL, Kachar B, Wu DK, Green ED. Targeted disruption of mouse Pds provides insight about the inner-ear defects encountered in Pendred syndrome. *Hum Mol Genet* 10: 153–161, 2001. doi:10.1093/hmg/10.2.153.

134. Everett LA, Glaser B, Beck JC, Idol JR, Buchs A, Heyman M, Adawi F, Hazani E, Nassir E, Baxevanis AD, Sheffield VC, Green ED. Pendred syndrome is caused by mutations in a putative sulphate transporter gene (PDS). *Nat Genet* 17: 411–422, 1997. doi:10.1038/ng1297-411.

135. Fagrell TG, Lingström P, Olsson S, Steiniger F, Norén JG. Bacterial invasion of dentinal tubules beneath apparently intact but hypomineralized enamel in molar teeth with molar incisor hypomineralization. *Int J Paediatr Dent* 18: 333–340, 2008. doi:10.1111/j.1365-263X.2007.00908.x.

136. Fang PA, Conway JF, Margolis HC, Simmer JP, Beniash E. Hierarchical self-assembly of amelogenin and the regulation of biomineralization at the nanoscale. *Proc Natl Acad Sci USA* 108: 14097–14102, 2011. doi:10.1073/pnas.1106228108.

137. Fang PA, Margolis HC, Conway JF, Simmer JP, Beniash E. CryoTEM study of effects of phosphorylation on the hierarchical assembly of porcine amelogenin and its regulation of mineralization in vitro. *J Struct Biol* 183: 250–257, 2013. doi:10.1016/j.jsb.2013.05.011.

138. Fang PA, Margolis HC, Conway JF, Simmer JP, Dickinson GH, Beniash E. Cryogenic transmission electron microscopy study of amelogenin self-assembly at different pH. *Cells Tissues Organs* 194: 166–170, 2011. doi:10.1159/000324250.

139. Featherstone JD. Prevention and reversal of dental caries: role of low level fluoride. *Community Dent Oral Epidemiol* 27: 31–40, 1999. doi:10.1111/j.1600-0528.1999.tb01989.x.

140. Featherstone JD. Remineralization, the natural caries repair process--the need for new approaches. *Adv Dent Res* 21: 4–7, 2009. doi:10.1177/0895937409335590.

141. Fejerskov O. Changing paradigms in concepts on dental caries: consequences for oral health care. *Caries Res* 38: 182–191, 2004. doi:10.1159/000077753.

142. Fejerskov O, Manji F, Baelum V. The nature and mechanisms of dental fluorosis in man. *J Dent Res* 69, 2_suppl: 692–700, 1990. doi:10.1177/00220345900690S135.

143. Ferrazzano GF, Sangianantoni G, Cantile T, Amato I, Orlando S, Ingenito A. Dental enamel defects in Italian children with cystic fibrosis: an observational study. *Community Dent Health* 29: 106–109, 2012.

144. Ferreira C, Bucchini D, Martin ME, Levi S, Arosio P, Grandchamp B, Beaumont C. Early embryonic lethality of H ferritin gene deletion in mice. *J Biol Chem* 275: 3021–3024, 2000. doi:10.1074/jbc.275.5.3021.

145. Feske S, Gwack Y, Prakriya M, Srikanth S, Puppel SH, Tanasa B, Hogan PG, Lewis RS, Daly M, Rao A. A mutation in Orai1 causes immune deficiency by abrogating CRAC channel function. *Nature* 441: 179–185, 2006. doi:10.1038/nature04702.

146. Feske S, Prakriya M. Conformational dynamics of STIM1 activation. *Nat Struct Mol Biol* 20: 918–919, 2013. doi:10.1038/nsmb.2647.

147. Fincham AG, Leung W, Tan J, Moradian-Oldak J. Does amelogenin nanosphere assembly proceed through intermediary-sized structures? *Connect Tissue Res* 38: 237–240, 1998. doi:10.3109/03008209809017042.

148. Fincham AG, Moradian-Oldak J, Diekwisch TGH, Lyaruu DM, Wright JT, Bringas P Jr, Slavkin HC. Evidence for amelogenin "nanospheres" as functional components of secretory-stage enamel matrix. *J Struct Biol* 115: 50–59, 1995. doi:10.1006/jsbi.1995.1029.

149. Fincham AG, Moradian-Oldak J, Sarte PE. Mass-spectrographic analysis of a porcine amelogenin identifies a single phosphorylated locus. *Calcif Tissue Int* 55: 398–400, 1994. doi:10.1007/BF00299322.

150. Fincham AG, Moradian-Oldak J, Simmer JP. The structural biology of the developing dental enamel matrix. *J Struct Biol* 126: 270–299, 1999. doi:10.1006/jsbi.1999.4130.

151. Fincham AG, Moradian-Oldak J, Simmer JP, Sarte P, Lau EC, Diekwisch T, Slavkin HC. Self-assembly of a recombinant amelogenin protein generates supramolecular structures. *J Struct Biol* 112: 103–109, 1994. doi:10.1006/jsbi.1994.1011.

152. Fong CD, Cerný R, Hammarström L, Slaby I. Sequential expression of an amelin gene in mesenchymal and epithelial cells during odontogenesis in rats. *Eur J Oral Sci* 106, Suppl 1: 324–330, 1998. doi:10.1111/j.1600-0722.1998.tb02193.x.

153. Fong CD, Slaby I, Hammarström L. Amelin: an enamel-related protein, transcribed in the cells of epithelial root sheath. *J Bone Miner Res* 11: 892–898, 1996. doi:10.1002/jbmr.5650110704.

154. Fong H, White SN, Paine ML, Luo W, Snead ML, Sarikaya M. Enamel structure properties controlled by engineered proteins in transgenic mice. *J Bone Miner Res* 18: 2052–2059, 2003. doi:10.1359/jbmr.2003.18.11.2052.

155. Forster I, Hernando N, Sorribas V, Werner A. Phosphate transporters in renal, gastrointestinal, and other tissues. *Adv Chronic Kidney Dis* 18: 63–76, 2011. doi:10.1053/j.ackd.2011.01.006.

156. Forster IC, Biber J, Murer H. Proton-sensitive transitions of renal type II $Na^+$-coupled phosphate cotransporter kinetics. *Biophys J* 79: 215–230, 2000. doi:10.1016/S0006-3495(00)76285-0.

157. Forster IC, Hernando N, Biber J, Murer H. Phosphate transporters of the SLC20 and SLC34 families. *Mol Aspects Med* 34: 386–395, 2013. doi:10.1016/j.mam.2012.07.007.

158. Foskett JK, White C, Cheung KH, Mak DO. Inositol trisphosphate receptor $Ca^{2+}$ release channels. *Physiol Rev* 87: 593–658, 2007. doi:10.1152/physrev.00035.2006.

159. Francès F, Portolés O, González JI, Coltell O, Verdú F, Castelló A, Corella D. Amelogenin test: from forensics to quality control in clinical and biochemical genomics. *Clin Chim Acta* 386: 53–56, 2007. doi:10.1016/j.cca.2007.07.020.

160. Franklin DL, Severs NJ, Katchburian E. Development of the distal end and Tomes' processes of ameloblasts observed by freeze-fracture and ultrathin section electron microscopy. *J Anat* 174: 103–114, 1991.

161. Franklin IK, Winz RA, Hubbard MJ. Endoplasmic reticulum $Ca^{2+}$-ATPase pump is up-regulated in calcium-transporting dental enamel cells: a non-housekeeping role for SERCA2b. *Biochem J* 358: 217–224, 2001. doi:10.1042/bj3580217.

162. Friddle RW, Battle K, Trubetskoy V, Tao J, Salter EA, Moradian-Oldak J, De Yoreo JJ, Wierzbicki A. Single-molecule determination of the face-specific adsorption of Amelogenin's C-terminus on hydroxyapatite. *Angew Chem Int Ed Engl* 50: 7541–7545, 2011. doi:10.1002/anie.201100181.

163. Fuchs S, Rensing-Ehl A, Speckmann C, Bengsch B, Schmitt-Graeff A, Bondzio I, Maul-Pavicic A, Bass T, Vraetz T, Strahm B, Ankermann T, Benson M, Caliebe A, Fölster-Holst R, Kaiser P, Thimme R, Schamel WW, Schwarz K, Feske S, Ehl S. Antiviral and regulatory T cell immunity in a patient with stromal interaction molecule 1 deficiency. *J Immunol* 188: 1523–1533, 2012. doi:10.4049/jimmunol.1102507.

164. Fukumoto S, Kiba T, Hall B, Iehara N, Nakamura T, Longenecker G, Krebsbach PH, Nanci A, Kulkarni AB, Yamada Y. Ameloblastin is a cell adhesion molecule required for maintaining the differentiation state of ameloblasts. *J Cell Biol* 167: 973–983, 2004. doi:10.1083/jcb.200409077.

165. Gadhia K, McDonald S, Arkutu N, Malik K. Amelogenesis imperfecta: an introduction. *Br Dent J* 212: 377–379, 2012. doi:10.1038/sj.bdj.2012.314.

166. Gallagher RR, Balooch M, Balooch G, Wilson RS, Marshall SJ, Marshall GW. Coupled nanomechanical and raman microspectroscopic investigation of human third molar DEJ. *J Dent Biomech* 2010: 256903, 2010. doi:10.4061/2010/256903.

167. Garant PR, Nagy A, Cho MI. A freeze-fracture study of ruffle-ended post-secretory ameloblasts. *J Dent Res* 63: 622–628, 1984. doi:10.1177/00220345840630050301.

168. Garcia-Margarit M, Catalá-Pizarro M, Montiel-Company JM, Almerich-Silla JM. Epidemiologic study of molar-incisor hypomineralization in 8-year-old Spanish children. *Int J Paediatr Dent* 24: 14–22, 2014. doi:10.1111/ipd.12020.

169. Gasse B, Chiari Y, Silvent J, Davit-Béal T, Sire JY. Amelotin: an enamel matrix protein that experienced distinct evolutionary histories in amphibians, sauropsids and mammals. *BMC Evol Biol* 15: 47, 2015. doi:10.1186/s12862-015-0329-x.

170. Gasse B, Liu X, Corre E, Sire JY. Amelotin gene structure and expression during enamel formation in the opossum *Monodelphis domestica*. *PLoS One* 10: e0133314, 2015. doi:10.1371/journal.pone.0133314.

171. Gawenis LR, Bradford EM, Prasad V, Lorenz JN, Simpson JE, Clarke LL, Woo AL, Grisham C, Sanford LP, Doetschman T, Miller ML, Shull GE. Colonic anion secretory defects and metabolic acidosis in mice lacking the NBC1 $Na^+/HCO_3^-$ cotransporter. *J Biol Chem* 282: 9042–9052, 2007. doi:10.1074/jbc.M607041200.

172. Gawenis LR, Ledoussal C, Judd LM, Prasad V, Alper SL, Stuart-Tilley A, Woo AL, Grisham C, Sanford LP, Doetschman T, Miller ML, Shull GE. Mice with a targeted disruption of the AE2 Cl-/HCO3- exchanger are achlorhydric. *J Biol Chem* 279: 30531–30539, 2004. doi:10.1074/jbc.M403779200.

173. Gerlach RF, de Souza AP, Cury JA, Line SR. Fluoride effect on the activity of enamel matrix proteinases in vitro. *Eur J Oral Sci* 108: 48–53, 2000. doi:10.1034/j.1600-0722.2000.00735.x.

174. Ghezzi C, Murer H, Forster IC. Substrate interactions of the electroneutral $Na^+$-coupled inorganic phosphate cotransporter (NaPi-IIc). *J Physiol* 587: 4293–4307, 2009. doi:10.1113/jphysiol.2009.175596.

175. Gibson CW, Golub EE, Abrams WR, Shen G, Ding W, Rosenbloom J. Bovine amelogenin message heterogeneity: alternative splicing and Y-chromosomal gene transcription. *Biochemistry* 31: 8384–8388, 1992. doi:10.1021/bi00150a036.

176. Gibson CW. Regulation of amelogenin gene expression. *Crit Rev Eukaryot Gene Expr* 9: 45–57, 1999.

177. Gibson CW, Li Y, Suggs C, Kuehl MA, Pugach MK, Kulkarni AB, Wright JT. Rescue of the murine amelogenin null phenotype with two amelogenin transgenes. *Eur J Oral Sci* 119, Suppl 1: 70–74, 2011. doi:10.1111/j.1600-0722.2011.00882.x.

178. Gibson CW, Yuan ZA, Hall B, Longenecker G, Chen E, Thyagarajan T, Sreenath T, Wright JT, Decker S, Piddington R, Harrison G, Kulkarni AB. Amelogenin-deficient mice display an amelogenesis imperfecta phenotype. *J Biol Chem* 276: 31871–31875, 2001. doi:10.1074/jbc.M104624200.

179. Gibson CW, Yuan ZA, Li Y, Daly B, Suggs C, Aragon MA, Alawi F, Kulkarni AB, Wright JT. Transgenic mice that express normal and mutated amelogenins. *J Dent Res* 86: 331–335, 2007. doi:10.1177/154405910708600406.

180. Gibson MP, Liu Q, Zhu Q, Lu Y, Jani P, Wang X, Liu Y, Paine ML, Snead ML, Feng JQ, Qin C. Role of the $NH_2$-terminal fragment of dentin sialophosphoprotein in dentinogenesis. *Eur J Oral Sci* 121: 76–85, 2013. doi:10.1111/eos.12020.

181. Gkouvatsos K, Papanikolaou G, Pantopoulos K. Regulation of iron transport and the role of transferrin. *Biochim Biophys Acta* 1820: 188–202, 2012. doi:10.1016/j.bbagen.2011.10.013.

182. Glimcher MJ, Daniel EJ, Travis DF, Kamhi S. Electron optical and X-ray diffraction studies of the organization of the inorganic crystals in embryonic bovine enamel. *J Ultrastruct Res* 50, Suppl 7: 7, 1965.

183. Go W, Korzh V. Plasma membrane Ca(2+) ATPase Atp2b1a regulates bone mineralization in zebrafish. *Bone* 54: 48–57, 2013. doi:10.1016/j.bone.2013.01.026.

184. Goldberg M, Genotelle-Septier D, Molon-Noblot M, Weill R. Ultrastructural study of the proteoglycans in enamel from rat incisors during late enamel maturation. *Arch Oral Biol* 23: 1007–1011, 1978. doi:10.1016/0003-9969(78)90258-3.

185. Goldberg M, Kellermann O, Dimitrova-Nakov S, Harichane Y, Baudry A. Comparative studies between mice molars and incisors are required to draw an overview of enamel structural complexity. *Front Physiol* 5: 359, 2014. doi:10.3389/fphys.2014.00359.

186. Goldberg M, Septier D. Phospholipids in amelogenesis and dentinogenesis. *Crit Rev Oral Biol Med* 13: 276–290, 2002. doi:10.1177/154411130201300305.

187. Goldberg M, Septier D, Bourd K, Hall R, George A, Goldberg H, Menashi S. Immunohistochemical localization of MMP-2, MMP-9, TIMP-1, and TIMP-2 in the forming rat incisor. *Connect Tissue Res* 44: 143–153, 2003. doi:10.1080/03008200390223927.

188. Goldberg M, Septier D, Lécolle S, Chardin H, Quintana MA, Acevedo AC, Gafni G, Dillouya D, Vermelin L, Thonemann B, et al. Dental mineralization. *Int J Dev Biol* 39: 93–110, 1995.

189. Goldberg M, Septier D, Rapoport O, Iozzo RV, Young MF, Ameye LG. Targeted disruption of two small leucine-rich proteoglycans, biglycan and decorin, excerpts divergent effects on enamel and dentin formation. *Calcif Tissue Int* 77: 297–310, 2005. doi:10.1007/s00223-005-0026-7.

190. Goldberg M, Septier D, Rapoport O, Young M, Ameye L. Biglycan is a repressor of amelogenin expression and enamel formation: an emerging hypothesis. *J Dent Res* 81: 520–524, 2002. doi:10.1177/154405910208100804.

191. González-Cabezas C, Jiang H, Fontana M, Eckert G. Effect of low pH on surface rehardening efficacy of high concentration fluoride treatments on non-cavitated lesions. *J Dent* 40: 522–526, 2012. doi:10.1016/j.jdent.2012.03.002.

192. Gordon LM, Cohen MJ, MacRenaris KW, Pasteris JD, Seda T, Joester D. Dental materials. Amorphous intergranular phases control the properties of rodent tooth enamel. *Science* 347: 746–750, 2015. doi:10.1126/science.1258950.

193. Gordon LM, Joester D. Mapping residual organics and carbonate at grain boundaries and the amorphous interphase in mouse incisor enamel. *Front Physiol* 6: 57, 2015. doi:10.3389/fphys.2015.00057.

194. Green DW, Goto TK, Kim KS, Jung HS. Calcifying tissue regeneration via biomimetic materials chemistry. *J R Soc Interface* 11: 20140537, 2014. doi:10.1098/rsif.2014.0537.

195. Green F, O'Hare T, Blackwell A, Enns CA. Association of human transferrin receptor with GABARAP. *FEBS Lett* 518: 101–106, 2002. doi:10.1016/S0014-5793(02)02655-8.

196. Gruenbaum-Cohen Y, Tucker AS, Haze A, Shilo D, Taylor AL, Shay B, Sharpe PT, Mitsiadis TA, Ornoy A, Blumenfeld A, Deutsch D. Amelogenin in cranio-facial development: the tooth as a model to study the role of amelogenin during embryogenesis. *J Exp Zool B Mol Dev Evol* 312B: 445–457, 2009. doi:10.1002/jez.b.21255.

197. Guo J, Bervoets TJ, Henriksen K, Everts V, Bronckers AL. Null mutation of chloride channel 7 (Clcn7) impairs dental root formation but does not affect enamel mineralization. *Cell Tissue Res* 363: 361–370, 2016. doi:10.1007/s00441-015-2263-z.

198. Habelitz S. Materials engineering by ameloblasts. *J Dent Res* 94: 759–767, 2015. doi:10.1177/0022034515577963.

199. Hall R, Septier D, Embery G, Goldberg M. Stromelysin-1 (MMP-3) in forming enamel and predentine in rat incisor-coordinated distribution with proteoglycans suggests a functional role. *Histochem J* 31: 761–770, 1999. doi:10.1023/A:1003945902473.

200. Hallsworth AS, Weatherell JA, Robinson C. Loss of carbonate during the first stages of enamel caries. *Caries Res* 7: 345–348, 1973. doi:10.1159/000259857.

201. Halse A, Selvig KA. Incorporation of iron in rat incisor enamel. *Scand J Dent Res* 82: 47–56, 1974.

202. Hanawa M, Takano Y, Wakita M. An autoradiographic study of calcium movement in the enamel organ of rat molar tooth germs. *Arch Oral Biol* 35: 899–906, 1990. doi:10.1016/0003-9969(90)90070-Q.

203. Hannig M, Hannig C. Nanotechnology and its role in caries therapy. *Adv Dent Res* 24: 53–57, 2012. doi:10.1177/0022034512450446.

204. Harada H, Kettunen P, Jung HS, Mustonen T, Wang YA, Thesleff I. Localization of putative stem cells in dental epithelium and their association with Notch and FGF signaling. *J Cell Biol* 147: 105–120, 1999. doi:10.1083/jcb.147.1.105.

205. Hariri I, Sadr A, Shimada Y, Tagami J, Sumi Y. Effects of structural orientation of enamel and dentine on light attenuation and local refractive index: an optical coherence tomography study. *J Dent* 40: 387–396, 2012. doi:10.1016/j.jdent.2012.01.017.

206. Harrison PM, Arosio P. The ferritins: molecular properties, iron storage function and cellular regulation. *Biochim Biophys Acta* 1275: 161–203, 1996. doi:10.1016/0005-2728(96)00022-9.

207. Hart PS, Hart TC, Michalec MD, Ryu OH, Simmons D, Hong S, Wright JT. Mutation in kallikrein 4 causes autosomal recessive hypomaturation amelogenesis imperfecta. *J Med Genet* 41: 545–549, 2004. doi:10.1136/jmg.2003.017657.

208. Hart PS, Michalec MD, Seow WK, Hart TC, Wright JT. Identification of the enamelin (g.8344delG) mutation in a new kindred and presentation of a standardized ENAM nomenclature. *Arch Oral Biol* 48: 589–596, 2003. doi:10.1016/S0003-9969(03)00114-6.

209. Hasegawa T, Sato F, Ishida N, Fukushima Y, Mukoyama H. Sex determination by simultaneous amplification of equine SRY and amelogenin genes. *J Vet Med Sci* 62: 1109–1110, 2000. doi:10.1292/jvms.62.1109.

210. Hayashi H, Suruga K, Yamashita Y. Regulation of intestinal $Cl^-/HCO_3^-$ exchanger SLC26A3 by intracellular pH. *Am J Physiol Cell Physiol* 296: C1279–C1290, 2009. doi:10.1152/ajpcell.00638.2008.

211. Haze A, Taylor AL, Blumenfeld A, Rosenfeld E, Leiser Y, Dafni L, Shay B, Gruenbaum-Cohen Y, Fermon E, Haegewald S, Bernimoulin JP, Deutsch D. Amelogenin expression in long bone and cartilage cells and in bone marrow progenitor cells. *Anat Rec (Hoboken)* 290: 455–460, 2007. doi:10.1002/ar.20520.

212. He X, Wu S, Martinez-Avila O, Cheng Y, Habelitz S. Self-aligning amelogenin nanoribbons in oil-water system. *J Struct Biol* 174: 203–212, 2011. doi:10.1016/j.jsb.2010.11.027.

213. Heaton FW. Effect of magnesium deficiency on plasma alkaline phosphatase activity. *Nature* 207: 1292–1293, 1965. doi:10.1038/2071292b0.

214. Hediger MA, Clémençon B, Burrier RE, Bruford EA. The ABCs of membrane transporters in health and disease (SLC series): introduction. *Mol Aspects Med* 34: 95–107, 2013. doi:10.1016/j.mam.2012.12.009.

215. Hetz C. The unfolded protein response: controlling cell fate decisions under ER stress and beyond. *Nat Rev Mol Cell Biol* 13: 89–102, 2012. doi:10.1038/nrm3270.

216. Hihnala S, Kujala M, Toppari J, Kere J, Holmberg C, Höglund P. Expression of SLC26A3, CFTR and NHE3 in the human male reproductive tract: role in male subfertility caused by congenital chloride diarrhoea. *Mol Hum Reprod* 12: 107–111, 2006. doi:10.1093/molehr/gal009.

217. Höglund P, Auranen M, Socha J, Popinska K, Nazer H, Rajaram U, Al Sanie A, Al-Ghanim M, Holmberg C, de la Chapelle A, Kere J. Genetic background of congenital chloride diarrhea in high-incidence populations: Finland, Poland, and Saudi Arabia and Kuwait. *Am J Hum Genet* 63: 760–768, 1998. doi:10.1086/301998.

218. Höglund P, Haila S, Socha J, Tomaszewski L, Saarialho-Kere U, Karjalainen-Lindsberg ML, Airola K, Holmberg C, de la Chapelle A, Kere J. Mutations of the Down-regulated in adenoma (DRA) gene cause congenital chloride diarrhoea. *Nat Genet* 14: 316–319, 1996. doi:10.1038/ng1196-316.

219. Höglund P, Sormaala M, Haila S, Socha J, Rajaram U, Scheurlen W, Sinaasappel M, de Jonge H, Holmberg C, Yoshikawa H, Kere J. Identification of seven novel mutations including the first two genomic rearrangements in SLC26A3 mutated in congenital chloride diarrhea. *Hum Mutat* 18: 233–242, 2001. doi:10.1002/humu.1179.

220. Holcroft J, Ganss B. Identification of amelotin- and ODAM-interacting enamel matrix proteins using the yeast two-hybrid system. *Eur J Oral Sci* 119, Suppl 1: 301–306, 2011. doi:10.1111/j.1600-0722.2011.00870.x.

221. Homma K, Miller KK, Anderson CT, Sengupta S, Du GG, Aguiñaga S, Cheatham M, Dallos P, Zheng J. Interaction between CFTR and prestin (SLC26A5). *Biochim Biophys Acta* 1798: 1029–1040, 2010. doi:10.1016/j.bbamem.2010.02.001.

222. Hong H, Xia Y, Sun Y, Ye L, Liu J, Bai J, Zhang H. Elevated NCX1 and NCKX4 expression in the patent postnatal ductus arteriosus of ductal-dependent congenital heart disease patients. *Pediatr Cardiol* 36: 743–751, 2015. doi:10.1007/s00246-014-1070-8.

223. Höning S, Griffith J, Geuze HJ, Hunziker W. The tyrosine-based lysosomal targeting signal in lamp-1 mediates sorting into Golgi-derived clathrin-coated vesicles. *EMBO J* 15: 5230–5239, 1996.

224. Horowitz AM. A report on the NIH Consensus Development Conference on Diagnosis and Management of Dental Caries Throughout Life. *J Dent Res* 83 Suppl: 15–17, 2004. doi:10.1177/154405910408301s03.

225. Hoshi K, Amizuka N, Oda K, Ikehara Y, Ozawa H. Immunolocalization of tissue non-specific alkaline phosphatase in mice. *Histochem Cell Biol* 107: 183–191, 1997. doi:10.1007/s004180050103.

226. Hu CC, Fukae M, Uchida T, Qian Q, Zhang CH, Ryu OH, Tanabe T, Yamakoshi Y, Murakami C, Dohi N, Shimizu M, Simmer JP. Cloning and characterization of porcine enamelin mRNAs. *J Dent Res* 76: 1720–1729, 1997. doi:10.1177/00220345970760110201.

227. Hu CC, Fukae M, Uchida T, Qian Q, Zhang CH, Ryu OH, Tanabe T, Yamakoshi Y, Murakami C, Dohi N, Shimizu M, Simmer JP. Sheathlin: cloning, cDNA/polypeptide sequences, and immunolocalization of porcine enamel sheath proteins. *J Dent Res* 76: 648–657, 1997. doi:10.1177/00220345970760020501.

228. Hu JC, Chun YH, Al Hazzazzi T, Simmer JP. Enamel formation and amelogenesis imperfecta. *Cells Tissues Organs* 186: 78–85, 2007. doi:10.1159/000102683.

229. Hu JC, Hu Y, Lu Y, Smith CE, Lertlam R, Wright JT, Suggs C, McKee MD, Beniash E, Kabir ME, Simmer JP. Enamelin is critical for ameloblast integrity and enamel ultrastructure formation. *PLoS One* 9: e89303, 2014. doi:10.1371/journal.pone.0089303.

230. Hu JC, Hu Y, Smith CE, McKee MD, Wright JT, Yamakoshi Y, Papagerakis P, Hunter GK, Feng JQ, Yamakoshi F, Simmer JP. Enamel defects and ameloblast-specific expression in Enam knock-out/lacz knock-in mice. *J Biol Chem* 283: 10858–10871, 2008. doi:10.1074/jbc.M710565200.

231. Hu JC, Lertlam R, Richardson AS, Smith CE, McKee MD, Simmer JP. Cell proliferation and apoptosis in enamelin null mice. *Eur J Oral Sci* 119, Suppl 1: 329–337, 2011. doi:10.1111/j.1600-0722.2011.00860.x.

232. Hu JC, Ryu OH, Chen JJ, Uchida T, Wakida K, Murakami C, Jiang H, Qian Q, Zhang C, Ottmers V, Bartlett JD, Simmer JP. Localization of EMSP1 expression during tooth formation and cloning of mouse cDNA. *J Dent Res* 79: 70–76, 2000. doi:10.1177/00220345000790011301.

233. Hu JC, Sun X, Zhang C, Liu S, Bartlett JD, Simmer JP. Enamelysin and kallikrein-4 mRNA expression in developing mouse molars. *Eur J Oral Sci* 110: 307–315, 2002. doi:10.1034/j.1600-0722.2002.21301.x.

234. Hu P, Lacruz RS, Smith CE, Smith SM, Kurtz I, Paine ML. Expression of the sodium/calcium/potassium exchanger, NCKX4, in ameloblasts. *Cells Tissues Organs* 196: 501–509, 2012. doi:10.1159/000337493.

235. Hu Y, Hu JC, Smith CE, Bartlett JD, Simmer JP. Kallikrein-related peptidase 4, matrix metalloproteinase 20, and the maturation of murine and porcine enamel. *Eur J Oral Sci* 119, Suppl 1: 217–225, 2011. doi:10.1111/j.1600-0722.2011.00859.x.

236. Hu Y, Smith CE, Cai Z, Donnelly LA, Yang J, Hu JC, Simmer JP. Enamel ribbons, surface nodules, and octacalcium phosphate in C57BL/6 Amelx(−/−) mice and Amelx(+/−) lyonization. *Mol Genet Genomic Med* 4: 641–661, 2016. doi:10.1002/mgg3.252.

237. Huang Z, Kim J, Lacruz RS, Bringas P Jr, Glogauer M, Bromage TG, Kaartinen VM, Snead ML. Epithelial-specific knockout of the Rac1 gene leads to enamel defects. *Eur J Oral Sci* 119, Suppl 1: 168–176, 2011. doi:10.1111/j.1600-0722.2011.00904.x.

238. Hubbard MJ. Abundant calcium homeostasis machinery in rat dental enamel cells. Up-regulation of calcium store proteins during enamel mineralization implicates the endoplasmic reticulum in calcium transcytosis. *Eur J Biochem* 239: 611–623, 1996. doi:10.1111/j.1432-1033.1996.0611u.x.

239. Hubbard MJ. Calbindin28kDa and calmodulin are hyperabundant in rat dental enamel cells. Identification of the protein phosphatase calcineurin as a principal calmodulin target and of a secretion-related role for calbindin28kDa. *Eur J Biochem* 230: 68–79, 1995. doi:10.1111/j.1432-1033.1995.tb20535.x.

240. Hubbard MJ. Calcium transport across the dental enamel epithelium. *Crit Rev Oral Biol Med* 11: 437–466, 2000. doi:10.1177/10454411000110040401.

241. Hubbard MJ, McHugh NJ. Calbindin28kDa and calbindin30kDa (calretinin) are substantially localised in the particulate fraction of rat brain. *FEBS Lett* 374: 333–337, 1995. doi:10.1016/0014-5793(95)01135-2.

242. Hubbard MJ, McHugh NJ, Carne DL. Isolation of ERp29, a novel endoplasmic reticulum protein, from rat enamel cells. Evidence for a unique role in secretory-protein synthesis. *Eur J Biochem* 267: 1945–1957, 2000. doi:10.1046/j.1432-1327.2000.01193.x.

243. Hubbard MJ, McHugh NJ, Mangum JE. Exclusion of all three calbindins from a calcium-ferry role in rat enamel cells. *Eur J Oral Sci* 119, Suppl 1: 112–119, 2011. doi:10.1111/j.1600-0722.2011.00890.x.

244. Huysseune A, Sire JY. Evolution of patterns and processes in teeth and tooth-related tissues in non-mammalian vertebrates. *Eur J Oral Sci* 106, Suppl 1: 437–481, 1998. doi:10.1111/j.1600-0722.1998.tb02211.x.

245. Ida-Yonemochi H, Ohshiro K, Swelam W, Metwaly H, Saku T. Perlecan, a basement membrane-type heparan sulfate proteoglycan, in the enamel organ: its intraepithelial localization in the stellate reticulum. *J Histochem Cytochem* 53: 763–772, 2005. doi:10.1369/jhc.4A6479.2005.

246. Igarashi T, Inatomi J, Sekine T, Cha SH, Kanai Y, Kunimi M, Tsukamoto K, Satoh H, Shimadzu M, Tozawa F, Mori T, Shiobara M, Seki G, Endou H. Mutations in SLC4A4 cause permanent isolated proximal renal tubular acidosis with ocular abnormalities. *Nat Genet* 23: 264–266, 1999. doi:10.1038/15440.

247. Igarashi T, Ishii T, Watanabe K, Hayakawa H, Horio K, Sone Y, Ohga K. Persistent isolated proximal renal tubular acidosis--a systemic disease with a distinct clinical entity. *Pediatr Nephrol* 8: 70–71, 1994. doi:10.1007/BF00868266.

248. Ihrke G, Kyttälä A, Russell MR, Rous BA, Luzio JP. Differential use of two AP-3-mediated pathways by lysosomal membrane proteins. *Traffic* 5: 946–962, 2004. doi:10.1111/j.1600-0854.2004.00236.x.

249. Imbeni V, Kruzic JJ, Marshall GW, Marshall SJ, Ritchie RO. The dentin-enamel junction and the fracture of human teeth. *Nat Mater* 4: 229–232, 2005. doi:10.1038/nmat1323.

250. Inaba D, Kawasaki K, Iijima Y, Taguchi N, Hayashida H, Yoshikawa T, Furugen R, Fukumoto E, Nishiyama T, Tanaka K, Takagi O. Enamel fluoride uptake from mouth-rinse solutions with different NaF concentrations. *Community Dent Oral Epidemiol* 30: 248–253, 2002. doi:10.1034/j.1600-0528.2002.00042.x.

251. Inatomi J, Horita S, Braverman N, Sekine T, Yamada H, Suzuki Y, Kawahara K, Moriyama N, Kudo A, Kawakami H, Shimadzu M, Endou H, Fujita T, Seki G, Igarashi T. Mutational and functional analysis of SLC4A4 in a patient with proximal renal tubular acidosis. *Pflugers Arch* 448: 438–444, 2004. doi:10.1007/s00424-004-1278-1.

252. Ismail AI. Clinical diagnosis of precavitated carious lesions. *Community Dent Oral Epidemiol* 25: 13–23, 1997. doi:10.1111/j.1600-0528.1997.tb00895.x.

253. Ito T, Choi BY, King KA, Zalewski CK, Muskett J, Chattaraj P, Shawker T, Reynolds JC, Butman JA, Brewer CC, Wangemann P, Alper SL, Griffith AJ. SLC26A4 genotypes and phenotypes associated with enlargement of the vestibular aqueduct. *Cell Physiol Biochem* 28: 545–552, 2011. doi:10.1159/000335119.

254. Ivanov SV, Kuzmin I, Wei MH, Pack S, Geil L, Johnson BE, Stanbridge EJ, Lerman MI. Down-regulation of transmembrane carbonic anhydrases in renal cell carcinoma cell lines by wild-type von Hippel-Lindau transgenes. *Proc Natl Acad Sci USA* 95: 12596–12601, 1998. doi:10.1073/pnas.95.21.12596.

255. Iwasaki K, Bajenova E, Somogyi-Ganss E, Miller M, Nguyen V, Nourkeyhani H, Gao Y, Wendel M, Ganss B. Amelotin--a novel secreted, ameloblast-specific protein. *J Dent Res* 84: 1127–1132, 2005. doi:10.1177/154405910508401207.

256. Iwase M, Satta Y, Hirai Y, Hirai H, Imai H, Takahata N. The amelogenin loci span an ancient pseudoautosomal boundary in diverse mammalian species. *Proc Natl Acad Sci USA* 100: 5258–5263, 2003. doi:10.1073/pnas.0635848100.

257. Iwata T, Yamakoshi Y, Hu JC, Ishikawa I, Bartlett JD, Krebsbach PH, Simmer JP. Processing of ameloblastin by MMP-20. *J Dent Res* 86: 153–157, 2007. doi:10.1177/154405910708600209.

258. Jalali R, Guo J, Zandieh-Doulabi B, Bervoets TJ, Paine ML, Boron WF, Parker MD, Bijvelds MJ, Medina JF, DenBesten PK, Bronckers AL. NBCe1 (SLC4A4) a potential pH regulator in enamel organ cells during enamel development in the mouse. *Cell Tissue Res* 358: 433–442, 2014. doi:10.1007/s00441-014-1935-4.

259. Jalali R, Zandieh-Doulabi B, DenBesten PK, Seidler U, Riederer B, Wedenoja S, Micha D, Bronckers AL. Slc26a3/Dra and Slc26a6 in murine ameloblasts. *J Dent Res* 94: 1732–1739, 2015. doi:10.1177/0022034515606873.

260. Jayasudha B, Baswaraj, H K N, K B P. Enamel regeneration: current progress and challenges. *J Clin Diagn Res* 8: ZE06–ZE09, 2014. doi:10.7860/JCDR/2014/10231.4883.

261. Jensen N, Schrøder HD, Hejbøl EK, Füchtbauer EM, de Oliveira JR, Pedersen L. Loss of function of Slc20a2 associated with familial idiopathic basal ganglia calcification in humans causes brain calcifications in mice. *J Mol Neurosci* 51: 994–999, 2013. doi:10.1007/s12031-013-0085-6.

262. Jernvall J, Thesleff I. Tooth shape formation and tooth renewal: evolving with the same signals. *Development* 139: 3487–3497, 2012. doi:10.1242/dev.085084.

263. Jheon AH, Seidel K, Biehs B, Klein OD. From molecules to mastication: the development and evolution of teeth. *Wiley Interdiscip Rev Dev Biol* 2: 165–182, 2013. doi:10.1002/wdev.63.

264. Ji C, Stockbridge RB, Miller C. Bacterial fluoride resistance, Fluc channels, and the weak acid accumulation effect. *J Gen Physiol* 144: 257–261, 2014. doi:10.1085/jgp.201411243.

265. Jiang Z, Asplin JR, Evan AP, Rajendran VM, Velazquez H, Nottoli TP, Binder HJ, Aronson PS. Calcium oxalate urolithiasis in mice lacking anion transporter Slc26a6. *Nat Genet* 38: 474–478, 2006. doi:10.1038/ng1762.

266. Jodaikin A, Traub W, Weiner S. Protein conformation in rat tooth enamel. *Arch Oral Biol* 31: 685–689, 1986. doi:10.1016/0003-9969(86)90098-1.

267. Jones RS, Fried D. Remineralization of enamel caries can decrease optical reflectivity. *J Dent Res* 85: 804–808, 2006. doi:10.1177/154405910608500905.

268. Josephsen K, Fejerskov O. Ameloblast modulation in the maturation zone of the rat incisor enamel organ. A light and electron microscopic study. *J Anat* 124: 45–70, 1977.

269. Josephsen K, Takano Y, Frische S, Praetorius J, Nielsen S, Aoba T, Fejerskov O. Ion transporters in secretory and cyclically modulating ameloblasts: a new hypothesis for cellular control of preeruptive enamel maturation. *Am J Physiol Cell Physiol* 299: C1299–C1307, 2010. doi:10.1152/ajpcell.00218.2010.

270. Juran BD, Atkinson EJ, Larson JJ, Schlicht EM, Lazaridis KN. Common genetic variation and haplotypes of the anion exchanger SLC4A2 in primary biliary cirrhosis. *Am J Gastroenterol* 104: 1406–1411, 2009. doi:10.1038/ajg.2009.103.

271. Jussila M, Thesleff I. Signaling networks regulating tooth organogenesis and regeneration, and the specification of dental mesenchymal and epithelial cell lineages. *Cold Spring Harb Perspect Biol* 4: a008425, 2012. doi:10.1101/cshperspect.a008425.

272. Juuri E, Saito K, Ahtiainen L, Seidel K, Tummers M, Hochedlinger K, Klein OD, Thesleff I, Michon F. Sox2+ stem cells contribute to all epithelial lineages of the tooth via Sfrp5+ progenitors. *Dev Cell* 23: 317–328, 2012. doi:10.1016/j.devcel.2012.05.012.

273. Kallenbach E. Electron microscopy of the differentiating rat incisor ameloblast. *J Ultrastruct Res* 35: 508–531, 1971. doi:10.1016/S0022-5320(71)80008-4.

274. Kallenbach E. Fine structure of rat incisor ameloblasts in transition between enamel secretion and maturation stages. *Tissue Cell* 6: 173–190, 1974. doi:10.1016/0040-8166(74)90030-5.

275. Kallenbach E. Fine structure of the stratum intermedium, stellate reticulum, and outer enamel epithelium in the enamel organ of the kitten. *J Anat* 126: 247–260, 1978.

276. Kallenbach E. The fine structure of Tomes' process of rat incisor ameloblasts and its relationship to the elaboration of enamel. *Tissue Cell* 5: 501–524, 1973. doi:10.1016/S0040-8166(73)80041-2.

277. Kaminsky LS, Mahoney MC, Leach J, Melius J, Miller MJ. Fluoride: benefits and risks of exposure. *Crit Rev Oral Biol Med* 1: 261–281, 1990. doi:10.1177/10454411900010040501.

278. Katsura KA, Horst JA, Chandra D, Le TQ, Nakano Y, Zhang Y, Horst OV, Zhu L, Le MH, DenBesten PK. WDR72 models of structure and function: a stage-specific regulator of enamel mineralization. *Matrix Biol* 38: 48–58, 2014. doi:10.1016/j.matbio.2014.06.005.

279. Kawamoto T, Shimizu M. Changes in the mode of calcium and phosphate transport during rat incisal enamel formation. *Calcif Tissue Int* 46: 406–414, 1990. doi:10.1007/BF02554972.

280. Kawasaki K. The SCPP gene family and the complexity of hard tissues in vertebrates. *Cells Tissues Organs* 194: 108–112, 2011. doi:10.1159/000324225.

281. Kawasaki K. The SCPP gene repertoire in bony vertebrates and graded differences in mineralized tissues. *Dev Genes Evol* 219: 147–157, 2009. doi:10.1007/s00427-009-0276-x.

282. Kawasaki K, Buchanan AV, Weiss KM. Biomineralization in humans: making the hard choices in life. *Annu Rev Genet* 43: 119–142, 2009. doi:10.1146/annurev-genet-102108-134242.

283. Kawasaki K, Buchanan AV, Weiss KM. Gene duplication and the evolution of vertebrate skeletal mineralization. *Cells Tissues Organs* 186: 7–24, 2007. doi:10.1159/000102678.

284. Kawasaki K, Lafont AG, Sire JY. The evolution of milk casein genes from tooth genes before the origin of mammals. *Mol Biol Evol* 28: 2053–2061, 2011. doi:10.1093/molbev/msr020.

285. Kawasaki K, Suzuki T, Weiss KM. Genetic basis for the evolution of vertebrate mineralized tissue. *Proc Natl Acad Sci USA* 101: 11356–11361, 2004. doi:10.1073/pnas.0404279101.

286. Kawasaki K, Weiss KM. Evolutionary genetics of vertebrate tissue mineralization: the origin and evolution of the secretory calcium-binding phosphoprotein family. *J Exp Zool B Mol Dev Evol* 306: 295–316, 2006. doi:10.1002/jez.b.21088.

287. Kawasaki K, Weiss KM. Mineralized tissue and vertebrate evolution: the secretory calcium-binding phosphoprotein gene cluster. *Proc Natl Acad Sci USA* 100: 4060–4065, 2003. doi:10.1073/pnas.0638023100.

288. Kawasaki K, Weiss KM. SCPP gene evolution and the dental mineralization continuum. *J Dent Res* 87: 520–531, 2008. doi:10.1177/154405910808700608.

289. Kay MI, Young RA, Posner AS. Crystal Structure of Hydroxyapatite. *Nature* 204: 1050–1052, 1964. doi:10.1038/2041050a0.

290. Kenny J, Lees MM, Drury S, Barnicoat A, Van't Hoff W, Palmer R, Morrogh D, Waters JJ, Lench NJ, Bockenhauer D. Sotos syndrome, infantile hypercalcemia, and nephrocalcinosis: a contiguous gene syndrome. *Pediatr Nephrol* 26: 1331–1334, 2011. doi:10.1007/s00467-011-1884-z.

291. Khalil IA, Kogure K, Akita H, Harashima H. Uptake pathways and subsequent intracellular trafficking in nonviral gene delivery. *Pharmacol Rev* 58: 32–45, 2006. doi:10.1124/pr.58.1.8.

292. Khandoudi N, Albadine J, Robert P, Krief S, Berrebi-Bertrand I, Martin X, Bevensee MO, Boron WF, Bril A. Inhibition of the cardiac electrogenic sodium bicarbonate cotransporter reduces ischemic injury. *Cardiovasc Res* 52: 387–396, 2001. doi:10.1016/S0008-6363(01)00430-8.

293. Kida M, Ariga T, Shirakawa T, Oguchi H, Sakiyama Y. Autosomal-dominant hypoplastic form of amelogenesis imperfecta caused by an enamelin gene mutation at the exon-intron boundary. *J Dent Res* 81: 738–742, 2002. doi:10.1177/0810738.

294. Kiefer CL, Hall KI, Grubb BR, Wright JT. Abnormal enamel development in a cystic fibrosis transgenic mouse model (Abstract). *J Dent Res* 74: 178, 1995.

295. Kim JW, Lee SK, Lee ZH, Park JC, Lee KE, Lee MH, Park JT, Seo BM, Hu JC, Simmer JP. FAM83H mutations in families with autosomal-dominant hypocalcified amelogenesis imperfecta. *Am J Hum Genet* 82: 489–494, 2008. doi:10.1016/j.ajhg.2007.09.020.

296. Kim JW, Seymen F, Lee KE, Ko J, Yildirim M, Tuna EB, Gencay K, Shin TJ, Kyun HK, Simmer JP, Hu JC. LAMB3 mutations causing autosomal-dominant amelogenesis imperfecta. *J Dent Res* 92: 899–904, 2013. doi:10.1177/0022034513502054.

297. Koenigswald WV, Clemens WA. Levels of complexity in the microstructure of mammalian enamel and their application in studies of systematics. *Scanning Microsc* 6: 195–217, 1992.

298. Kondo K, Kuriaki K. Carbonic anhydrases in dental tissue and effect of parathyroid hormone and fluoride on its activity. *J Dent Res* 40: 971–974, 1961. doi:10.1177/00220345610400052301.

299. Kondo S, Tamura Y, Bawden JW, Tanase S. The immunohistochemical localization of Bax and Bcl-2 and their relation to apoptosis during amelogenesis in developing rat molars. *Arch Oral Biol* 46: 557–568, 2001. doi:10.1016/S0003-9969(00)00139-4.

300. Kopp P, Arseven OK, Sabacan L, Kotlar T, Dupuis J, Cavaliere H, Santos CL, Jameson JL, Medeiros-Neto G. Phenocopies for deafness and goiter development in a large inbred Brazilian kindred with Pendred's syndrome associated with a novel mutation in the PDS gene. *J Clin Endocrinol Metab* 84: 336–341, 1999.

301. Kopp P, Pesce L, Solis-S JC. Pendred syndrome and iodide transport in the thyroid. *Trends Endocrinol Metab* 19: 260–268, 2008. doi:10.1016/j.tem.2008.07.001.

302. Koster MI. p63 in skin development and ectodermal dysplasias. *J Invest Dermatol* 130: 2352–2358, 2010. doi:10.1038/jid.2010.119.

303. Kozawa Y, Sakae T, Mishima H, Barckhaus RH, Krefting ER, Schmidt PF, Höhling HJ. Electron-microscopic and microprobe analyses on the pigmented and unpigmented enamel of Sorex (Insectivora). *Histochemistry* 90: 61–65, 1988. doi:10.1007/BF00495708.

304. Kozyraki R, Fyfe J, Verroust PJ, Jacobsen C, Dautry-Varsat A, Gburek J, Willnow TE, Christensen EI, Moestrup SK. Megalin-dependent cubilin-mediated endocytosis is a major pathway for the apical uptake of transferrin in polarized epithelia. *Proc Natl Acad Sci USA* 98: 12491–12496, 2001. doi:10.1073/pnas.211291398.

305. Krebsbach PH, Lee SK, Matsuki Y, Kozak CA, Yamada KM, Yamada Y. Full-length sequence, localization, and chromosomal mapping of ameloblastin. A novel tooth-specific gene. *J Biol Chem* 271: 4431–4435, 1996. doi:10.1074/jbc.271.8.4431.

306. Kubota K, Lee DH, Tsuchiya M, Young CS, Everett ET, Martinez-Mier EA, Snead ML, Nguyen L, Urano F, Bartlett JD. Fluoride induces endoplasmic reticulum stress in ameloblasts responsible for dental enamel formation. *J Biol Chem* 280: 23194–23202, 2005. doi:10.1074/jbc.M503288200.

307. Kuga T, Sasaki M, Mikami T, Miake Y, Adachi J, Shimizu M, Saito Y, Koura M, Takeda Y, Matsuda J, Tomonaga T, Nakayama Y. FAM83H and casein kinase I regulate the organization of the keratin cytoskeleton and formation of desmosomes. *Sci Rep* 6: 26557, 2016. doi:10.1038/srep26557.

308. Kühnisch J, Thiering E, Heitmüller D, Tiesler CM, Grallert H, Heinrich-Weltzien R, Hickel R, Heinrich J; GINI-10 Plus Study Group; LISA-10Plus Study Group. Genome-wide association study (GWAS) for molar-incisor hypomineralization (MIH). *Clin Oral Invest* 18: 677–682, 2014. doi:10.1007/s00784-013-1054-8.

309. Kulkarni AP, Mittal SP, Devasagayam TP, Pal JK. Hsp90 mediates activation of the heme regulated eIF-2 alpha kinase during oxidative stress. *Indian J Biochem Biophys* 47: 67–74, 2010.

310. Kulkarni AP, Mittal SP, Devasagayam TP, Pal JK. Oxidative stress perturbs cell proliferation in human K562 cells by modulating protein synthesis and cell cycle. *Free Radic Res* 43: 1090–1100, 2009. doi:10.1080/10715760903179673.

311. Kurahashi Y, Yoshiki S. Electron microscopic localization of alkaline phosphatase in the enamel organ of the young rat. *Arch Oral Biol* 17: 155–163, 1972. doi:10.1016/0003-9969(72)90143-4.

312. Kutuzova GD, Akhter S, Christakos S, Vanhooke J, Kimmel-Jehan C, Deluca HF. Calbindin D(9k) knockout mice are indistinguishable from wild-type mice in phenotype and serum calcium level. *Proc Natl Acad Sci USA* 103: 12377–12381, 2006. doi:10.1073/pnas.0605252103.

313. Lacruz RS, Brookes SJ, Wen X, Jimenez JM, Vikman S, Hu P, White SN, Lyngstadaas SP, Okamoto CT, Smith CE, Paine ML. Adaptor protein complex 2-mediated, clathrin-dependent endocytosis, and related gene activities, are a prominent feature during maturation stage amelogenesis. *J Bone Miner Res* 28: 672–687, 2013. doi:10.1002/jbmr.1779.

314. Lacruz RS, Feske S. Diseases caused by mutations in ORAI1 and STIM1. *Ann NY Acad Sci* 1356: 45–79, 2015. doi:10.1111/nyas.12938.

315. Lacruz RS, Hilvo M, Kurtz I, Paine ML. A survey of carbonic anhydrase mRNA expression in enamel cells. *Biochem Biophys Res Commun* 393: 883–887, 2010. doi:10.1016/j.bbrc.2010.02.116.

316. Lacruz RS, Nanci A, Kurtz I, Wright JT, Paine ML. Regulation of pH during amelogenesis. *Calcif Tissue Int* 86: 91–103, 2010. doi:10.1007/s00223-009-9326-7.

317. Lacruz RS, Nanci A, White SN, Wen X, Wang H, Zalzal SF, Luong VQ, Schuetter VL, Conti PS, Kurtz I, Paine ML. The sodium bicarbonate cotransporter (NBCe1) is essential for normal development of mouse dentition. *J Biol Chem* 285: 24432–24438, 2010. doi:10.1074/jbc.M110.115188.

318. Lacruz RS, Smith CE, Bringas P Jr, Chen YB, Smith SM, Snead ML, Kurtz I, Hacia JG, Hubbard MJ, Paine ML. Identification of novel candidate genes involved in mineralization of dental enamel by genome-wide transcript profiling. *J Cell Physiol* 227: 2264–2275, 2012. doi:10.1002/jcp.22965.

319. Lacruz RS, Smith CE, Chen YB, Hubbard MJ, Hacia JG, Paine ML. Gene-expression analysis of early- and late-maturation-stage rat enamel organ. *Eur J Oral Sci* 119, Suppl 1: 149–157, 2011. doi:10.1111/j.1600-0722.2011.00881.x.

320. Lacruz RS, Smith CE, Kurtz I, Hubbard MJ, Paine ML. New paradigms on the transport functions of maturation-stage ameloblasts. *J Dent Res* 92: 122–129, 2013. doi:10.1177/0022034512470954.

321. Lacruz RS, Smith CE, Moffatt P, Chang EH, Bromage TG, Bringas P Jr, Nanci A, Baniwal SK, Zabner J, Welsh MJ, Kurtz I, Paine ML. Requirements for ion and solute transport, and pH regulation during enamel maturation. *J Cell Physiol* 227: 1776–1785, 2012. doi:10.1002/jcp.22911.

322. Lacruz RS, Smith CE, Smith SM, Hu P, Bringas P Jr, Sahin-Tóth M, Moradian-Oldak J, Paine ML. Chymotrypsin C (caldecrin) is associated with enamel development. *J Dent Res* 90: 1228–1233, 2011. doi:10.1177/0022034511418231.

323. Last NB, Miller C. Functional monomerization of a ClC-type fluoride transporter. *J Mol Biol* 427: 3607–3612, 2015. doi:10.1016/j.jmb.2015.09.027.

324. Latysheva N, Muratov G, Rajesh S, Padgett M, Hotchin NA, Overduin M, Berditchevski F. Syntenin-1 is a new component of tetraspanin-enriched microdomains: mechanisms and consequences of the interaction of syntenin-1 with CD63. *Mol Cell Biol* 26: 7707–7718, 2006. doi:10.1128/MCB.00849-06.

325. Lau EC, Mohandas TK, Shapiro LJ, Slavkin HC, Snead ML. Human and mouse amelogenin gene loci are on the sex chromosomes. *Genomics* 4: 162–168, 1989. doi:10.1016/0888-7543(89)90295-4.

326. Lau EC, Simmer JP, Bringas P Jr, Hsu DD, Hu CC, Zeichner-David M, Thiemann F, Snead ML, Slavkin HC, Fincham AG. Alternative splicing of the mouse amelogenin primary RNA transcript contributes to amelogenin heterogeneity. *Biochem Biophys Res Commun* 188: 1253–1260, 1992. doi:10.1016/0006-291X(92)91366-X.

327. Le Roy C, Wrana JL. Clathrin- and non-clathrin-mediated endocytic regulation of cell signalling. *Nat Rev Mol Cell Biol* 6: 112–126, 2005. doi:10.1038/nrm1571.

328. Le TQ, Gochin M, Featherstone JD, Li W, DenBesten PK. Comparative calcium binding of leucine-rich amelogenin peptide and full-length amelogenin. *Eur J Oral Sci* 114, Suppl 1: 320–326, 2006. doi:10.1111/j.1600-0722.2006.00313.x.

329. Lee BS, Chou PH, Chen SY, Liao HY, Chang CC. Prevention of enamel demineralization with a novel fluoride strip: enamel surface composition and depth profile. *Sci Rep* 5: 13352, 2015. doi:10.1038/srep13352.

330. Lee GS, Lee KY, Choi KC, Ryu YH, Paik SG, Oh GT, Jeung EB. Phenotype of a calbindin-D9k gene knockout is compensated for by the induction of other calcium transporter genes in a mouse model. *J Bone Miner Res* 22: 1968–1978, 2007. doi:10.1359/jbmr.070801.

331. LeFevre ML, Manly RS. Moisture, inorganic and organic contents of enamel and dentin from carious teeth. *J Am Dent Assoc* 25: 233–242, 1938.

332. LeGeros RZ, Trautz OR, Klein E, LeGeros JP. Two types of carbonate substitution in the apatite structure. *Experientia* 25: 5–7, 1969. doi:10.1007/BF01903856.

333. Lekic P, McCulloch CA. Periodontal ligament cell population: the central role of fibroblasts in creating a unique tissue. *Anat Rec* 245: 327–341, 1996. doi:10.1002/(SICI)1097-0185(199606)245:2<327::AID-AR15>3.0.CO;2-R.

334. Lenzi TL, Montagner AF, Soares FZ, de Oliveira Rocha R. Are topical fluorides effective for treating incipient carious lesions? A systematic review and meta-analysis. *J Am Dent Assoc* 147: 84–91, 2016. doi:10.1016/j.adaj.2015.06.018.

335. Leppäniemi A, Lukinmaa PL, Alaluusua S. Nonfluoride hypomineralizations in the permanent first molars and their impact on the treatment need. *Caries Res* 35: 36–40, 2001.

336. Li CY, Cha W, Luder HU, Charles RP, McMahon M, Mitsiadis TA, Klein OD. E-cadherin regulates the behavior and fate of epithelial stem cells and their progeny in the mouse incisor. *Dev Biol* 366: 357–366, 2012. doi:10.1016/j.ydbio.2012.03.012.

337. Li X, Wang J, Joiner A, Chang J. The remineralisation of enamel: a review of the literature. *J Dent* 42, Suppl 1: S12–S20, 2014. doi:10.1016/S0300-5712(14)50003-6.

338. Lignon G, de la Dure-Molla M, Dessombz A, Berdal A, Babajko S. [Enamel: a unique self-assembling in mineral world]. *Med Sci (Paris)* 31: 515–521, 2015. doi:10.1051/medsci/20153105013.

339. Lim HH, Stockbridge RB, Miller C. Fluoride-dependent interruption of the transport cycle of a CLC $Cl^-/H^+$ antiporter. *Nat Chem Biol* 9: 721–725, 2013. doi:10.1038/nchembio.1336.

340. Limeback H, Simic A. Biochemical characterization of stable high molecular-weight aggregates of amelogenins formed during porcine enamel development. *Arch Oral Biol* 35: 459–468, 1990. doi:10.1016/0003-9969(90)90209-S.

341. Lin CP, Douglas WH, Erlandsen SL. Scanning electron microscopy of type I collagen at the dentin-enamel junction of human teeth. *J Histochem Cytochem* 41: 381–388, 1993. doi:10.1177/41.3.8429200.

342. Lin HM, Nakamura H, Noda T, Ozawa H. Localization of $H^+$-ATPase and carbonic anhydrase II in ameloblasts at maturation. *Calcif Tissue Int* 55: 38–45, 1994. doi:10.1007/BF00310167.

343. Liu H, Yan X, Pandya M, Luan X, Diekwisch TG. Daughters of the enamel organ: development, fate, and function of the stratum intermedium, stellate reticulum, and outer enamel epithelium. *Stem Cells Dev* 25: 1580–1590, 2016. doi:10.1089/scd.2016.0267.

344. Llano E, Pendás AM, Knäuper V, Sorsa T, Salo T, Salido E, Murphy G, Simmer JP, Bartlett JD, López-Otín C. Identification and structural and functional characterization of human enamelysin (MMP-20). *Biochemistry* 36: 15101–15108, 1997. doi:10.1021/bi972120y.

345. Lu JX, Xu YS, Buchko GW, Shaw WJ. Mineral association changes the secondary structure and dynamics of murine amelogenin. *J Dent Res* 92: 1000–1004, 2013. doi:10.1177/0022034513504929.

346. Lu L, Han AP, Chen JJ. Translation initiation control by heme-regulated eukaryotic initiation factor 2alpha kinase in erythroid cells under cytoplasmic stresses. *Mol Cell Biol* 21: 7971–7980, 2001. doi:10.1128/MCB.21.23.7971-7980.2001.

347. Lu X, Sun D, Xu B, Pan J, Wei Y, Mao X, Yu D, Liu H, Gao B. In silico screening and molecular dynamic study of nonsynonymous single nucleotide polymorphisms associated with kidney stones in the SLC26A6 gene. *J Urol* 196: 118–123, 2016. doi:10.1016/j.juro.2016.01.093.

348. Lu Y, Papagerakis P, Yamakoshi Y, Hu JC, Bartlett JD, Simmer JP. Functions of KLK4 and MMP-20 in dental enamel formation. *Biol Chem* 389: 695–700, 2008. doi:10.1515/BC.2008.080.

349. Luder HU, Gerth-Kahlert C, Ostertag-Benzinger S, Schorderet DF. Dental phenotype in Jalili syndrome due to a c.1312 dupC homozygous mutation in the CNNM4 gene. *PLoS One* 8: e78529, 2013. doi:10.1371/journal.pone.0078529.

350. Lyaruu DM, Bronckers AL, Mulder L, Mardones P, Medina JF, Kellokumpu S, Oude Elferink RP, Everts V. The anion exchanger Ae2 is required for enamel maturation in mouse teeth. *Matrix Biol* 27: 119–127, 2008. doi:10.1016/j.matbio.2007.09.006.

351. Lyaruu DM, Medina JF, Sarvide S, Bervoets TJ, Everts V, DenBesten P, Smith CE, Bronckers AL. Barrier formation: potential molecular mechanism of enamel fluorosis. *J Dent Res* 93: 96–102, 2014. doi:10.1177/0022034513510944.

352. Lyman GE, Waddell WJ. pH gradients in the developing teeth of young mice from autoradiography of [$^{14}$C]DMO. *Am J Physiol* 232: F364–F367, 1977.

353. Lynch RJ, Smith SR. Remineralization agents--new and effective or just marketing hype? *Adv Dent Res* 24: 63–67, 2012. doi:10.1177/0022034512454295.

354. Lyngstadaas SP, Møinichen CB, Risnes S. Crown morphology, enamel distribution, and enamel structure in mouse molars. *Anat Rec* 250: 268–280, 1998. doi:10.1002/(SICI)1097-0185(199803)250:3<268::AID-AR2>3.0.CO;2-X.

355. Maeda T, Sato O, Kobayashi S, Iwanaga T, Fujita T. The ultrastructure of Ruffini endings in the periodontal ligament of rat incisors with special reference to the terminal Schwann cells (K-cells). *Anat Rec* 223: 95–103, 1989. doi:10.1002/ar.1092230114.

356. Magen D, Berger L, Coady MJ, Ilivitzki A, Militianu D, Tieder M, Selig S, Lapointe JY, Zelikovic I, Skorecki K. A loss-of-function mutation in NaPi-IIa and renal Fanconi's syndrome. *N Engl J Med* 362: 1102–1109, 2010. doi:10.1056/NEJMoa0905647.

357. Mäkelä S, Kere J, Holmberg C, Höglund P. SLC26A3 mutations in congenital chloride diarrhea. *Hum Mutat* 20: 425–438, 2002. doi:10.1002/humu.10139.

358. Mårdh CK, Bäckman B, Holmgren G, Hu JC, Simmer JP, Forsman-Semb K. A nonsense mutation in the enamelin gene causes local hypoplastic autosomal dominant amelogenesis imperfecta (AIH2). *Hum Mol Genet* 11: 1069–1074, 2002. doi:10.1093/hmg/11.9.1069.

359. Margolis HC, Beniash E, Fowler CE. Role of macromolecular assembly of enamel matrix proteins in enamel formation. *J Dent Res* 85: 775–793, 2006. doi:10.1177/154405910608500902.

360. Margolis HC, Moreno EC. Physicochemical perspectives on the cariostatic mechanisms of systemic and topical fluorides. *J Dent Res* 69, Suppl 2: 606–613, 1990. doi:10.1177/00220345900690S119.

361. Martinez-Avila O, Wu S, Kim SJ, Cheng Y, Khan F, Samudrala R, Sali A, Horst JA, Habelitz S. Self-assembly of filamentous amelogenin requires calcium and phosphate: from dimers via nanoribbons to fibrils. *Biomacromolecules* 13: 3494–3502, 2012. doi:10.1021/bm300942c.

362. Martinez-Avila OM, Wu S, Cheng Y, Lee R, Khan F, Habelitz S. Self-assembly of amelogenin proteins at the water-oil interface. *Eur J Oral Sci* 119, Suppl 1: 75–82, 2011. doi:10.1111/j.1600-0722.2011.00907.x.

363. Mathias RS, Mathews CH, Machule C, Gao D, Li W, DenBesten PK. Identification of the calcium-sensing receptor in the developing tooth organ. *J Bone Miner Res* 16: 2238–2244, 2001. doi:10.1359/jbmr.2001.16.12.2238.

364. Matsuki Y, Nakashima M, Amizukal N, Warshawsky H, Goltzman D, Yamada KM, Yamada Y. A compilation of partial sequences of randomly selected cDNA clones from the rat incisor. *J Dent Res* 74: 307–312, 1995. doi:10.1177/00220345950740010401.

365. Matsunaga T, Fujioka M, Hosoya M. [Current status and perspectives of the research in Pendred syndrome]. *Nihon Rinsho* 71: 2215–2222, 2013.

366. Matthiessen ME, Rømert P. Ultrastructure of the human enamel organ. I. External enamel epithelium, stellate reticulum, and stratum intermedium. *Cell Tissue Res* 205: 361–370, 1980. doi:10.1007/BF00232278.

367. Matthiessen ME, Rømert P. Ultrastructure of the human enamel organ. II. Internal enamel epithelium, preameloblasts, and secretory ameloblasts. *Cell Tissue Res* 205: 371–382, 1980. doi:10.1007/BF00232279.

368. Maurer ME, Cooper JA. The adaptor protein Dab2 sorts LDL receptors into coated pits independently of AP-2 and ARH. *J Cell Sci* 119: 4235–4246, 2006. doi:10.1242/jcs.03217.

369. Maycock J, Wood SR, Brookes SJ, Shore RC, Robinson C, Kirkham J. Characterization of a porcine amelogenin preparation, EMDOGAIN, a biological treatment for periodontal disease. *Connect Tissue Res* 43: 472–476, 2002. doi:10.1080/03008200290000880.

370. McCarl CA, Khalil S, Ma J, Oh-hora M, Yamashita M, Roether J, Kawasaki T, Jairaman A, Sasaki Y, Prakriya M, Feske S. Store-operated $Ca^{2+}$ entry through ORAI1 is critical for T cell-mediated autoimmunity and allograft rejection. *J Immunol* 185: 5845–5858, 2010. doi:10.4049/jimmunol.1001796.

371. McGuire JD, Gorski JP, Dusevich V, Wang Y, Walker MP. Type IV collagen is a novel DEJ biomarker that is reduced by radiotherapy. *J Dent Res* 93: 1028–1034, 2014. doi:10.1177/0022034514548221.

372. McGuire JD, Walker MP, Mousa A, Wang Y, Gorski JP. Type VII collagen is enriched in the enamel organic matrix associated with the dentin-enamel junction of mature human teeth. *Bone* 63: 29–35, 2014. doi:10.1016/j.bone.2014.02.012.

373. McKee MD, Nakano Y, Masica DL, Gray JJ, Lemire I, Heft R, Whyte MP, Crine P, Millán JL. Enzyme replacement therapy prevents dental defects in a model of hypophosphatasia. *J Dent Res* 90: 470–476, 2011. doi:10.1177/0022034510393517.

374. McKee MD, Zerounian C, Martineau-Doizé B, Warshawsky H. Specific binding sites for transferrin on ameloblasts of the enamel maturation zone in the rat incisor. *Anat Rec* 218: 123–127, 1987. doi:10.1002/ar.1092180205.

375. Medina JF. Role of the anion exchanger 2 in the pathogenesis and treatment of primary biliary cirrhosis. *Dig Dis* 29: 103–112, 2011. doi:10.1159/000324144.

376. Medina JF, Recalde S, Prieto J, Lecanda J, Saez E, Funk CD, Vecino P, van Roon MA, Ottenhoff R, Bosma PJ, Bakker CT, Elferink RP. Anion exchanger 2 is essential for spermiogenesis in mice. *Proc Natl Acad Sci USA* 100: 15847–15852, 2003. doi:10.1073/pnas.2536127100.

377. Miletich I, Sharpe PT. Neural crest contribution to mammalian tooth formation. *Birth Defects Res C Embryo Today* 72: 200–212, 2004. doi:10.1002/bdrc.20012.

378. Miletich I, Sharpe PT. Normal and abnormal dental development. *Hum Mol Genet* 12: R69–R73, 2003. doi:10.1093/hmg/ddg085.

379. Mitsiadis TA, Barrandon O, Rochat A, Barrandon Y, De Bari C. Stem cell niches in mammals. *Exp Cell Res* 313: 3377–3385, 2007. doi:10.1016/j.yexcr.2007.07.027.

380. Mitsiadis TA, Graf D. Cell fate determination during tooth development and regeneration. *Birth Defects Res C Embryo Today* 87: 199–211, 2009. doi:10.1002/bdrc.20160.

381. Miyamoto K, Haito-Sugino S, Kuwahara S, Ohi A, Nomura K, Ito M, Kuwahata M, Kido S, Tatsumi S, Kaneko I, Segawa H. Sodium-dependent phosphate cotransporters: lessons from gene knockout and mutation studies. *J Pharm Sci* 100: 3719–3730, 2011. doi:10.1002/jps.22614.

382. Miyamoto K, Ito M, Tatsumi S, Kuwahata M, Segawa H. New aspect of renal phosphate reabsorption: the type IIc sodium-dependent phosphate transporter. *Am J Nephrol* 27: 503–515, 2007. doi:10.1159/000107069.

383. Miyazaki Y, Sakai H, Shibata Y, Shibata M, Mataki S, Kato Y. Expression and localization of ferritin mRNA in ameloblasts of rat incisor. *Arch Oral Biol* 43: 367–378, 1998. doi:10.1016/S0003-9969(98)00014-4.

384. Moestrup SK, Verroust PJ. Megalin- and cubilin-mediated endocytosis of protein-bound vitamins, lipids, and hormones in polarized epithelia. *Annu Rev Nutr* 21: 407–428, 2001. doi:10.1146/annurev.nutr.21.1.407.

385. Moffatt P, Smith CE, Sooknanan R, St-Arnaud R, Nanci A. Identification of secreted and membrane proteins in the rat incisor enamel organ using a signal-trap screening approach. *Eur J Oral Sci* 114, Suppl 1: 139–146, 2006. doi:10.1111/j.1600-0722.2006.00318.x.

386. Moffatt P, Smith CE, St-Arnaud R, Nanci A. Characterization of Apin, a secreted protein highly expressed in tooth-associated epithelia. *J Cell Biochem* 103: 941–956, 2008. doi:10.1002/jcb.21465.

387. Moradian-Oldak J. Protein-mediated enamel mineralization. *Front Biosci (Landmark Ed)* 17: 1996–2023, 2012. doi:10.2741/4034.

388. Moradian-Oldak J, Du C, Falini G. On the formation of amelogenin microribbons. *Eur J Oral Sci* 114, Suppl 1: 289–296, 2006. doi:10.1111/j.1600-0722.2006.00285.x.

389. Moradian-Oldak J, Goldberg M. Amelogenin supra-molecular assembly in vitro compared with the architecture of the forming enamel matrix. *Cells Tissues Organs* 181: 202–218, 2005. doi:10.1159/000091382.

390. Moradian-Oldak J, Leung W, Fincham AG. Temperature and pH-dependent supramolecular self-assembly of amelogenin molecules: a dynamic light-scattering analysis. *J Struct Biol* 122: 320–327, 1998. doi:10.1006/jsbi.1998.4008.

391. Moradian-Oldak J, Paine ML, Lei YP, Fincham AG, Snead ML. Self-assembly properties of recombinant engineered amelogenin proteins analyzed by dynamic light scattering and atomic force microscopy. *J Struct Biol* 131: 27–37, 2000. doi:10.1006/jsbi.2000.4237.

392. Moreno EC, Aoba T. Calcium bonding in enamel fluid and driving force for enamel mineralization in the secretory stage of amelogenesis. *Adv Dent Res* 1: 245–251, 1987. doi:10.1177/08959374870010021301.

393. Moreno EC, Kresak M, Zahradnik RT. Physicochemical aspects of fluoride-apatite systems relevant to the study of dental caries. *Caries Res* 11, Suppl 1: 142–171, 1977. doi:10.1159/000260299.

394. Motley A, Bright NA, Seaman MN, Robinson MS. Clathrin-mediated endocytosis in AP-2-depleted cells. *J Cell Biol* 162: 909–918, 2003. doi:10.1083/jcb.200305145.

395. Mukhopadhyay S, Roy P, Mandal B, Ghosh C, Chakraborty B. Enamel hypoplasia of primary canine: its prevalence and degree of expression. *J Nat Sci Biol Med* 5: 43–46, 2014. doi:10.4103/0976-9668.127283.

396. Munhoz CO, Leblond CP. Deposition of calcium phosphate into dentin and enamel as shown by radioautography of sections of incisor teeth following injection of $^{45}Ca$ into rats. *Calcif Tissue Res* 15: 221–235, 1974. doi:10.1007/BF02059059.

397. Murray JJ, Shaw L. Classification and prevalence of enamel opacities in the human deciduous and permanent dentitions. *Arch Oral Biol* 24: 7–13, 1979. doi:10.1016/0003-9969(79)90168-7.

398. Nagai R, Kooh SW, Balfe JW, Fenton T, Halperin ML. Renal tubular acidosis and osteopetrosis with carbonic anhydrase II deficiency: pathogenesis of impaired acidification. *Pediatr Nephrol* 11: 633–636, 1997. doi:10.1007/s004670050354.

399. Nagano T, Kakegawa A, Yamakoshi Y, Tsuchiya S, Hu JC, Gomi K, Arai T, Bartlett JD, Simmer JP. Mmp-20 and Klk4 cleavage site preferences for amelogenin sequences. *J Dent Res* 88: 823–828, 2009. doi:10.1177/0022034509342694.

400. Nakahori Y, Takenaka O, Nakagome Y. A human X-Y homologous region encodes "amelogenin". *Genomics* 9: 264–269, 1991. doi:10.1016/0888-7543(91)90251-9.

401. Nakano Y, Le MH, Abduweli D, Ho SP, Ryazanova LV, Hu Z, Ryazanov AG, Den Besten PK, Zhang Y. A critical role of TRPM7 as an ion channel protein in mediating the mineralization of the craniofacial hard tissues. *Front Physiol* 7: 258, 2016. doi:10.3389/fphys.2016.00258.

402. Nakayama Y, Holcroft J, Ganss B. Enamel hypomineralization and structural defects in amelotin-deficient mice. *J Dent Res* 94: 697–705, 2015. doi:10.1177/0022034514566214.

403. Nanci A. *Ten Cate's Oral Histology: Development, Structure, and Function*. St. Louis, MO: Mosby Elsevier, 2008.

404. Nichols BJ, Lippincott-Schwartz J. Endocytosis without clathrin coats. *Trends Cell Biol* 11: 406–412, 2001. doi:10.1016/S0962-8924(01)02107-9.

405. Nishimura M, Naito S. Tissue-specific mRNA expression profiles of human solute carrier transporter superfamilies. *Drug Metab Pharmacokinet* 23: 22–44, 2008. doi:10.2133/dmpk.23.22.

406. Nishio C, Wazen R, Kuroda S, Moffatt P, Nanci A. Expression pattern of odontogenic ameloblast-associated and amelotin during formation and regeneration of the junctional epithelium. *Eur Cell Mater* 20: 393–402, 2010. doi:10.22203/eCM.v020a32.

407. Nishio C, Wazen R, Moffatt P, Nanci A. Expression of odontogenic ameloblast-associated and amelotin proteins in the junctional epithelium. *Periodontol 2000* 63: 59–66, 2013. doi:10.1111/prd.12031.

408. Nongonierma AB, Fitzgerald RJ. Biofunctional properties of caseinophosphopeptides in the oral cavity. *Caries Res* 46: 234–267, 2012. doi:10.1159/000338381.

409. Nurbaeva MK, Eckstein M, Concepcion AR, Smith CE, Srikanth S, Paine ML, Gwack Y, Hubbard MJ, Feske S, Lacruz RS. Dental enamel cells express functional SOCE channels. *Sci Rep* 5: 15803, 2015. doi:10.1038/srep15803.

410. Nurbaeva MK, Eckstein M, Feske S, Lacruz RS. Ca(2+) transport and signalling in enamel cells [In press]. *J Physiol*, 2016. doi:10.1113/JP272775.

411. Nurbaeva MK, Eckstein M, Snead ML, Feske S, Lacruz RS. Store-operated $Ca^{2+}$ entry modulates the expression of enamel genes. *J Dent Res* 94: 1471–1477, 2015. doi:10.1177/0022034515598144.

411a. Nusier M, Yassin O, Hart TC, Samimi A, Wright JT. Phenotypic diversity and revision of the nomenclature for autosomal recessive amelogenesis imperfecta. *Oral Surg Oral Med Oral Pathol Oral Radiol Endod* 97: 220–230, 2004.

412. Odajima T, Onishi M. The state of chlorine in human enamel and dentine. In: *Tooth Enamel V*, edited by Fearnhead R. Tsurumi, Japan: Florence Publishers, 1989, p. 360–366.

413. Ohi A, Hanabusa E, Ueda O, Segawa H, Horiba N, Kaneko I, Kuwahara S, Mukai T, Sasaki S, Tominaga R, Furutani J, Aranami F, Ohtomo S, Oikawa Y, Kawase Y, Wada NA, Tachibe T, Kakefuda M, Tateishi H, Matsumoto K, Tatsumi S, Kido S, Fukushima N, Jishage K, Miyamoto K. Inorganic phosphate homeostasis in sodium-dependent phosphate cotransporter $Npt2b^{+/-}$ mice. *Am J Physiol Renal Physiol* 301: F1105–F1113, 2011. doi:10.1152/ajprenal.00663.2010.

414. Ohshima H, Maeda T, Takano Y. Cytochrome oxidase activity in the enamel organ during amelogenesis in rat incisors. *Anat Rec* 252: 519–531, 1998. doi:10.1002/(SICI)1097-0185(199812)252:4<519::AID-AR3>3.0.CO;2-I.

415. Okazaki M, Takahashi J, Kimura H. Iron uptake of hydroxyapatite. *J Osaka Univ Dent Sch* 25: 17–24, 1985.

416. Okumura R, Shibukawa Y, Muramatsu T, Hashimoto S, Nakagawa K, Tazaki M, Shimono M. Sodium-calcium exchangers in rat ameloblasts. *J Pharmacol Sci* 112: 223–230, 2010. doi:10.1254/jphs.09267FP.

417. Olszta MJ, Cheng X, Jee SS, Kumar R, Kim Y-Y, Kaufman MJ, Douglas EP, Gower LB. Bone structure and formation: a new perspective. *Mater Sci Eng Rep* 58: 77–116, 2008. doi:10.1016/j.mser.2007.05.001.

418. Omelon S, Georgiou J, Henneman ZJ, Wise LM, Sukhu B, Hunt T, Wynnyckyj C, Holmyard D, Bielecki R, Grynpas MD. Control of vertebrate skeletal mineralization by polyphosphates. *PLoS One* 4: e5634, 2009. doi:10.1371/journal.pone.0005634.

419. Omelon SJ, Grynpas MD. Relationships between polyphosphate chemistry, biochemistry and apatite biomineralization. *Chem Rev* 108: 4694–4715, 2008. doi:10.1021/cr0782527.

420. Orsini G, Jimenez-Rojo L, Natsiou D, Putignano A, Mitsiadis TA. In vivo administration of dental epithelial stem cells at the apical end of the mouse incisor. *Front Physiol* 6: 112, 2015. doi:10.3389/fphys.2015.00112.

421. Ozdemir D, Hart PS, Ryu OH, Choi SJ, Ozdemir-Karatas M, Firatli E, Piesco N, Hart TC. MMP20 active-site mutation in hypomaturation amelogenesis imperfecta. *J Dent Res* 84: 1031–1035, 2005. doi:10.1177/154405910508401112.

422. Paine ML, Krebsbach PH, Chen LS, Paine CT, Yamada Y, Deutsch D, Snead ML. Protein-to-protein interactions: criteria defining the assembly of the enamel organic matrix. *J Dent Res* 77: 496–502, 1998. doi:10.1177/00220345980770030901.

423. Paine ML, Lei YP, Dickerson K, Snead ML. Altered amelogenin self-assembly based on mutations observed in human X-linked amelogenesis imperfecta (AIH1). *J Biol Chem* 277: 17112–17116, 2002. doi:10.1074/jbc.M110473200.

424. Paine ML, Luo W, Wang HJ, Bringas P Jr, Ngan AYW, Miklus VG, Zhu DH, MacDougall M, White SN, Snead ML. Dentin sialoprotein and dentin phosphoprotein overexpression during amelogenesis. *J Biol Chem* 280: 31991–31998, 2005. doi:10.1074/jbc.M502991200.

425. Paine ML, Luo W, Zhu DH, Bringas P Jr, Snead ML. Functional domains for amelogenin revealed by compound genetic defects. *J Bone Miner Res* 18: 466–472, 2003. doi:10.1359/jbmr.2003.18.3.466.

426. Paine ML, Slots J, Rich SK. Fluoride use in periodontal therapy: a review of the literature. *J Am Dent Assoc* 129: 69–77, 1998. doi:10.14219/jada.archive.1998.0023.

427. Paine ML, Snead ML. Protein interactions during assembly of the enamel organic extracellular matrix. *J Bone Miner Res* 12: 221–227, 1997. doi:10.1359/jbmr.1997.12.2.221.

428. Paine ML, Snead ML. Tooth developmental biology: disruptions to enamel-matrix assembly and its impact on biomineralization. *Orthod Craniofac Res* 8: 239–251, 2005. doi:10.1111/j.1601-6343.2005.00346.x.

429. Paine ML, Snead ML, Wang HJ, Abuladze N, Pushkin A, Liu W, Kao LY, Wall SM, Kim YH, Kurtz I. Role of NBCe1 and AE2 in secretory ameloblasts. *J Dent Res* 87: 391–395, 2008. doi:10.1177/154405910808700415.

430. Paine ML, White SN, Luo W, Fong H, Sarikaya M, Snead ML. Regulated gene expression dictates enamel structure and tooth function. *Matrix Biol* 20: 273–292, 2001. doi:10.1016/S0945-053X(01)00153-6.

431. Paine ML, Zhu DH, Luo W, Bringas P Jr, Goldberg M, White SN, Lei YP, Sarikaya M, Fong HK, Snead ML. Enamel biomineralization defects result from alterations to amelogenin self-assembly. *J Struct Biol* 132: 191–200, 2000. doi:10.1006/jsbi.2000.4324.

432. Palmer LC, Newcomb CJ, Kaltz SR, Spoerke ED, Stupp SI. Biomimetic systems for hydroxyapatite mineralization inspired by bone and enamel. *Chem Rev* 108: 4754–4783, 2008. doi:10.1021/cr8004422.

433. Pan P, Leppilampi M, Pastorekova S, Pastorek J, Waheed A, Sly WS, Parkkila S. Carbonic anhydrase gene expression in CA II-deficient (Car2−/−) and CA IX-deficient (Car9−/−) mice. *J Physiol* 571: 319–327, 2006. doi:10.1113/jphysiol.2005.102590.

434. Pantopoulos K, Porwal SK, Tartakoff A, Devireddy L. Mechanisms of mammalian iron homeostasis. *Biochemistry* 51: 5705–5724, 2012. doi:10.1021/bi300752r.

435. Parekh AB, Putney JW Jr. Store-operated calcium channels. *Physiol Rev* 85: 757–810, 2005. doi:10.1152/physrev.00057.2003.

436. Parker MD, Boron WF. The divergence, actions, roles, and relatives of sodium-coupled bicarbonate transporters. *Physiol Rev* 93: 803–959, 2013. doi:10.1152/physrev.00023.2012.

437. Parry DA, Brookes SJ, Logan CV, Poulter JA, El-Sayed W, Al-Bahlani S, Al Harasi S, Sayed J, Raïf M, Shore RC, Dashash M, Barron M, Morgan JE, Carr IM, Taylor GR, Johnson CA, Aldred MJ, Dixon MJ, Wright JT, Kirkham J, Inglehearn CF, Mighell AJ. Mutations in C4orf26, encoding a peptide with in vitro hydroxyapatite crystal nucleation and growth activity, cause amelogenesis imperfecta. *Am J Hum Genet* 91: 565–571, 2012. doi:10.1016/j.ajhg.2012.07.020.

438. Parry DA, Mighell AJ, El-Sayed W, Shore RC, Jalili IK, Dollfus H, Bloch-Zupan A, Carlos R, Carr IM, Downey LM, Blain KM, Mansfield DC, Shahrabi M, Heidari M, Aref P, Abbasi M, Michaelides M, Moore AT, Kirkham J, Inglehearn CF. Mutations in CNNM4 cause Jalili syndrome, consisting of autosomal-recessive cone-rod dystrophy and amelogenesis imperfecta. *Am J Hum Genet* 84: 266–273, 2009. doi:10.1016/j.ajhg.2009.01.009.

439. Parry DA, Poulter JA, Logan CV, Brookes SJ, Jafri H, Ferguson CH, Anwari BM, Rashid Y, Zhao H, Johnson CA, Inglehearn CF, Mighell AJ. Identification of mutations in SLC24A4, encoding a potassium-dependent sodium/calcium exchanger, as a cause of amelogenesis imperfecta. *Am J Hum Genet* 92: 307–312, 2013. doi:10.1016/j.ajhg.2013.01.003.

440. Parry DA, Smith CE, El-Sayed W, Poulter JA, Shore RC, Logan CV, Mogi C, Sato K, Okajima F, Harada A, Zhang H, Koruyucu M, Seymen F, Hu JC, Simmer JP, Ahmed M, Jafri H, Johnson CA, Inglehearn CF, Mighell AJ. Mutations in the pH-sensing G-protein-coupled receptor GPR68 cause amelogenesis imperfecta. *Am J Hum Genet* 99: 984–990, 2016. doi:10.1016/j.ajhg.2016.08.020.

441. Pastorekova S, Parkkila S, Pastorek J, Supuran CT. Carbonic anhydrases: current state of the art, therapeutic applications and future prospects. *J Enzyme Inhib Med Chem* 19: 199–229, 2004. doi:10.1080/14756360410001689540.

442. Pautard FG. An X-ray diffraction pattern from human enamel matrix. *Arch Oral Biol* 3: 217–220, 1961. doi:10.1016/0003-9969(61)90139-X.

443. Pearse BM. Clathrin: a unique protein associated with intracellular transfer of membrane by coated vesicles. *Proc Natl Acad Sci USA* 73: 1255–1259, 1976. doi:10.1073/pnas.73.4.1255.

444. Peden AA, Oorschot V, Hesser BA, Austin CD, Scheller RH, Klumperman J. Localization of the AP-3 adaptor complex defines a novel endosomal exit site for lysosomal membrane proteins. *J Cell Biol* 164: 1065–1076, 2004. doi:10.1083/jcb.200311064.

445. Peker S, Mete S, Gokdemir Y, Karadag B, Kargul B. Related factors of dental caries and molar incisor hypomineralisation in a group of children with cystic fibrosis. *Eur Arch Paediatr Dent* 15: 275–280, 2014. doi:10.1007/s40368-014-0112-5.

446. Perdok WG, Gustafson G. X-ray diffraction studies of the insoluble protein in mature human enamel. *Arch Oral Biol* 4: 70–75, 1961. doi:10.1016/0003-9969(61)90081-4.

447. Picard C, McCarl CA, Papolos A, Khalil S, Lüthy K, Hivroz C, LeDeist F, Rieux-Laucat F, Rechavi G, Rao A, Fischer A, Feske S. STIM1 mutation associated with a syndrome of immunodeficiency and autoimmunity. *N Engl J Med* 360: 1971–1980, 2009. doi:10.1056/NEJMoa0900082.

448. Pidancier N, Jordan S, Luikart G, Taberlet P. Evolutionary history of the genus *Capra* (Mammalia, Artiodactyla): discordance between mitochondrial DNA and Y-chromosome phylogenies. *Mol Phylogenet Evol* 40: 739–749, 2006. doi:10.1016/j.ympev.2006.04.002.

449. Pindborg JJ. The pigmentation of the rat incisor as an index of metabolic disturbances. *Oral Surg Oral Med Oral Pathol* 6: 780–789, 1953. doi:10.1016/0030-4220(53)90205-9.

450. Pindborg JJ, Weinmann JP. Morphologic and functional correlations in the enamel organ of the rat incisor during amelogenesis. *Acta Anat (Basel)* 36: 367–381, 1959. doi:10.1159/000141450.

451. Pollick HF. Scientific evidence continues to support fluoridation of public water supplies. *Int J Occup Environ Health* 11: 322–326, 2005. doi:10.1179/oeh.2005.11.3.322.

452. Pols MS, Klumperman J. Trafficking and function of the tetraspanin CD63. *Exp Cell Res* 315: 1584–1592, 2009. doi:10.1016/j.yexcr.2008.09.020.

453. Poulter JA, El-Sayed W, Shore RC, Kirkham J, Inglehearn CF, Mighell AJ. Whole-exome sequencing, without prior linkage, identifies a mutation in LAMB3 as a cause of dominant hypoplastic amelogenesis imperfecta. *Eur J Hum Genet* 22: 132–135, 2014. doi:10.1038/ejhg.2013.76.

454. Prajapati S, Tao J, Ruan Q, De Yoreo JJ, Moradian-Oldak J. Matrix metalloproteinase-20 mediates dental enamel biomineralization by preventing protein occlusion inside apatite crystals. *Biomaterials* 75: 260–270, 2016. doi:10.1016/j.biomaterials.2015.10.031.

455. Prakriya M, Lewis RS. Store-operated calcium channels. *Physiol Rev* 95: 1383–1436, 2015. doi:10.1152/physrev.00020.2014.

456. Pretty IA, Ellwood RP. The caries continuum: opportunities to detect, treat and monitor the re-mineralization of early caries lesions. *J Dent* 41, Suppl 2: S12–S21, 2013. doi:10.1016/j.jdent.2010.04.003.

457. Prié D, Huart V, Bakouh N, Planelles G, Dellis O, Gérard B, Hulin P, Benqué-Blanchet F, Silve C, Grandchamp B, Friedlander G. Nephrolithiasis and osteoporosis associated with hypophosphatemia caused by mutations in the type 2a sodium-phosphate cotransporter. *N Engl J Med* 347: 983–991, 2002. doi:10.1056/NEJMoa020028.

458. Prime SS, MacDonald DG, Noble HW, Rennie JS. Effect of prolonged iron deficiency on enamel pigmentation and tooth structure in rat incisors. *Arch Oral Biol* 29: 905–909, 1984. doi:10.1016/0003-9969(84)90090-6.

459. Prout RE, Odutuga AA, Tring FC. Lipid analysis of rat enamel and dentine. *Arch Oral Biol* 18: 373–380, 1973. doi:10.1016/0003-9969(73)90161-1.

460. Pushkin A, Kurtz I. SLC4 base ($HCO3^-$, $CO_3^{2-}$) transporters: classification, function, structure, genetic diseases, and knockout models. *Am J Physiol Renal Physiol* 290: F580–F599, 2006. doi:10.1152/ajprenal.00252.2005.

461. Putney JW. Capacitative calcium entry: from concept to molecules. *Immunol Rev* 231: 10–22, 2009. doi:10.1111/j.1600-065X.2009.00810.x.

462. Quilter CR, Blott SC, Mileham AJ, Affara NA, Sargent CA, Griffin DK. A mapping and evolutionary study of porcine sex chromosome genes. *Mamm Genome* 13: 588–594, 2002. doi:10.1007/s00335-002-3026-1.

463. Reibring CG, El Shahawy M, Hallberg K, Kannius-Janson M, Nilsson J, Parkkila S, Sly WS, Waheed A, Linde A, Gritli-Linde A. Expression patterns and subcellular localization of carbonic anhydrases are developmentally regulated during tooth formation. *PLoS One* 9: e96007, 2014. doi:10.1371/journal.pone.0096007.

464. Reith EJ. The stages of amelogenesis as observed in molar teeth of young rats. *J Ultrastruct Res* 30: 111–151, 1970. doi:10.1016/S0022-5320(70)90068-7.

465. Reith EJ. The ultrastructure of ameloblasts during matrix formation and the maturation of enamel. *J Biophys Biochem Cytol* 9: 825–839, 1961. doi:10.1083/jcb.9.4.825.

466. Reith EJ, Boyde A. The arrangement of ameloblasts on the surface of maturing enamel of the rat incisor tooth. *J Anat* 133: 381–388, 1981.

467. Reith EJ, Boyde A. Autoradiographic evidence of cyclical entry of calcium into maturing enamel of the rat incisor tooth. *Arch Oral Biol* 26: 983–987, 1981. doi:10.1016/0003-9969(81)90107-2.

468. Reith EJ, Boyde A. A correlated scanning and transmission electron microscopic study of maturation ameloblasts in developing molar teeth of rats. *Cell Tissue Res* 197: 421–431, 1979. doi:10.1007/BF00233567.

469. Reith EJ, Boyde A. The pyroantimonate reaction and transcellular transport of calcium in rat molar enamel organs. *Histochemistry* 83: 539–543, 1985. doi:10.1007/BF00492457.

470. Rej R, Bretaudiere JP. Effects of metal ions on the measurement of alkaline phosphatase activity. *Clin Chem* 26: 423–428, 1980.

471. Richards A, Kragstrup J, Josephsen K, Fejerskov O. Dental fluorosis developed in post-secretory enamel. *J Dent Res* 65: 1406–1409, 1986. doi:10.1177/00220345860650120501.

472. Risnes S. The prism pattern of rat molar enamel: a scanning electron microscope study. *Am J Anat* 155: 245–257, 1979. doi:10.1002/aja.1001550207.

473. Risnes S. A scanning electron microscope study of aberrations in the prism pattern of rat incisor inner enamel. *Am J Anat* 154: 419–436, 1979. doi:10.1002/aja.1001540307.

474. Robinson C. Self-oriented assembly of nano-apatite particles: a subunit mechanism for building biological mineral crystals. *J Dent Res* 86: 677–679, 2007. doi:10.1177/154405910708600801.

475. Robinson C, Brookes SJ, Shore RC, Kirkham J. The developing enamel matrix: nature and function. *Eur J Oral Sci* 106, Suppl 1: 282–291, 1998. doi:10.1111/j.1600-0722.1998.tb02188.x.

476. Robinson C, Connell S, Kirkham J, Brookes SJ, Shore RC, Smith AM. The effect of fluoride on the developing tooth. *Caries Res* 38: 268–276, 2004. doi:10.1159/000077766.

477. Robinson C, Hiller CR, Weatherell JA. Uptake of $^{32}$P-labelled phosphate into developing rat incisor enamel. *Calcif Tissue Res* 15: 143–152, 1974. doi:10.1007/BF02059052.

478. Robinson C, Shore RC, Brookes SJ, Strafford S, Wood SR, Kirkham J. The chemistry of enamel caries. *Crit Rev Oral Biol Med* 11: 481–495, 2000. doi:10.1177/10454411000110040601.

479. Robinson C, Weatherell JA, Hallsworth AS. Variation in composition of dental enamel within thin ground tooth sections. *Caries Res* 5: 44–57, 1971. doi:10.1159/000259731.

480. Robinson MS, Bonifacino JS. Adaptor-related proteins. *Curr Opin Cell Biol* 13: 444–453, 2001. doi:10.1016/S0955-0674(00)00235-0.

481. Romero MF, Chen AP, Parker MD, Boron WF. The SLC4 family of bicarbonate ($HCO_3^-$) transporters. *Mol Aspects Med* 34: 159–182, 2013. doi:10.1016/j.mam.2012.10.008.

482. Rosset EM, Bradshaw AD. SPARC/osteonectin in mineralized tissue. *Matrix Biol* 52-54: 78–87, 2016. doi:10.1016/j.matbio.2016.02.001.

483. Rous BA, Reaves BJ, Ihrke G, Briggs JA, Gray SR, Stephens DJ, Banting G, Luzio JP. Role of adaptor complex AP-3 in targeting wild-type and mutated CD63 to lysosomes. *Mol Biol Cell* 13: 1071–1082, 2002. doi:10.1091/mbc.01-08-0409.

484. Ruan Q, Liberman D, Bapat R, Chandrababu KB, Phark JH, Moradian-Oldak J. Efficacy of amelogenin-chitosan hydrogel in biomimetic repair of human enamel in pH-cycling systems. *J Biomed Eng Inform* 2: 119–128, 2016. doi:10.5430/jbei.v2n1p119.

485. Ruan Q, Moradian-Oldak J. Amelogenin and enamel biomimetics. *J Mater Chem B Mater Biol Med* 3: 3112–3129, 2015. doi:10.1039/C5TB00163C.

486. Ruan Q, Zhang Y, Yang X, Nutt S, Moradian-Oldak J. An amelogenin-chitosan matrix promotes assembly of an enamel-like layer with a dense interface. *Acta Biomater* 9: 7289–7297, 2013. doi:10.1016/j.actbio.2013.04.004.

487. Rugg-Gunn A. Dental caries: strategies to control this preventable disease. *Acta Med Acad* 42: 117–130, 2013. doi:10.5644/ama2006-124.80.

488. Ryu OH, Fincham AG, Hu CC, Zhang C, Qian Q, Bartlett JD, Simmer JP. Characterization of recombinant pig enamelysin activity and cleavage of recombinant pig and mouse amelogenins. *J Dent Res* 78: 743–750, 1999. doi:10.1177/00220345990780030601.

489. Saito A, Sato H, Iino N, Takeda T. Molecular mechanisms of receptor-mediated endocytosis in the renal proximal tubular epithelium. *J Biomed Biotechnol* 2010: 403272, 2010. doi:10.1155/2010/403272.

490. Salama AH, Zaki AE, Eisenmann DR. Cytochemical localization of $Ca^{2+}$-$Mg^{2+}$ adenosine triphosphatase in rat incisor ameloblasts during enamel secretion and maturation. *J Histochem Cytochem* 35: 471–482, 1987. doi:10.1177/35.4.2950164.

491. Salas JT, Banales JM, Sarvide S, Recalde S, Ferrer A, Uriarte I, Oude Elferink RP, Prieto J, Medina JF. Ae2a,b-deficient mice develop antimitochondrial antibodies and other features resembling primary biliary cirrhosis. *Gastroenterology* 134: 1482–1493, 2008. doi:10.1053/j.gastro.2008.02.020.

492. Salido EC, Yen PH, Koprivnikar K, Yu LC, Shapiro LJ. The human enamel protein gene amelogenin is expressed from both the X and the Y chromosomes. *Am J Hum Genet* 50: 303–316, 1992.

493. Sanii B, Martinez-Avila O, Simpliciano C, Zuckermann RN, Habelitz S. Matching 4.7-Å XRD spacing in amelogenin nanoribbons and enamel matrix. *J Dent Res* 93: 918–922, 2014. doi:10.1177/0022034514544216.

494. Sarkar J, Simanian EJ, Tuggy SY, Bartlett JD, Snead ML, Sugiyama T, Paine ML. Comparison of two mouse ameloblast-like cell lines for enamel-specific gene expression. *Front Physiol* 5: 277, 2014. doi:10.3389/fphys.2014.00277.

495. Sarkar J, Wen X, Simanian EJ, Paine ML. V-type ATPase proton pump expression during enamel formation. *Matrix Biol* 52-54: 234–245, 2016. doi:10.1016/j.matbio.2015.11.004.

496. Sasaki S, Shimokawa H. The amelogenin gene. *Int J Dev Biol* 39: 127–133, 1995.

497. Sasaki S, Takagi T, Suzuki M. Cyclical changes in pH in bovine developing enamel as sequential bands. *Arch Oral Biol* 36: 227–231, 1991. doi:10.1016/0003-9969(91)90090-H.

498. Sasaki T. Endocytotic pathways at the ruffled borders of rat maturation ameloblasts. *Histochemistry* 80: 263–268, 1984. doi:10.1007/BF00495775.

499. Sasaki T. Tracer, cytochemical, and freeze-fracture study on the mechanisms whereby secretory ameloblasts absorb exogeneous proteins. *Acta Anat (Basel)* 118: 23–33, 1984. doi:10.1159/000145817.

500. Sasaki T. Ultrastructural and cytochemical studies of resorptive and digestive functions of secretory ameloblasts in kitten tooth germs. *Acta Anat (Basel)* 115: 361–375, 1983. doi:10.1159/000145713.

501. Sasaki T, Debari K, Garant PR. Ameloblast modulation and changes in the Ca, P, and S content of developing enamel matrix as revealed by SEM-EDX. *J Dent Res* 66: 778–783, 1987. doi:10.1177/00220345870660031501.

502. Sasaki T, Goldberg M, Takuma S, Garant PR. Cell biology of tooth enamel formation. Functional electron microscopic monographs. *Monogr Oral Sci* 14: 1–199, 1990. doi:10.1159/000417939.

503. Sasaki T, Higashi S, Tachikawa T, Yoshiki S. Formation of tight junctions in differentiating and secretory ameloblasts of rat molar tooth germs. *Arch Oral Biol* 27: 1059–1068, 1982. doi:10.1016/0003-9969(82)90012-7.

504. Sasaki T, Higashi S, Tachikawa T, Yoshiki S. Morphology and permeability of junctional complexes in maturing ameloblasts of rat incisors. *Acta Anat (Basel)* 116: 74–83, 1983. doi:10.1159/000145728.

505. Sasaki T, Higashi S, Tachikawa T, Yoshiki S. Thin-section, tracer, and freeze-fracture study of the smooth-ended maturation ameloblasts in rat incisors. *Acta Anat (Basel)* 117: 303–313, 1983. doi:10.1159/000145802.

506. Sasaki T, Segawa K, Takiguchi R, Higashi S. Intercellular junctions in the cells of the human enamel organ as revealed by freeze-fracture. *Arch Oral Biol* 29: 275–286, 1984. doi:10.1016/0003-9969(84)90101-8.

507. Sato O, Maeda T, Iwanaga T, Kobayashi S. Innervation of the incisors and periodontal ligament in several rodents: an immunohistochemical study of neurofilament protein and glia-specific S-100 protein. *Acta Anat (Basel)* 134: 94–99, 1989. doi:10.1159/000146671.

508. Schiavi SC, Tang W, Bracken C, O'Brien SP, Song W, Boulanger J, Ryan S, Phillips L, Liu S, Arbeeny C, Ledbetter S, Sabbagh Y. Npt2b deletion attenuates hyperphosphatemia

associated with CKD. *J Am Soc Nephrol* 23: 1691–1700, 2012. doi:10.1681/ASN.2011121213.

509. Schmitz JE, Teepe JD, Hu Y, Smith CE, Fajardo RJ, Chun YH. Estimating mineral changes in enamel formation by ashing/BSE and microCT. *J Dent Res* 93: 256–262, 2014. doi:10.1177/0022034513520548.

510. Schossig A, Wolf NI, Fischer C, Fischer M, Stocker G, Pabinger S, Dander A, Steiner B, Tönz O, Kotzot D, Haberlandt E, Amberger A, Burwinkel B, Wimmer K, Fauth C, Grond-Ginsbach C, Koch MJ, Deichmann A, von Kalle C, Bartram CR, Kohlschütter A, Trajanoski Z, Zschocke J. Mutations in ROGDI cause Kohlschütter-Tönz syndrome. *Am J Hum Genet* 90: 701–707, 2012. doi:10.1016/j.ajhg.2012.02.012.

511. Schweinfest CW, Spyropoulos DD, Henderson KW, Kim JH, Chapman JM, Barone S, Worrell RT, Wang Z, Soleimani M. slc26a3 (dra)-deficient mice display chloride-losing diarrhea, enhanced colonic proliferation, and distinct up-regulation of ion transporters in the colon. *J Biol Chem* 281: 37962–37971, 2006. doi:10.1074/jbc.M607527200.

512. Seymen F, Kim YJ, Lee YJ, Kang J, Kim TH, Choi H, Koruyucu M, Kasimoglu Y, Tuna EB, Gencay K, Shin TJ, Hyun HK, Kim YJ, Lee SH, Lee ZH, Zhang H, Hu JC, Simmer JP, Cho ES, Kim JW. Recessive mutations in ACPT, encoding testicular acid phosphatase, cause hypoplastic amelogenesis imperfecta. *Am J Hum Genet* 99: 1199–1205, 2016. doi:10.1016/j.ajhg.2016.09.018.

513. Sferra TJ, Collins FS. The molecular biology of cystic fibrosis. *Annu Rev Med* 44: 133–144, 1993. doi:10.1146/annurev.me.44.020193.001025.

514. Shapiro IM, Wuthier RE. A study of the phospholipids of bovine dental tissues. II. Developing bovine foetal dental pulp. *Arch Oral Biol* 11: 513–519, 1966. doi:10.1016/0003-9969(66)90157-9.

515. Shapiro IM, Wuthier RE, Irving JT. A study of the phospholipids of bovine dental tissues. I. Enamel matrix and dentine. *Arch Oral Biol* 11: 501–512, 1966. doi:10.1016/0003-9969(66)90156-7.

516. Shapiro JL, Wang H, Wen X, Tannukit S, Paine ML. An amelogenin minigene to study alternative splicing. *DNA Cell Biol* 25: 1–5, 2006. doi:10.1089/dna.2006.25.1.

517. Sharma CG, Pradeep AR. Localized attachment loss in Pendred syndrome: incidental? *J Periodontol* 78: 948–954, 2007. doi:10.1902/jop.2007.060270.

518. Sharma R, Tsuchiya M, Tannous BA, Bartlett JD. Measurement of fluoride-induced endoplasmic reticulum stress using Gaussia luciferase. *Methods Enzymol* 491: 111–125, 2011. doi:10.1016/B978-0-12-385928-0.00007-9.

519. Shaw JH, Yen PK. Sodium, potassium, and magnesium concentrations in the enamel and dentin of human and rhesus monkey teeth. *J Dent Res* 51: 95–101, 1972. doi:10.1177/00220345720510013701.

520. Shaw WJ, Campbell AA, Paine ML, Snead ML. The COOH terminus of the amelogenin, LRAP, is oriented next to the hydroxyapatite surface. *J Biol Chem* 279: 40263–40266, 2004. doi:10.1074/jbc.C400322200.

521. Shin M, Hu Y, Tye CE, Guan X, Deagle CC, Antone JV, Smith CE, Simmer JP, Bartlett JD. Matrix metalloproteinase-20 over-expression is detrimental to enamel development: a *Mus musculus* model. *PLoS One* 9: e86774, 2014. doi:10.1371/journal.pone.0086774.

522. Sierant ML, Bartlett JD. Stress response pathways in ameloblasts: implications for amelogenesis and dental fluorosis. *Cells* 1: 631–645, 2012. doi:10.3390/cells1030631.

523. Simmer JP, Fincham AG. Molecular mechanisms of dental enamel formation. *Crit Rev Oral Biol Med* 6: 84–108, 1995. doi:10.1177/10454411950060020701.

524. Simmer JP, Hu JC. Expression, structure, and function of enamel proteinases. *Connect Tissue Res* 43: 441–449, 2002. doi:10.1080/03008200290001159.

525. Simmer JP, Hu Y, Lertlam R, Yamakoshi Y, Hu JC. Hypomaturation enamel defects in Klk4 knockout/LacZ knockin mice. *J Biol Chem* 284: 19110–19121, 2009. doi:10.1074/jbc.M109.013623.

526. Simmer JP, Hu Y, Richardson AS, Bartlett JD, Hu JC. Why does enamel in Klk4-null mice break above the dentino-enamel junction? *Cells Tissues Organs* 194: 211–215, 2011. doi:10.1159/000324260.

527. Simmer JP, Papagerakis P, Smith CE, Fisher DC, Rountrey AN, Zheng L, Hu JC. Regulation of dental enamel shape and hardness. *J Dent Res* 89: 1024–1038, 2010. doi:10.1177/0022034510375829.

528. Simmer JP, Snead ML. Molecular biology of the amelogenin gene. In: *Dental Enamel: Formation to Destruction*, edited by Robinson C, Kirkham J, Shore R. Boca Raton, FL: CRC, 1995, p. 59–84.

529. Simmer JP, Hu CC, Lau EC, Sarte P, Slavkin HC, Fincham AG. Alternative splicing of the mouse amelogenin primary RNA transcript. *Calcif Tissue Int* 55: 302–310, 1994. doi:10.1007/BF00310410.

530. Simmons D, Gu TT, Krebsbach PH, Yamada Y, MacDougall M. Identification and characterization of a cDNA for mouse ameloblastin. *Connect Tissue Res* 39: 3–12, 1998. doi:10.3109/03008209809023907.

531. Singh AK, Sjöblom M, Zheng W, Krabbenhöft A, Riederer B, Rausch B, Manns MP, Soleimani M, Seidler U. CFTR and its key role in in vivo resting and luminal acid-induced duodenal $HCO_3^-$ secretion. *Acta Physiol (Oxf)* 193: 357–365, 2008. doi:10.1111/j.1748-1716.2008.01854.x.

532. Sire JY, Davit-Béal T, Delgado S, Gu X. The origin and evolution of enamel mineralization genes. *Cells Tissues Organs* 186: 25–48, 2007. doi:10.1159/000102679.

533. Sire JY, Delgado S, Fromentin D, Girondot M. Amelogenin: lessons from evolution. *Arch Oral Biol* 50: 205–212, 2005. doi:10.1016/j.archoralbio.2004.09.004.

534. Sire JY, Delgado S, Girondot M. The amelogenin story: origin and evolution. *Eur J Oral Sci* 114, Suppl 1: 64–77, 2006. doi:10.1111/j.1600-0722.2006.00297.x.

535. Skinner MF, Hung JT. Social and biological correlates of localized enamel hypoplasia of the human deciduous canine tooth. *Am J Phys Anthropol* 79: 159–175, 1989. doi:10.1002/ajpa.1330790204.

536. Skobe Z, Prostak KS, Stern DN. A scanning electron microscope study of monkey maturation-stage ameloblasts. *J Dent Res* 67: 1396–1401, 1988. doi:10.1177/00220345880670110701.

537. Slavkin HC, Bessem C, Fincham AG, Bringas P Jr, Santos V, Snead ML, Zeichner-David M. Human and mouse cementum proteins immunologically related to enamel proteins. *Biochim Biophys Acta* 991: 12–18, 1989. doi:10.1016/0304-4165(89)90021-4.

538. Slayton RL, Warren JJ, Kanellis MJ, Levy SM, Islam M. Prevalence of enamel hypoplasia and isolated opacities in the primary dentition. *Pediatr Dent* 23: 32–36, 2001.

539. Sly WS, Hu PY. Human carbonic anhydrases and carbonic anhydrase deficiencies. *Annu Rev Biochem* 64: 375–401, 1995. doi:10.1146/annurev.bi.64.070195.002111.

540. Smith CE. Ameloblasts: secretory and resorptive functions. *J Dent Res* 58, Suppl 2: 695–707, 1979. doi:10.1177/00220345790580022011.

541. Smith CE. Cellular and chemical events during enamel maturation. *Crit Rev Oral Biol Med* 9: 128–161, 1998. doi:10.1177/10454411980090020101.

542. Smith CE, Chong DL, Bartlett JD, Margolis HC. Mineral acquisition rates in developing enamel on maxillary and mandibular incisors of rats and mice: implications for extracellular acid loading as apatite crystals mature. *J Bone Miner Res* 20: 240–249, 2005. doi:10.1359/JBMR.041002.

543. Smith CE, Hu Y, Hu JC, Simmer JP. Ultrastructure of early amelogenesis in wild-type, Amelx(−/−), and Enam(−/−) mice: enamel ribbon initiation on dentin mineral and ribbon orientation by ameloblasts. *Mol Genet Genomic Med* 4: 662–683, 2016. doi:10.1002/mgg3.253.

544. Smith CE, Issid M, Margolis HC, Moreno EC. Developmental changes in the pH of enamel fluid and its effects on matrix-resident proteinases. *Adv Dent Res* 10: 159–169, 1996. doi:10.1177/08959374960100020701.

545. Smith CE, McKee MD, Nanci A. Cyclic induction and rapid movement of sequential waves of new smooth-ended ameloblast modulation bands in rat incisors as visualized by polychrome fluorescent labeling and GBHA-staining of maturing enamel. *Adv Dent Res* 1: 162–175, 1987. doi:10.1177/08959374870010020401.

546. Smith CE, Murillo G, Brookes SJ, Poulter JA, Silva S, Kirkham J, Inglehearn CF, Mighell AJ. Deletion of amelotin exons 3-6 is associated with amelogenesis imperfecta. *Hum Mol Genet* 25: 3578–3587, 2016. doi:10.1093/hmg/ddw203.

547. Smith CE, Nanci A. A method for sampling the stages of amelogenesis on mandibular rat incisors using the molars as a reference for dissection. *Anat Rec* 225: 257–266, 1989. doi:10.1002/ar.1092250312.

548. Smith CE, Nanci A. Protein dynamics of amelogenesis. *Anat Rec* 245: 186–207, 1996. doi:10.1002/(SICI)1097-0185(199606)245:2<186::AID-AR7>3.0.CO;2-V.

549. Smith CE, Nanci A, Moffatt P. Evidence by signal peptide trap technology for the expression of carbonic anhydrase 6 in rat incisor enamel organs. *Eur J Oral Sci* 114, Suppl 1: 147–153, 2006. doi:10.1111/j.1600-0722.2006.00273.x.

550. Smith CE, Warshawsky H. Quantitative analysis of cell turnover in the enamel organ of the rat incisor. Evidence for ameloblast death immediately after enamel matrix secretion. *Anat Rec* 187: 63–98, 1977. doi:10.1002/ar.1091870106.

551. Smith KD, Gordon PB, Rivetta A, Allen KE, Berbasova T, Slayman C, Strobel SA. Yeast Fex1p is a constitutively expressed fluoride channel with functional asymmetry of its two homologous domains. *J Biol Chem* 290: 19874–19887, 2015. doi:10.1074/jbc.M115.651976.

552. Snead ML, Lau EC, Fincham AG, Zeichner-David M, Davis C, Slavkin HC. Of mice and men: anatomy of the amelogenin gene. *Connect Tissue Res* 22: 101–109, 1989. doi:10.3109/03008208909114125.

553. Snead ML, Lau EC, Zeichner-David M, Fincham AG, Woo SL, Slavkin HC. DNA sequence for cloned cDNA for murine amelogenin reveal the amino acid sequence for enamel-specific protein. *Biochem Biophys Res Commun* 129: 812–818, 1985. doi:10.1016/0006-291X(85)91964-3.

554. Snead ML, Luo W, Lau EC, Slavkin HC. Spatial- and temporal-restricted pattern for amelogenin gene expression during mouse molar tooth organogenesis. *Development* 104: 77–85, 1988.

555. Snead ML, Zeichner-David M, Chandra T, Robson KJ, Woo SL, Slavkin HC. Construction and identification of mouse amelogenin cDNA clones. *Proc Natl Acad Sci USA* 80: 7254–7258, 1983. doi:10.1073/pnas.80.23.7254.

556. Snead ML, Zhu DH, Lei Y, Luo W, Bringas PO Jr, Sucov HM, Rauth RJ, Paine ML, White SN. A simplified genetic design for mammalian enamel. *Biomaterials* 32: 3151–3157, 2011. doi:10.1016/j.biomaterials.2011.01.024.

557. Spahr A, Lyngstadaas SP, Slaby I, Pezeshki G. Ameloblastin expression during craniofacial bone formation in rats. *Eur J Oral Sci* 114: 504–511, 2006. doi:10.1111/j.1600-0722.2006.00403.x.

558. Spoonhower KA, Davis PB. Epidemiology of cystic fibrosis. *Clin Chest Med* 37: 1–8, 2016. doi:10.1016/j.ccm.2015.10.002.

559. Stathopulos PB, Seo MD, Enomoto M, Amador FJ, Ishiyama N, Ikura M. Themes and variations in ER/SR calcium release channels: structure and function. *Physiology (Bethesda)* 27: 331–342, 2012. doi:10.1152/physiol.00013.2012.

560. Stein G, Boyle PE. Pigmentation of the enamel of albino rat incisor teeth. *Arch Oral Biol* 1: 97–105, 1959. doi:10.1016/0003-9969(59)90002-0.

561. Stephanopoulos G, Garefalaki ME, Lyroudia K. Genes and related proteins involved in amelogenesis imperfecta. *J Dent Res* 84: 1117–1126, 2005. doi:10.1177/154405910508401206.

562. Stockbridge RB, Lim HH, Otten R, Williams C, Shane T, Weinberg Z, Miller C. Fluoride resistance and transport by riboswitch-controlled CLC antiporters. *Proc Natl Acad Sci USA* 109: 15289–15294, 2012. doi:10.1073/pnas.1210896109.

563. Stockbridge RB, Robertson JL, Kolmakova-Partensky L, Miller C. A family of fluoride-specific ion channels with dual-topology architecture. *Elife* 2: e01084, 2013.

564. Stoltz DA, Meyerholz DK, Pezzulo AA, Ramachandran S, Rogan MP, Davis GJ, Hanfland RA, Wohlford-Lenane C, Dohrn CL, Bartlett JA, Nelson GA IV, Chang EH, Taft PJ, Ludwig PS, Estin M, Hornick EE, Launspach JL, Samuel M, Rokhlina T, Karp PH, Ostedgaard LS, Uc A, Starner TD, Horswill AR, Brogden KA, Prather RS, Richter SS, Shilyansky J, McCray PB Jr, Zabner J, Welsh MJ. Cystic fibrosis pigs develop lung disease and exhibit defective bacterial eradication at birth. *Sci Transl Med* 2: 29ra31, 2010. doi:10.1126/scitranslmed.3000928.

565. Stoltz DA, Meyerholz DK, Welsh MJ. Origins of cystic fibrosis lung disease. *N Engl J Med* 372: 1574–1575, 2015. doi:10.1056/NEJMc1502191.

566. Storch S, Kübler B, Höning S, Ackmann M, Zapf J, Blum W, Braulke T. Transferrin binds insulin-like growth factors and affects binding properties of insulin-like growth factor binding protein-3. *FEBS Lett* 509: 395–398, 2001. doi:10.1016/S0014-5793(01)03204-5.

567. Strisciuglio P, Sartorio R, Pecoraro C, Lotito F, Sly WS. Variable clinical presentation of carbonic anhydrase deficiency: evidence for heterogeneity? *Eur J Pediatr* 149: 337–340, 1990. doi:10.1007/BF02171561.

568. Stuart-Tilley A, Sardet C, Pouyssegur J, Schwartz MA, Brown D, Alper SL. Immunolocalization of anion exchanger AE2 and cation exchanger NHE-1 in distinct adjacent cells of gastric mucosa. *Am J Physiol Cell Physiol* 266: C559–C568, 1994.

569. Stuart-Tilley AK, Shmukler BE, Brown D, Alper SL. Immunolocalization and tissue-specific splicing of AE2 anion exchanger in mouse kidney. *J Am Soc Nephrol* 9: 946–959, 1998.

570. Suckling GW, Brown RH, Herbison GP. The prevalence of developmental defects of enamel in 696 nine-year-old New Zealand children participating in a health and development study. *Community Dent Health* 2: 303–313, 1985.

571. Suckling GW, Pearce EI. Developmental defects of enamel in a group of New Zealand children: their prevalence and some associated etiological factors. *Community Dent Oral Epidemiol* 12: 177–184, 1984. doi:10.1111/j.1600-0528.1984.tb01434.x.

572. Sui W, Boyd C, Wright JT. Altered pH regulation during enamel development in the cystic fibrosis mouse incisor. *J Dent Res* 82: 388–392, 2003. doi:10.1177/154405910308200512.

573. Supuran CT. Carbonic anhydrases--an overview. *Curr Pharm Des* 14: 603–614, 2008. doi:10.2174/138161208783877884.

574. Supuran CT. Carbonic anhydrases: novel therapeutic applications for inhibitors and activators. *Nat Rev Drug Discov* 7: 168–181, 2008. doi:10.1038/nrd2467.

575. Suzuki M, Shin M, Simmer JP, Bartlett JD. Fluoride affects enamel protein content via TGF-$\beta$1-mediated KLK4 inhibition. *J Dent Res* 93: 1022–1027, 2014. doi:10.1177/0022034514545629.

576. Suzuki M, Sierant ML, Antone JV, Everett ET, Whitford GM, Bartlett JD. Uncoupling protein-2 is an antioxidant that is up-regulated in the enamel organ of fluoride-treated rats. *Connect Tissue Res* 55, Suppl 1: 25–28, 2014. doi:10.3109/03008207.2014.923854.

577. Takagi T, Ogasawara T, Tagami J, Akao M, Kuboki Y, Nagai N, LeGeros RZ. pH and carbonate levels in developing enamel. *Connect Tissue Res* 38: 181–187, 1998. doi:10.3109/03008209809017035.

578. Takagi T, Suzuki M, Baba T, Minegishi K, Sasaki S. Complete amino acid sequence of amelogenin in developing bovine enamel. *Biochem Biophys Res Commun* 121: 592–597, 1984. doi:10.1016/0006-291X(84)90223-7.

579. Takano Y. Enamel mineralization and the role of ameloblasts in calcium transport. *Connect Tissue Res* 33: 127–137, 1995. doi:10.3109/03008209509016992.

580. Takano Y, Crenshaw MA. The penetration of intravascularly perfused lanthanum into the ameloblast layer of developing rat molar teeth. *Arch Oral Biol* 25: 505–511, 1980. doi:10.1016/0003-9969(80)90061-8.

581. Takano Y, Crenshaw MA, Bawden JW, Hammarström L, Lindskog S. The visualization of the patterns of ameloblast modulation by the glyoxal bis(2-hydroxyanil) staining method. *J Dent Res* (Spec No): 1580–1587, 1982.

582. Takano Y, Crenshaw MA, Reith EJ. Correlation of $^{45}$Ca incorporation with maturation ameloblast morphology in the rat incisor. *Calcif Tissue Int* 34: 211–213, 1982. doi:10.1007/BF02411236.

583. Takano Y, Ozawa H. Ultrastructural and cytochemical observations on the alternating morphologic changes of the ameloblasts at the stage of enamel maturation. *Arch Histol Jpn* 43: 385–399, 1980. doi:10.1679/aohc1950.43.385.

584. Takei K, Haucke V. Clathrin-mediated endocytosis: membrane factors pull the trigger. *Trends Cell Biol* 11: 385–391, 2001. doi:10.1016/S0962-8924(01)02082-7.

585. Takei K, Haucke V, Slepnev V, Farsad K, Salazar M, Chen H, De Camilli P. Generation of coated intermediates of clathrin-mediated endocytosis on protein-free liposomes. *Cell* 94: 131–141, 1998. doi:10.1016/S0092-8674(00)81228-3.

586. Takei K, Slepnev VI, Haucke V, De Camilli P. Functional partnership between amphiphysin and dynamin in clathrin-mediated endocytosis. *Nat Cell Biol* 1: 33–39, 1999.

587. Tamburstuen MV, Reppe S, Spahr A, Sabetrasekh R, Kvalheim G, Slaby I, Syversen U, Lyngstadaas SP, Reseland JE. Ameloblastin promotes bone growth by enhancing proliferation of progenitor cells and by stimulating immunoregulators. *Eur J Oral Sci* 118: 451–459, 2010. doi:10.1111/j.1600-0722.2010.00760.x.

588. Tao J, Buchko GW, Shaw WJ, De Yoreo JJ, Tarasevich BJ. Sequence-defined energetic shifts control the disassembly kinetics and microstructure of amelogenin adsorbed

onto hydroxyapatite (100). *Langmuir* 31: 10451–10460, 2015. doi:10.1021/acs.langmuir.5b02549.

589. Ten Cate JM. Review on fluoride, with special emphasis on calcium fluoride mechanisms in caries prevention. *Eur J Oral Sci* 105: 461–465, 1997. doi:10.1111/j.1600-0722.1997.tb00231.x.

590. Ten Cate JM, Featherstone JD. Mechanistic aspects of the interactions between fluoride and dental enamel. *Crit Rev Oral Biol Med* 2: 283–296, 1991. doi:10.1177/10454411910020030101.

591. Termine JD, Belcourt AB, Christner PJ, Conn KM, Nylen MU. Properties of dissociatively extracted fetal tooth matrix proteins. I. Principal molecular species in developing bovine enamel. *J Biol Chem* 255: 9760–9768, 1980.

592. Tomes J. On the development of the enamel. *J Microsc Sci* 4: 213–220, 1856.

593. Tomoe Y, Segawa H, Shiozawa K, Kaneko I, Tominaga R, Hanabusa E, Aranami F, Furutani J, Kuwahara S, Tatsumi S, Matsumoto M, Ito M, Miyamoto K. Phosphaturic action of fibroblast growth factor 23 in Npt2 null mice. *Am J Physiol Renal Physiol* 298: F1341–F1350, 2010. doi:10.1152/ajprenal.00375.2009.

594. Tompkins K. Molecular mechanisms of cytodifferentiation in mammalian tooth development. *Connect Tissue Res* 47: 111–118, 2006. doi:10.1080/03008200600727756.

595. Toyosawa S, Ogawa Y, Inagaki T, Ijuhin N. Immunohistochemical localization of carbonic anhydrase isozyme II in rat incisor epithelial cells at various stages of amelogenesis. *Cell Tissue Res* 285: 217–225, 1996. doi:10.1007/s004410050639.

596. Travis DF, Glimcher MJ. The structure and organization of, and the relationship between the organic matrix and the inorganic crystals of embryonic bovine enamel. *J Cell Biol* 23: 447–497, 1964. doi:10.1083/jcb.23.3.447.

597. Triller M. [Fluoride, a preventive agent of caries: mechanisms, sources, risks]. *Arch Pediatr* 5: 1149–1152, 1998. doi:10.1016/S0929-693X(99)80016-5.

598. Türeci O, Sahin U, Vollmar E, Siemer S, Göttert E, Seitz G, Parkkila AK, Shah GN, Grubb JH, Pfreundschuh M, Sly WS. Human carbonic anhydrase XII: cDNA cloning, expression, and chromosomal localization of a carbonic anhydrase gene that is overexpressed in some renal cell cancers. *Proc Natl Acad Sci USA* 95: 7608–7613, 1998. doi:10.1073/pnas.95.13.7608.

599. Turnbull CI, Looi K, Mangum JE, Meyer M, Sayer RJ, Hubbard MJ. Calbindin independence of calcium transport in developing teeth contradicts the calcium ferry dogma. *J Biol Chem* 279: 55850–55854, 2004. doi:10.1074/jbc.M409299200.

600. Tye CE, Antone JV, Bartlett JD. Fluoride does not inhibit enamel protease activity. *J Dent Res* 90: 489–494, 2011. doi:10.1177/0022034510390043.

601. Tye CE, Pham CT, Simmer JP, Bartlett JD. DPPI may activate KLK4 during enamel formation. *J Dent Res* 88: 323–327, 2009. doi:10.1177/0022034509334240.

602. Uchida T, McKee MD, Warshawsky H. A radioautographic study of the effects of vinblastine on the fate of injected $^{45}$calcium and [$^{125}$I]-insulin in the rat incisor. *Arch Oral Biol* 32: 433–437, 1987. doi:10.1016/0003-9969(87)90079-3.

603. Uchida T, Tanabe T, Fukae M, Shimizu M. Immunocytochemical and immunochemical detection of a 32 kDa nonamelogenin and related proteins in porcine tooth germs. *Arch Histol Cytol* 54: 527–538, 1991. doi:10.1679/aohc.54.527.

604. Urzúa B, Ortega-Pinto A, Morales-Bozo I, Rojas-Alcayaga G, Cifuentes V. Defining a new candidate gene for amelogenesis imperfecta: from molecular genetics to biochemistry. *Biochem Genet* 49: 104–121, 2011. doi:10.1007/s10528-010-9392-6.

605. Usami S, Abe S, Weston MD, Shinkawa H, Van Camp G, Kimberling WJ. Non-syndromic hearing loss associated with enlarged vestibular aqueduct is caused by PDS mutations. *Hum Genet* 104: 188–192, 1999. doi:10.1007/s004390050933.

606. Van Hauwe P, Everett LA, Coucke P, Scott DA, Kraft ML, Ris-Stalpers C, Bolder C, Otten B, de Vijlder JJ, Dietrich NL, Ramesh A, Srisailapathy SC, Parving A, Cremers CW, Willems PJ, Smith RJ, Green ED, Van Camp G. Two frequent missense mutations in Pendred syndrome. *Hum Mol Genet* 7: 1099–1104, 1998. doi:10.1093/hmg/7.7.1099.

607. Vieira AP, Hanocock R, Eggertsson H, Everett ET, Grynpas MD. Tooth quality in dental fluorosis genetic and environmental factors. *Calcif Tissue Int* 76: 17–25, 2005. doi:10.1007/s00223-004-0075-3.

608. Vieira AP, Mousny M, Maia R, Hancock R, Everett ET, Grynpas MD. Assessment of teeth as biomarkers for skeletal fluoride exposure. *Osteoporos Int* 16: 1576–1582, 2005. doi:10.1007/s00198-005-1870-z.

609. Vieira AR, Kup E. On the etiology of molar-incisor hypomineralization. *Caries Res* 50: 166–169, 2016. doi:10.1159/000445128.

610. Virkki LV, Biber J, Murer H, Forster IC. Phosphate transporters: a tale of two solute carrier families. *Am J Physiol Renal Physiol* 293: F643–F654, 2007. doi:10.1152/ajprenal.00228.2007.

611. Von Wurmb-Schwark N, Bosinski H, Ritz-Timme S. What do the X and Y chromosomes tell us about sex and gender in forensic case analysis? *J Forensic Leg Med* 14: 27–30, 2007. doi:10.1016/j.jcfm.2005.09.003.

612. Wald T, Osickova A, Sulc M, Benada O, Semeradtova A, Rezabkova L, Veverka V, Bednarova L, Maly J, Macek P, Sebo P, Slaby I, Vondrasek J, Osicka R. Intrinsically disordered enamel matrix protein ameloblastin forms ribbon-like supramolecular structures via an N-terminal segment encoded by exon 5. *J Biol Chem* 288: 22333–22345, 2013. doi:10.1074/jbc.M113.456012.

613. Wang C, Li Y, Shi L, Ren J, Patti M, Wang T, de Oliveira JR, Sobrido MJ, Quintáns B, Baquero M, Cui X, Zhang XY, Wang L, Xu H, Wang J, Yao J, Dai X, Liu J, Zhang L, Ma H, Gao Y, Ma X, Feng S, Liu M, Wang QK, Forster IC, Zhang X, Liu JY. Mutations in SLC20A2 link familial idiopathic basal ganglia calcification with phosphate homeostasis. *Nat Genet* 44: 254–256, 2012. doi:10.1038/ng.1077.

614. Wang H, Tannukit S, Zhu D, Snead ML, Paine ML. Enamel matrix protein interactions. *J Bone Miner Res* 20: 1032–1040, 2005. doi:10.1359/JBMR.050111.

615. Wang S, Choi M, Richardson AS, Reid BM, Seymen F, Yildirim M, Tuna E, Gençay K, Simmer JP, Hu JC. STIM1 and SLC24A4 are critical for enamel maturation. *J Dent Res* 93, Suppl: 94S–100S, 2014. doi:10.1177/0022034514527971.

616. Wang SK, Hu Y, Yang J, Smith CE, Nunez SM, Richardson AS, Pal S, Samann AC, Hu JC, Simmer JP. Critical roles for WDR72 in calcium transport and matrix protein removal during enamel maturation. *Mol Genet Genomic Med* 3: 302–319, 2015. doi:10.1002/mgg3.143.

617. Wang X, Xia C, Zhang Z, Deng X, Wei S, Zheng G, Chen H. Direct growth of human enamel-like calcium phosphate microstructures on human tooth. *J Nanosci Nanotechnol* 9: 1361–1364, 2009. doi:10.1166/jnn.2009.C157.

618. Wang X, Zhao Y, Yang Y, Qin M. Novel ENAM and LAMB3 mutations in Chinese families with hypoplastic amelogenesis imperfecta. *PLoS One* 10: e0116514, 2015. doi:10.1371/journal.pone.0116514.

619. Wang Y, Soyombo AA, Shcheynikov N, Zeng W, Dorwart M, Marino CR, Thomas PJ, Muallem S. Slc26a6 regulates CFTR activity in vivo to determine pancreatic duct $HCO_3^-$ secretion: relevance to cystic fibrosis. *EMBO J* 25: 5049–5057, 2006. doi:10.1038/sj.emboj.7601387.

620. Wang Z, Wang T, Petrovic S, Tuo B, Riederer B, Barone S, Lorenz JN, Seidler U, Aronson PS, Soleimani M. Renal and intestinal transport defects in Slc26a6-null mice. *Am J Physiol Cell Physiol* 288: C957–C965, 2005. doi:10.1152/ajpcell.00505.2004.

621. Warshawsky H. The fine structure of secretory ameloblasts in rat incisors. *Anat Rec* 161: 211–229, 1968. doi:10.1002/ar.1091610207.

622. Warshawsky H, Smith CE. Morphological classification of rat incisor ameloblasts. *Anat Rec* 179: 423–446, 1974. doi:10.1002/ar.1091790403.

623. Wazen RM, Moffatt P, Ponce KJ, Kuroda S, Nishio C, Nanci A. Inactivation of the odontogenic ameloblast-associated gene affects the integrity of the junctional epithelium and gingival healing. *Eur Cell Mater* 30: 187–199, 2015. doi:10.22203/eCM.v030a13.

624. Wazen RM, Moffatt P, Zalzal SF, Yamada Y, Nanci A. A mouse model expressing a truncated form of ameloblastin exhibits dental and junctional epithelium defects. *Matrix Biol* 28: 292–303, 2009. doi:10.1016/j.matbio.2009.04.004.

625. Weatherell JA, Deutsch D, Robinson C, Hallsworth AS. Assimilation of fluoride by enamel throughout the life of the tooth. *Caries Res* 11, Suppl 1: 85–115, 1977. doi:10.1159/000260297.

626. Weatherell JA, Deutsch D, Robinson C, Hallsworth AS. Fluoride concentrations in developing enamel. *Nature* 256: 230–232, 1975. doi:10.1038/256230a0.

627. Weerheijm KL. Molar incisor hypomineralization (MIH): clinical presentation, aetiology and management. *Dent Update* 31: 9–12, 2004.

628. Wei W, Gao Y, Wang C, Zhao L, Sun D. Excessive fluoride induces endoplasmic reticulum stress and interferes enamel proteinases secretion. *Environ Toxicol* 28: 332–341, 2013. doi:10.1002/tox.20724.

629. Weinzimer SA, Gibson TB, Collett-Solberg PF, Khare A, Liu B, Cohen P. Transferrin is an insulin-like growth factor-binding protein-3 binding protein. *J Clin Endocrinol Metab* 86: 1806–1813, 2001.

630. Wen HB, Fincham AG, Moradian-Oldak J. Progressive accretion of amelogenin molecules during nanospheres assembly revealed by atomic force microscopy. *Matrix Biol* 20: 387–395, 2001. doi:10.1016/S0945-053X(01)00144-5.

631. Wen X, Lacruz RS, Paine ML. Dental and cranial pathologies in mice lacking the Cl(−)/H(+) exchanger ClC-7. *Anat Rec (Hoboken)* 298: 1502–1508, 2015. doi:10.1002/ar.23118.

632. Wen X, Paine ML. Iron deposition and ferritin heavy chain (Fth) localization in rodent teeth. *BMC Res Notes* 6: 1, 2013. doi:10.1186/1756-0500-6-1.

633. White SN, Miklus VG, Chang PP, Caputo AA, Fong H, Sarikaya M, Luo W, Paine ML, Snead ML. Controlled failure mechanisms toughen the dentino-enamel junction zone. *J Prosthet Dent* 94: 330–335, 2005. doi:10.1016/j.prosdent.2005.08.013.

634. White SN, Paine ML, Ngan AY, Miklus VG, Luo W, Wang H, Snead ML. Ectopic expression of dentin sialoprotein during amelogenesis hardens bulk enamel. *J Biol Chem* 282: 5340–5345, 2007. doi:10.1074/jbc.M604814200.

635. White SN, Paine ML, Sarikaya M, Fong H, Yu Z, Li ZC, Snead ML. Dentino-enamel junction is a broad transitional zone uniting dissimilar bioceramic composites. *J Am Ceram Soc* 83: 238–240, 2000. doi:10.1111/j.1151-2916.2000.tb01181.x.

636. Wiedemann-Bidlack FB, Beniash E, Yamakoshi Y, Simmer JP, Margolis HC. pH triggered self-assembly of native and recombinant amelogenins under physiological pH and temperature in vitro. *J Struct Biol* 160: 57–69, 2007. doi:10.1016/j.jsb.2007.06.007.

637. William V, Messer LB, Burrow MF. Molar incisor hypomineralization: review and recommendations for clinical management. *Pediatr Dent* 28: 224–232, 2006.

638. Witkop CJ. Hereditary defects in enamel and dentin. *Acta Genet Stat Med* 7: 236–239, 1957.

639. Witkop CJ Jr. Amelogenesis imperfecta, dentinogenesis imperfecta and dentin dysplasia revisited: problems in classification. *J Oral Pathol* 17: 547–553, 1988. doi:10.1111/j.1600-0714.1988.tb01332.x.

640. Wöltgens JHM, Lyaruu DM, Bronckers ALJJ, Bervoets TJM, Van Duin M. Biomineralization during early stages of the developing tooth in vitro with special reference to secretory stage of amelogenesis. *Int J Dev Biol* 39: 203–212, 1995.

641. Wright JT. The molecular etiologies and associated phenotypes of amelogenesis imperfecta. *Am J Med Genet A* 140: 2547–2555, 2006. doi:10.1002/ajmg.a.31358.

642. Wright JT, Carrion IA, Morris C. The molecular basis of hereditary enamel defects in humans. *J Dent Res* 94: 52–61, 2015. doi:10.1177/0022034514556708.

643. Wright JT, Chen SC, Hall KI, Yamauchi M, Bawden JW. Protein characterization of fluorosed human enamel. *J Dent Res* 75: 1936–1941, 1996. doi:10.1177/00220345960750120401.

644. Wright JT, Frazier-Bowers S, Simmons D, Alexander K, Crawford P, Han ST, Hart PS, Hart TC. Phenotypic variation in FAM83H-associated amelogenesis imperfecta. *J Dent Res* 88: 356–360, 2009. doi:10.1177/0022034509333822.

645. Wright JT, Hall KI, Deaton TG, Fine JD. Structural and compositional alteration of tooth enamel in hereditary epidermolysis bullosa. *Connect Tissue Res* 34: 271–279, 1996. doi:10.3109/03008209609005271.

646. Wright JT, Hall KI, Grubb BR. Enamel mineral composition of normal and cystic fibrosis transgenic mice. *Adv Dent Res* 10: 270–274, 1996. doi:10.1177/08959374960100022501.

647. Wright JT, Hall KI, Yamauche M. The enamel proteins in human amelogenesis imperfecta. *Arch Oral Biol* 42: 149–159, 1997. doi:10.1016/S0003-9969(96)00096-9.

648. Wright JT, Hart PS, Aldred MJ, Seow K, Crawford PJ, Hong SP, Gibson CW, Hart TC. Relationship of phenotype and genotype in X-linked amelogenesis imperfecta. *Connect Tissue Res* 44, Suppl 1: 72–78, 2003. doi:10.1080/03008200390152124.

649. Wright JT, Hart TC, Hart PS, Simmons D, Suggs C, Daley B, Simmer J, Hu J, Bartlett JD, Li Y, Yuan ZA, Seow WK, Gibson CW. Human and mouse enamel phenotypes resulting from mutation or altered expression of AMEL, ENAM, MMP20 and KLK4. *Cells Tissues Organs* 189: 224–229, 2009. doi:10.1159/000151378.

649a. Wright JT, Johnson LB, Fine JD. Development defects of enamel in humans with hereditary epidermolysis bullosa. *Arch Oral Biol* 38: 945–955, 1993.

650. Wright JT, Kiefer CL, Hall KI, Grubb BR. Abnormal enamel development in a cystic fibrosis transgenic mouse model. *J Dent Res* 75: 966–973, 1996. doi:10.1177/00220345960750041101.

651. Wright JT, Kula K, Hall K, Simmons JH, Hart TC. Analysis of the tricho-dento-osseous syndrome genotype and phenotype. *Am J Med Genet* 72: 197–204, 1997. doi:10.1002/(SICI)1096-8628(19971017)72:2<197::AID-AJMG14>3.0.CO;2-I.

652. Wright JT, Li Y, Suggs C, Kuehl MA, Kulkarni AB, Gibson CW. The role of amelogenin during enamel-crystallite growth and organization in vivo. *Eur J Oral Sci* 119, Suppl 1: 65–69, 2011. doi:10.1111/j.1600-0722.2011.00883.x.

653. Xia Y, Ren A, Pugach MK. Truncated amelogenin and LRAP transgenes improve Amelx null mouse enamel. *Matrix Biol* 52-54: 198–206, 2016. doi:10.1016/j.matbio.2015.11.005.

654. Xu R, Zhou Y, Zhang B, Shen J, Gao B, Xu X, Ye L, Zheng L, Zhou X. Enamel regeneration in making a bioengineered tooth. *Curr Stem Cell Res Ther* 10: 434–442, 2015. doi:10.2174/1574888X10666150305104116.

655. Yahyazadehfar M, Ivancik J, Majd H, An B, Zhang D, Arola D. On the mechanics of fatigue and fracture in teeth. *Appl Mech Rev* 66: 0308031–3080319, 2014. doi:10.1115/1.4027431.

656. Yamakoshi Y. Porcine amelogenin: alternative splicing, proteolytic processing, protein-protein interactions, and possible functions. *J Oral Biosci* 53: 275–283, 2011. doi:10.1016/S1349-0079(11)80011-3.

657. Yamakoshi Y, Hu JC, Fukae M, Yamakoshi F, Simmer JP. How do enamelysin and kallikrein 4 process the 32-kDa enamelin? *Eur J Oral Sci* 114, Suppl 1: 45–51, 2006. doi:10.1111/j.1600-0722.2006.00281.x.

658. Yamakoshi Y, Hu JC, Zhang H, Iwata T, Yamakoshi F, Simmer JP. Proteomic analysis of enamel matrix using a two-dimensional protein fractionation system. *Eur J Oral Sci* 114, Suppl 1: 266–271, 2006. doi:10.1111/j.1600-0722.2006.00279.x.

659. Yamakoshi Y, Hu JCC, Fukae M, Tanabe T, Oida S, Simmer JP. *Amelogenin and 32 kDa Enamelin Protein-Protein Interactions*. Kanagawa: Tokai Univ. Press, 2003, p. 338–342.

660. Yamakoshi Y, Richardson AS, Nunez SM, Yamakoshi F, Milkovich RN, Hu JC, Bartlett JD, Simmer JP. Enamel proteins and proteases in Mmp20 and Klk4 null and double-null mice. *Eur J Oral Sci* 119, Suppl 1: 206–216, 2011. doi:10.1111/j.1600-0722.2011.00866.x.

661. Yamazaki D, Funato Y, Miura J, Sato S, Toyosawa S, Furutani K, Kurachi Y, Omori Y, Furukawa T, Tsuda T, Kuwabata S, Mizukami S, Kikuchi K, Miki H. Basolateral $Mg^{2+}$ extrusion via CNNM4 mediates transcellular $Mg^{2+}$ transport across epithelia: a mouse model. *PLoS Genet* 9: e1003983, 2013. doi:10.1371/journal.pgen.1003983.

662. Yang X, Wang L, Qin Y, Sun Z, Henneman ZJ, Moradian-Oldak J, Nancollas GH. How amelogenin orchestrates the organization of hierarchical elongated microstructures of apatite. *J Phys Chem B* 114: 2293–2300, 2010. doi:10.1021/jp910219s.

663. Yilmaz ED, Bechtle S, Özcoban H, Kieser JA, Swain MV, Schneider GA. Micromechanical characterization of prismless enamel in the tuatara, *Sphenodon punctatus*. *J Mech Behav Biomed Mater* 39: 210–217, 2014. doi:10.1016/j.jmbbm.2014.07.024.

664. Yin K, Hacia JG, Zhong Z, Paine ML. Genome-wide analysis of miRNA and mRNA transcriptomes during amelogenesis. *BMC Genomics* 15: 998, 2014. doi:10.1186/1471-2164-15-998.

665. Yin K, Lei Y, Wen X, Lacruz RS, Soleimani M, Kurtz I, Snead ML, White SN, Paine ML. SLC26A gene family participate in pH regulation during enamel maturation. *PLoS One* 10: e0144703, 2015. doi:10.1371/journal.pone.0144703.

666. Yokozeki M, Afanador E, Nishi M, Kaneko K, Shimokawa H, Yokote K, Deng C, Tsuchida K, Sugino H, Moriyama K. Smad3 is required for enamel biomineralization. *Biochem Biophys Res Commun* 305: 684–690, 2003. doi:10.1016/S0006-291X(03)00806-4.

667. Young RA. Biological apatite vs hydroxyapatite at the atomic level. *Clin Orthop Relat Res* 113: 249–262, 1975. doi:10.1097/00003086-197511000-00036.

668. Young RA. Implications of atomic substitutions and other structural details in apatites. *J Dent Res* 53: 193–203, 1974. doi:10.1177/00220345740530020601.

669. Zaki AE, Hand AR, Mednieks MI, Eisenmann DR, Borke JL. Quantitative immunocytochemistry of $Ca^{2+}$-$Mg^{2+}$ ATPase in ameloblasts associated with enamel secretion and maturation in the rat incisor. *Adv Dent Res* 10: 245–251, 1996. doi:10.1177/08959374960100022101.

670. Zeichner-David M, Chen LS, Hsu Z, Reyna J, Caton J, Bringas P. Amelogenin and ameloblastin show growth-factor like activity in periodontal ligament cells. *Eur J Oral Sci* 114, Suppl 1: 244–253, 2006. doi:10.1111/j.1600-0722.2006.00322.x.

671. Zhang JW, Nancollas GH. Mechanisms of growth and dissolution of sparingly soluble salts. *Rev Mineral Geochem* 23: 365–396, 1990.

672. Zhang Y, Kim JY, Horst O, Nakano Y, Zhu L, Radlanski RJ, Ho S, DenBesten PK. Fluorosed mouse ameloblasts have increased SATB1 retention and Gαq activity. *PLoS One* 9: e103994, 2014. doi:10.1371/journal.pone.0103994.

673. Zhang Y, Yan Q, Li W, DenBesten PK. Fluoride down-regulates the expression of matrix metalloproteinase-20 in human fetal tooth ameloblast-lineage cells in vitro. *Eur J Oral Sci* 114, Suppl 1: 105–110, 2006. doi:10.1111/j.1600-0722.2006.00303.x.

674. Zhu D, Paine ML, Luo W, Bringas P Jr, Snead ML. Altering biomineralization by protein design. *J Biol Chem* 281: 21173–21182, 2006. doi:10.1074/jbc.M510757200.

675. Zou Y, Wang H, Shapiro JL, Okamoto CT, Brookes SJ, Lyngstadaas SP, Snead ML, Paine ML. Determination of protein regions responsible for interactions of amelogenin with CD63 and LAMP1. *Biochem J* 408: 347–354, 2007. doi:10.1042/BJ20070881.